Nanoimaging using soft X-ray and EUV sources

Przemyslaw Wachulak
wachulak@gmail.com

http://www.ztl.wat.edu.pl/zoplzm

LASER-MATTER INTERACTION LABORATORY
Institute of Optoelectronics, Military University of Technology

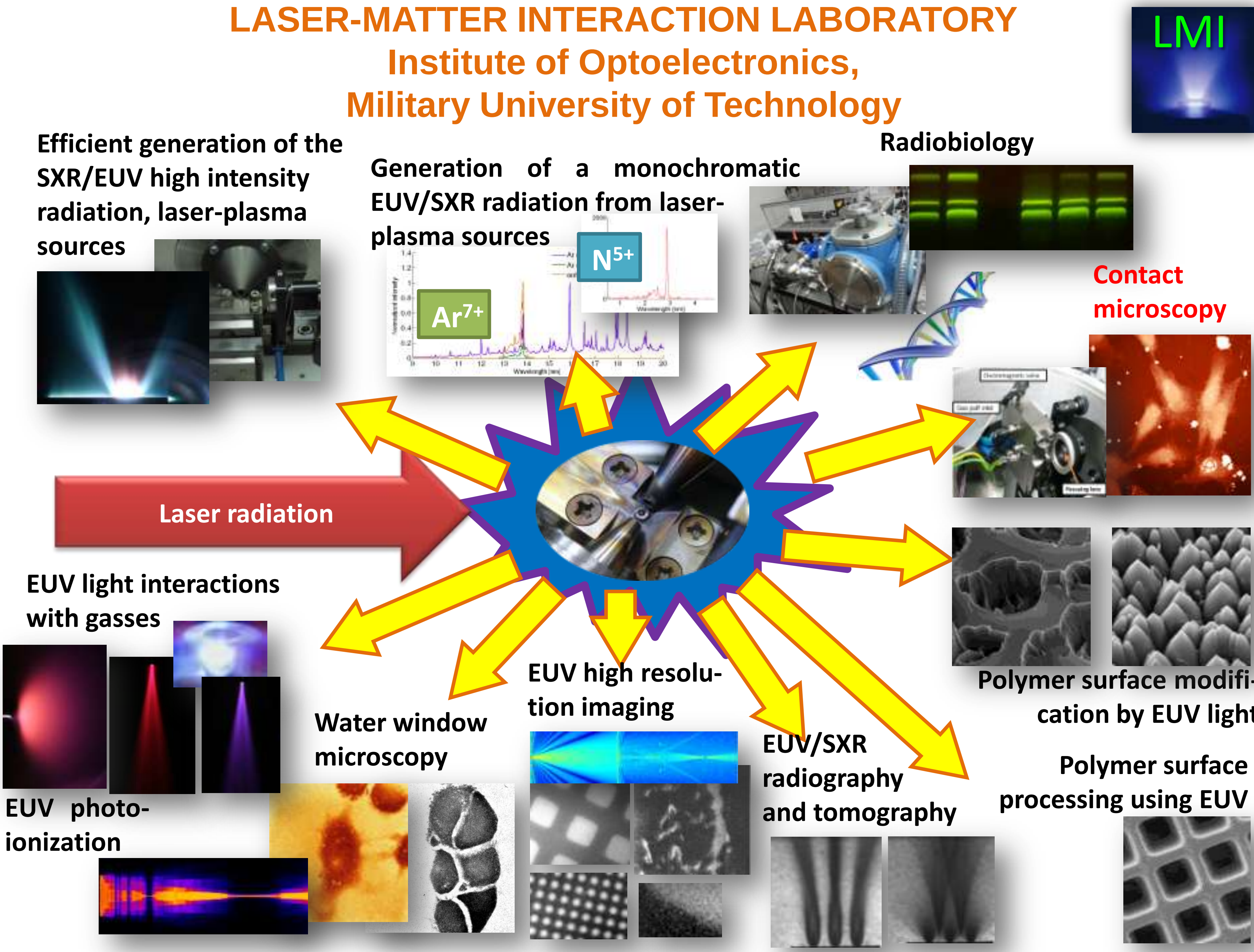

Outline

- Nanotechnology and nanoimaging
- EUV and SXR radiation, motivation and sources
- EUV holography (Gabor, Fourier)
- Reconstruction of CG holograms
- Talbot imaging
- Coherent diffraction (lens-less) imaging
- Ptychography
- Zone plates for various wavelengths
- EUV microscopy using FZP
- Scanning EUV microscopy
- SXR and „water-window” microscopy
- EUV, SXR HXR tomography
- Contact microscopy

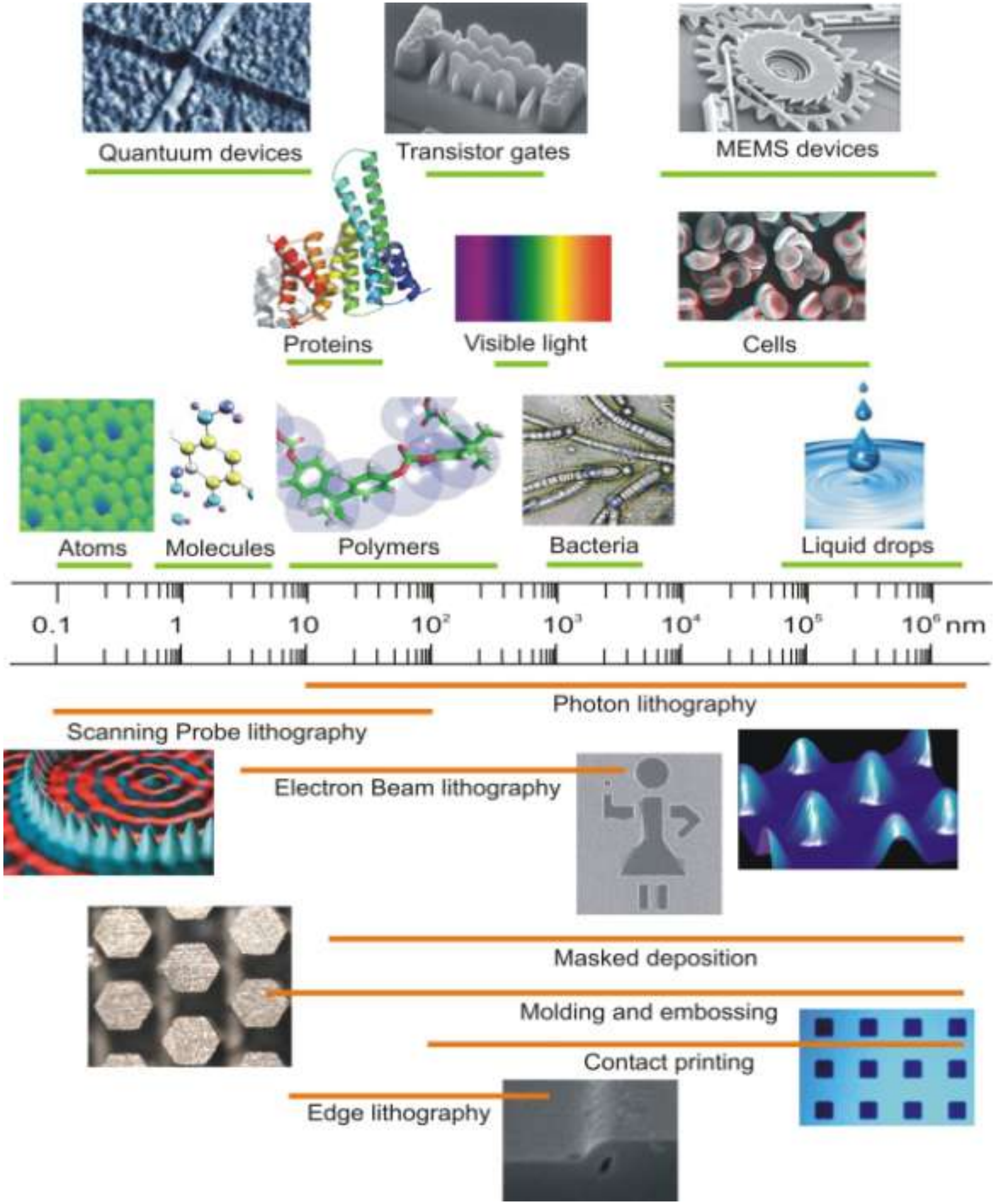

Nanotechnology:

Manipulation on objects like atoms and molecules and the observation of the results of such manipulation in the nanometer scale

„NANO”

1nm =0.000 000 001m= 10 H atoms

Diameter of a human hair: 50 000nm

Smallest feature seen by a human eye: 10 000 nm

Nanoimaging:

Imaging in the nanometer scale: **<1um or <100nm**

Electromagnetic Spectrum

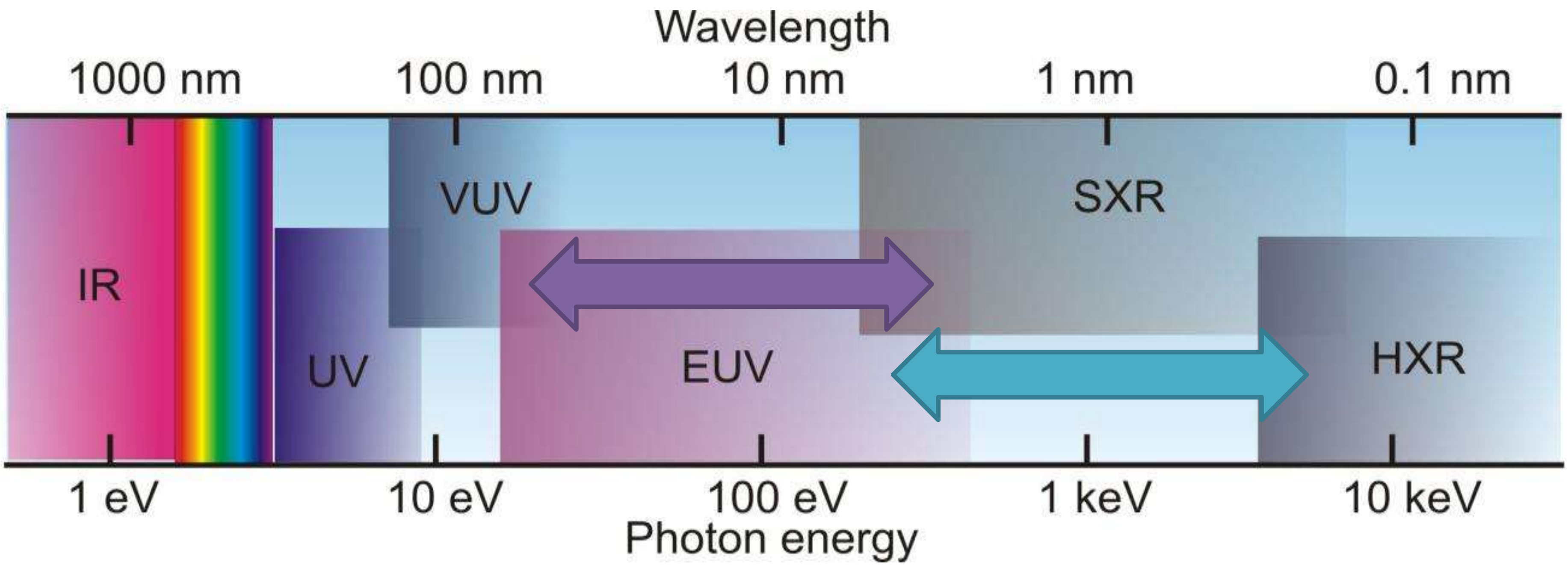

Adequate wavelengths of light:

Extreme Ultraviolet (EUV)
λ~10-120nm
Eph~10-120eV

Soft X-rays (SXR)
λ~1Å-10nm
Eph~120 – 10keV

Motivation for EUV and SXR imaging

EUV (λ=10-120nm)

• shorter wavelength λ – better spatial resolution

$$\delta = \frac{k \cdot \lambda}{NA}$$

λ = 500 nm

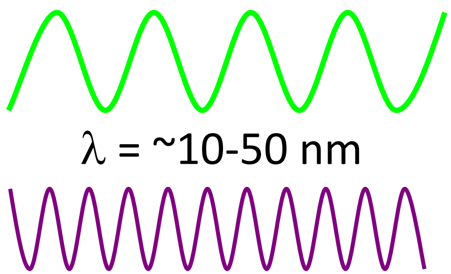

λ = ~10-50 nm

EUV/SXR radiation „see" 10-100x smaller features

• strong optical contrast in the EUV; **very high absorption of EUV light in very thin layers**, practically almost all materials are opaque, including gasses, which allows for (**direct – based on light absorption - obserwation of gasses**).

• EUV light is used in lithography

• short EUV pulses allow to study transient processes

SXR (λ=0.1-10nm)

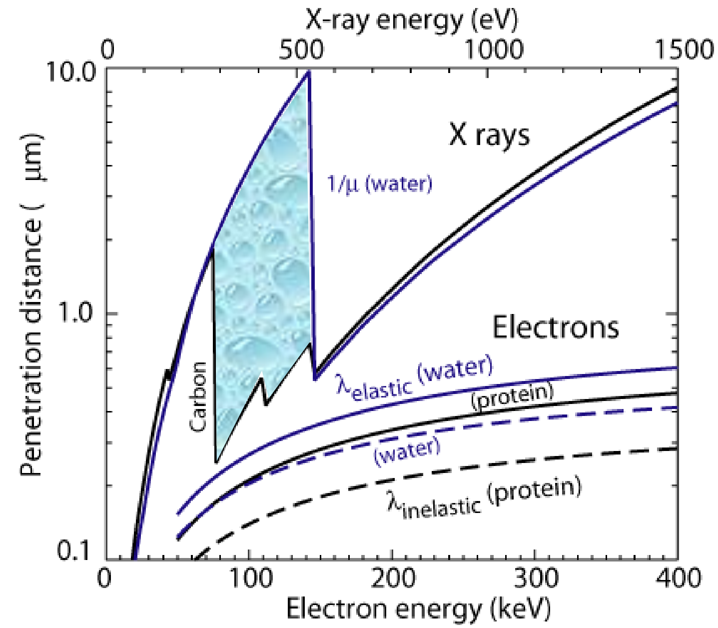

xray1.physics.sunysb.edu

Water window: 284 - 543 eV, λ = 2.3 – 4.4 nm

• short wavelength-> possible **high spatial resolution** : **δ=kλ/NA**.

• very high **optical contrast between organic material (barbon based) and water (oxygen)**

• **radiation with relatively large penetration depth** tens of microns for biological samples.

Synchrotrons and FEL used for nanoimaging

BERKELEY LAB
LAWRENCE BERKELEY NATIONAL LABORATORY
Advanced Light Source
An Office of Science User Facility

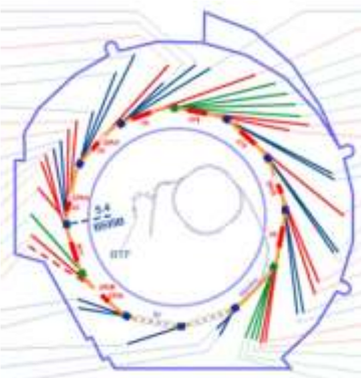

XM-1 microscope

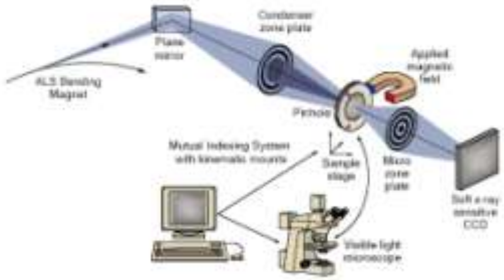

http://www-als.lbl.gov/

http://www.lightsources.org/facility/hzb-helmholtz-zentrum-berlin

BESSY II – Helmholtz-Zentrum Berlin (HZB)

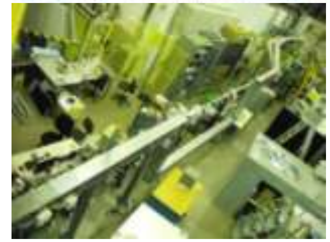

XM, X-ray Microscopy **U41-TXM**
X-ray-Microscopy, X-ray-Tomography

PAUL SCHERRER INSTITUT
PSI

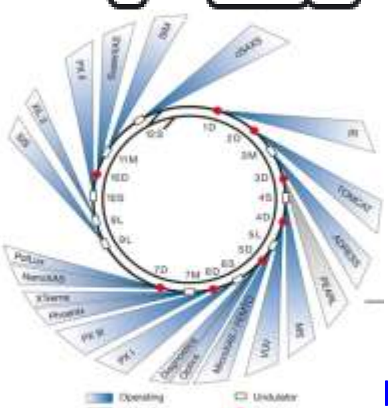

TOMCAT - X02DA: Tomography
A beamline for TOmographic Microscopy and Coherent rAdiology experimenTs

SIM - X11MA: Surfaces / Interfaces: Microscopy

http://www.psi.ch/sls/sim/sim

ALBA

Transmission X-ray Microscopy beamline MISTRAL

https://www.cells.es/Beamlines/XM/

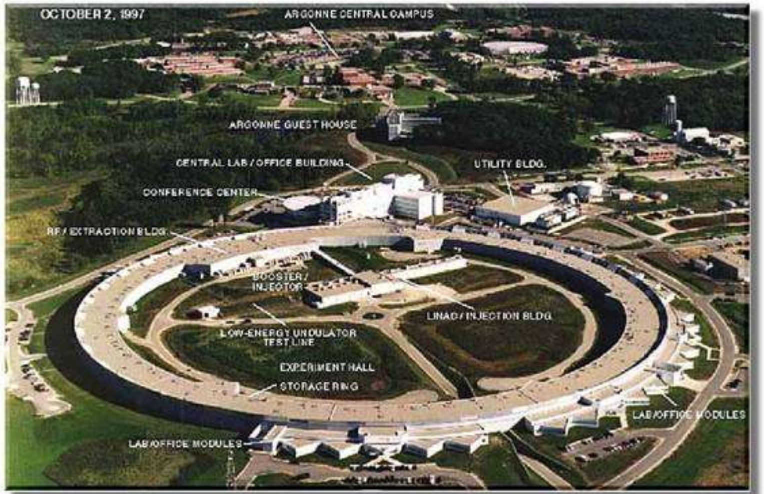

Advanced Photon Source, Argonne National Lab, USA

Stanford Linear Accelerator Center – SLAC and Linac Coherent Light Source - LCLS (USA)

Free Electron Laser (FEL), Hamburg, Germany

Compact sources

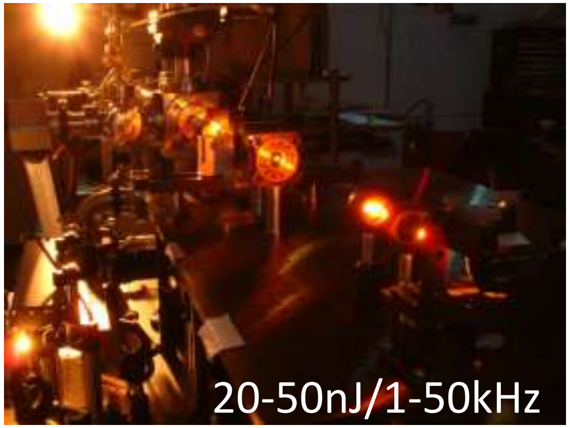

High Harmonic Geneation (HHG) system, James R., Macdonald Laboratory, Atomic, Molecular & Optical Physics Research Facility, Kansan State University, KS, USA

Capillary discharge type EUV laser (fast electric discharge in Ar filled capillary), EUV ERC, Prof. Jorge Rocca, Fort Collins, USA

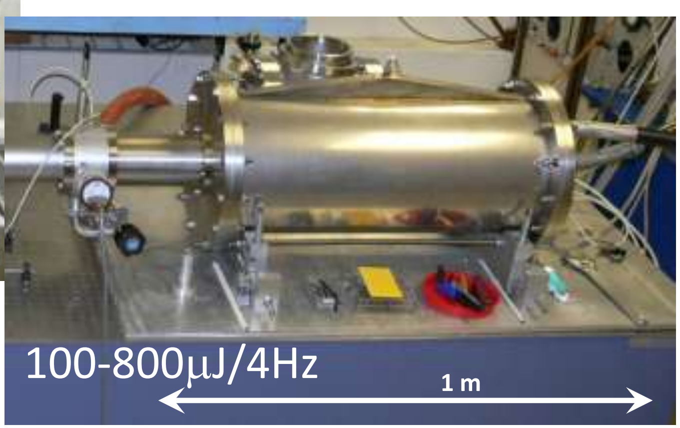

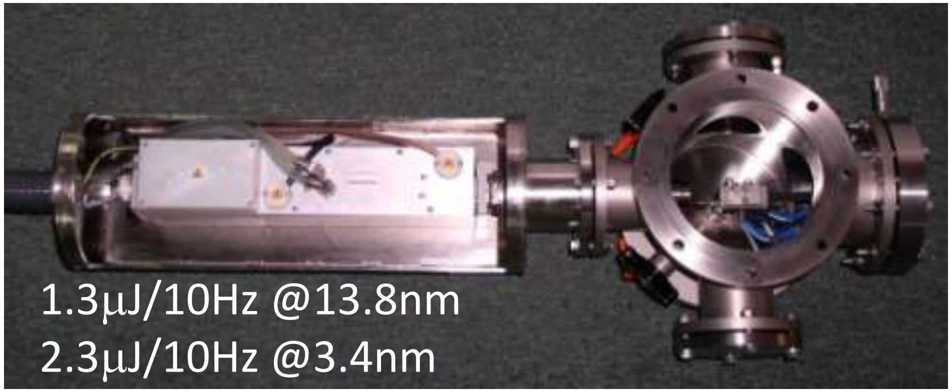

EUV/SXR lamp for metrology and microscopy, Prof. Henryk Fiedorowicz, IOE WAT, Warsaw, Poland

Compact sources:

- possibility to perform imaging experiments **in the laboratory environment**
- higher chances for **future commercialization**
- **easy, low cost operation, easy access to the user**

Gabor Holography: Coherent EUV source – Capillary discharge laser λ=46.9nm

- High fluence
mW average power

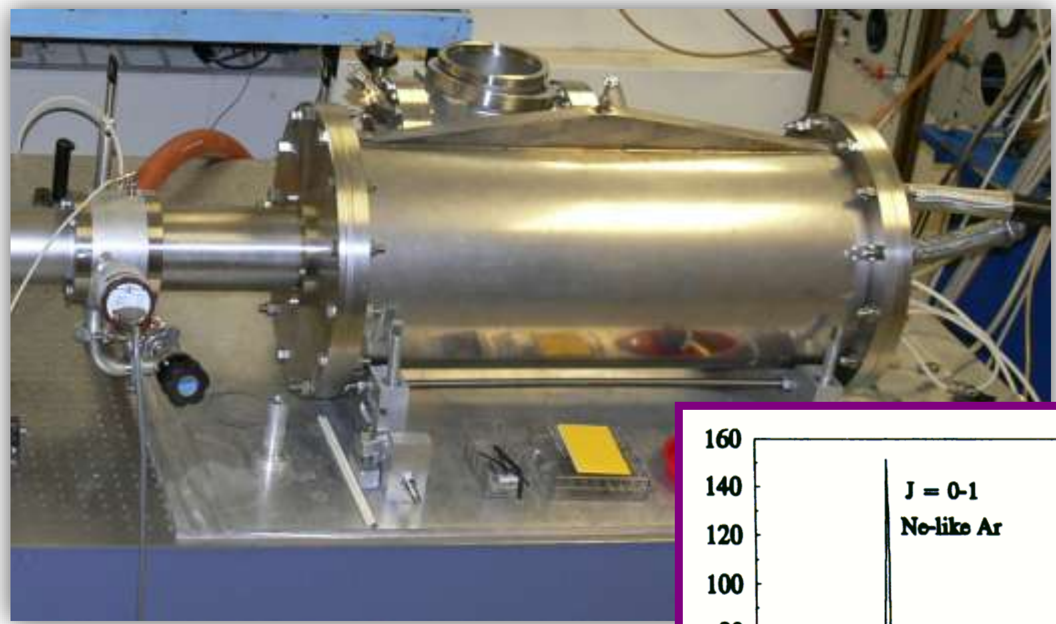

- High monochromaticity

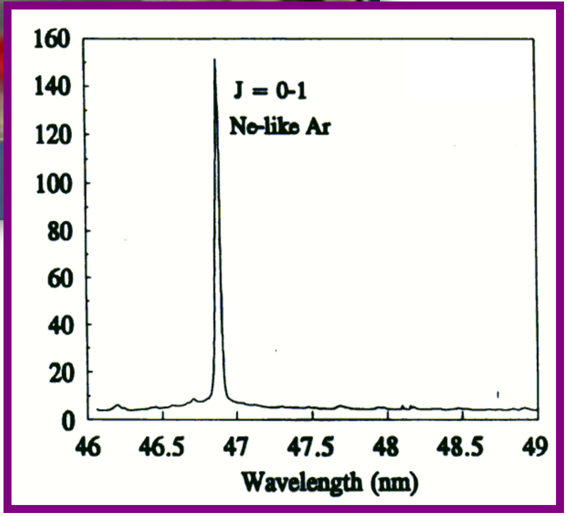

J.J. Rocca, el al. Phys. Rev. Lett. 73, 2192 (1994).

- High spatial coherence

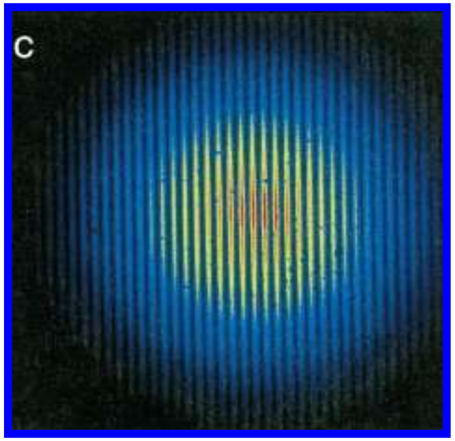

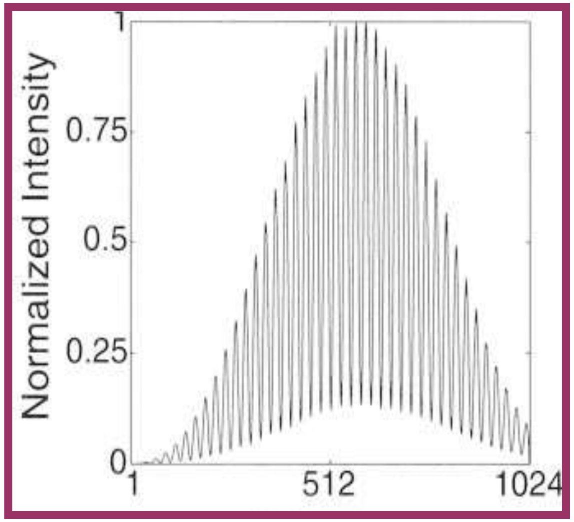

Y. Liu, et al. Phys. Rev. A, 63, 033802 (2001).

- Repetition rate: 4 Hz
- High energy per pulse max - 0.8 mJ
- Average power ~ 3 mW
  - High monochromaticity: $\Delta\lambda/\lambda<10^{-4}$
- Coherence radius: R_c = 550 μm at 0.157m from 36cm capillary
- Very compact

Gabor holography - recording and reconstruction

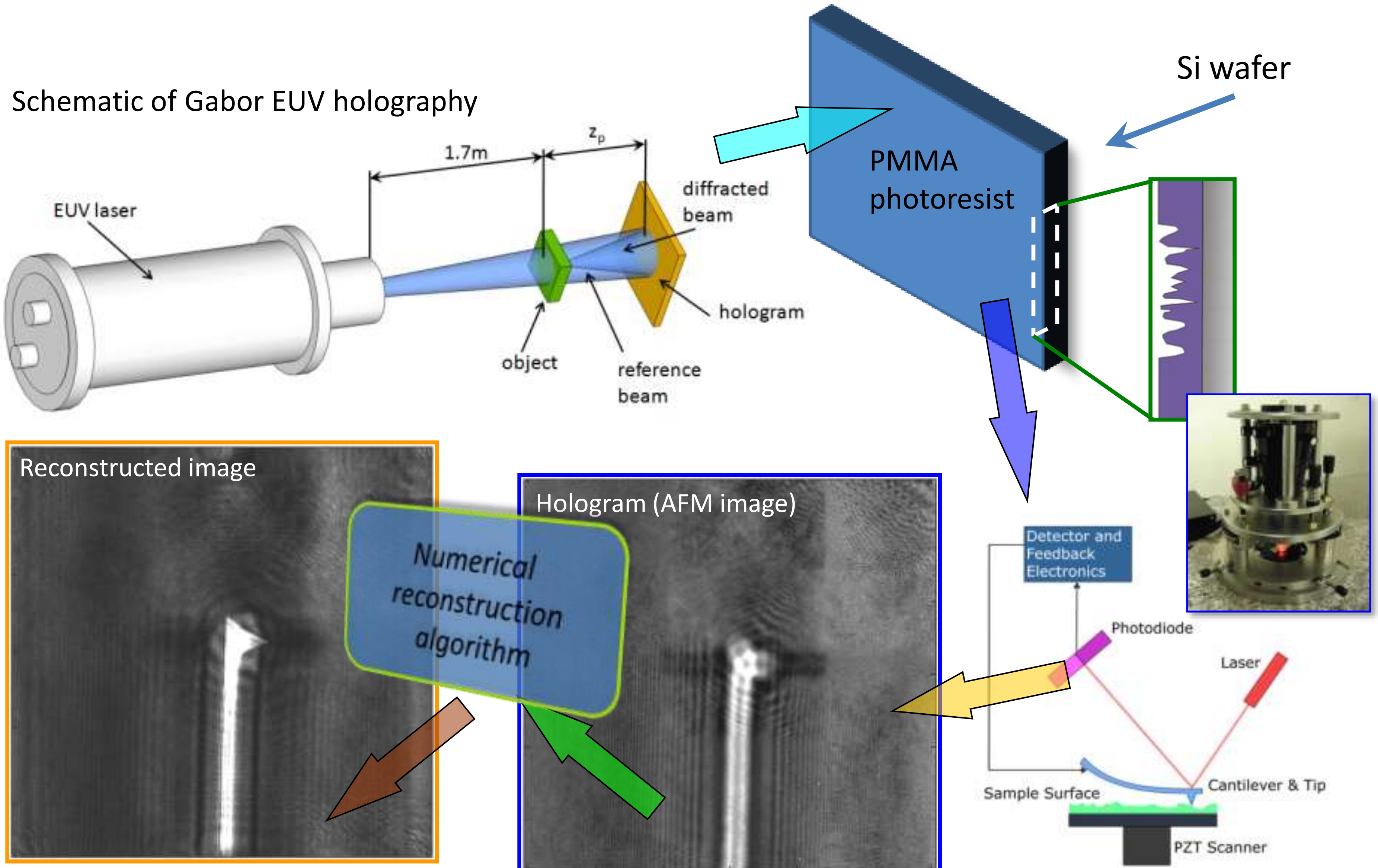

Wavelength resolution holographic scheme

Experimental arrangement

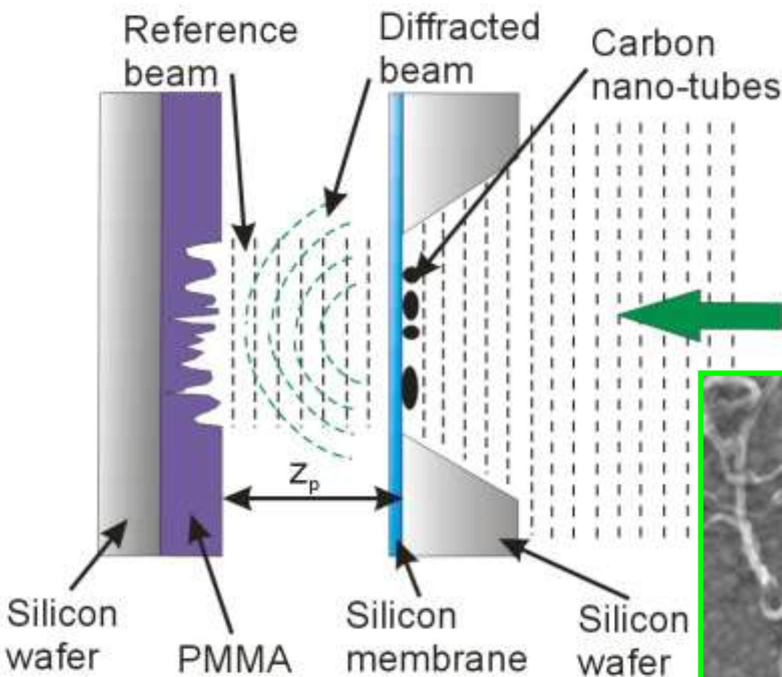

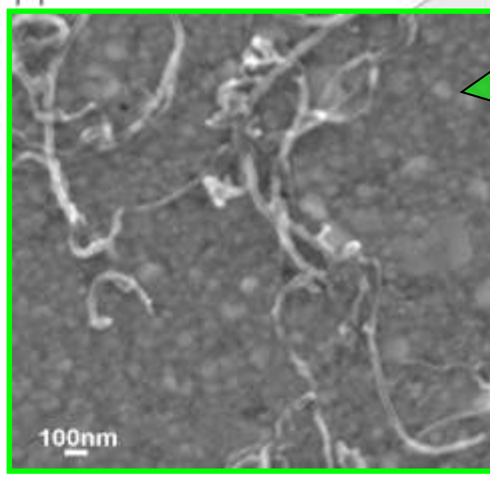

SEM image of carbon nanotubes

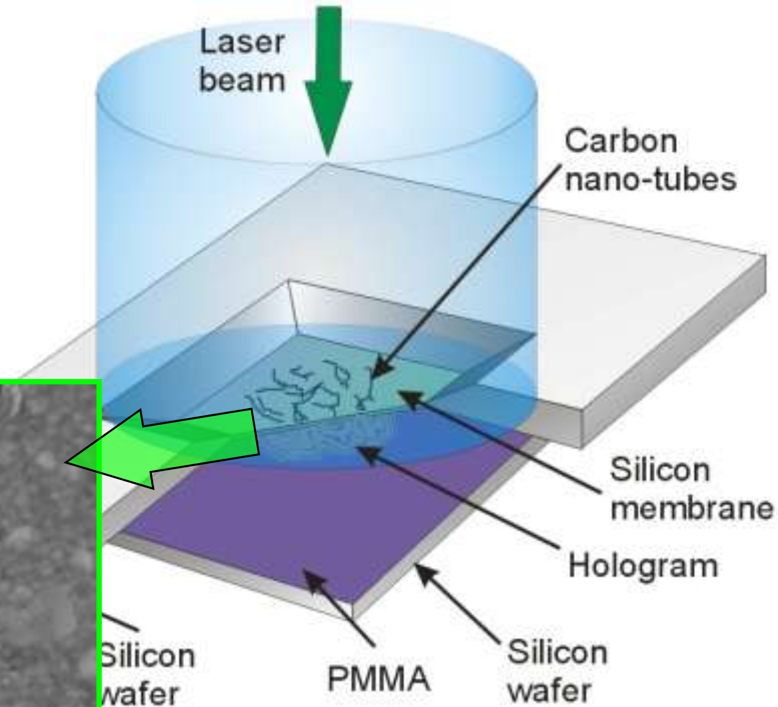

Object characteristics:

Multi-Wall Carbon Nanotubes

- Outer Diameter 50-80nm
- Length 10-20μm

Experimental details:

- Illumination wavelength λ= 46.9nm
- Object-photoresist distance z_p ~2.5 - 4μm
- Laser-object distance z_s =75cm
- Required number of laser shots = 150, => Dose = 53mJ/cm^2
- Membrane transmission T~15-20%

2-D holograms and reconstructions of CNT

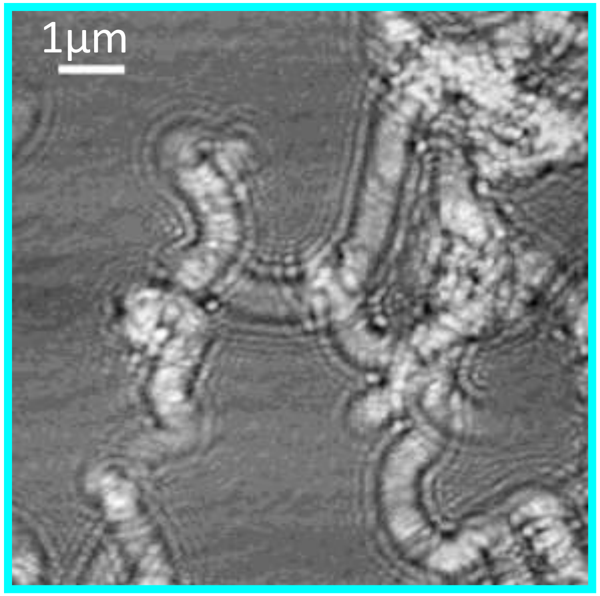

hologram

Reconstruction parameters:

- z_p = 2.66 µm
- pixel size = 9.7nm

- scan size typically 10x10 μm^2
- max scan size 42x42 μm^2

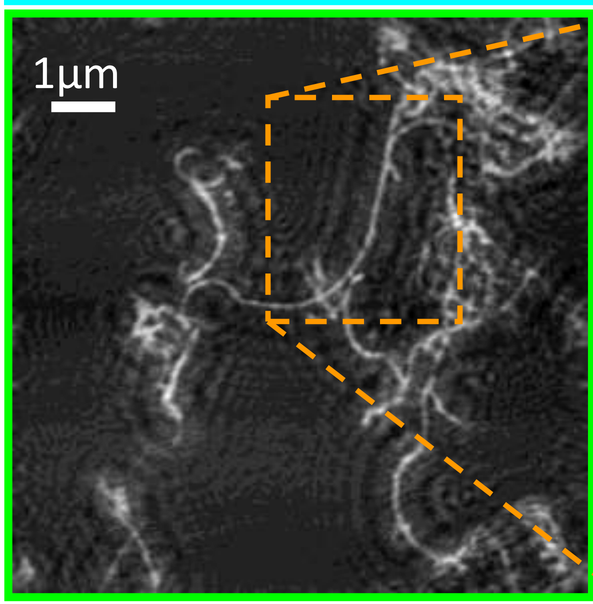

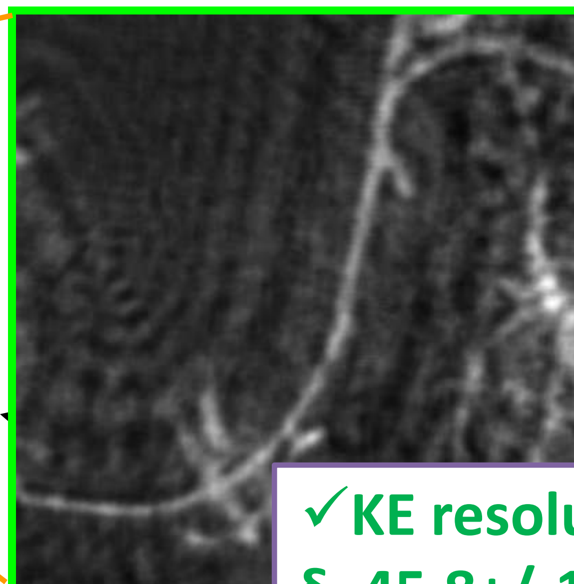

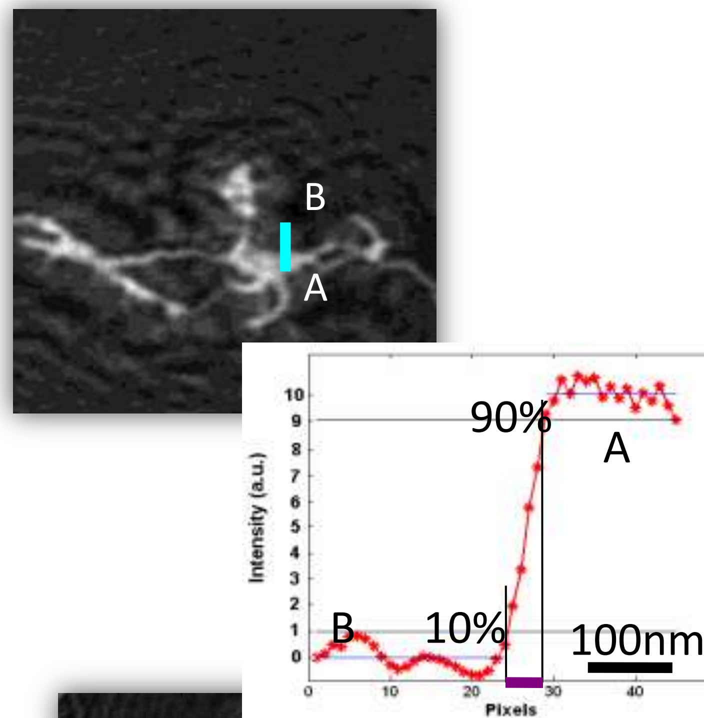

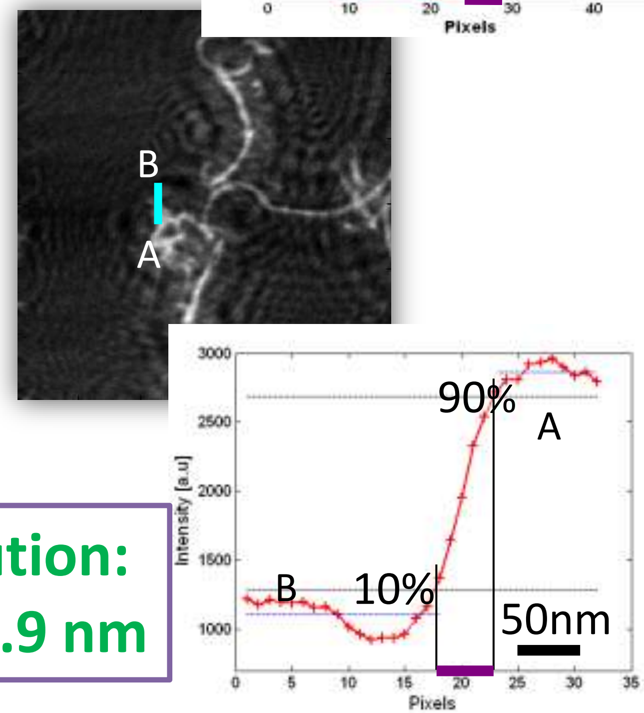

✓KE resolution:
δ=45.8+/-1.9 nm

P. W. Wachulak, et al., J. Opt. Soc. Am. B, 25, 11, 1811 (2008).

Single-shot EUV Fourier transform holography of an extended object

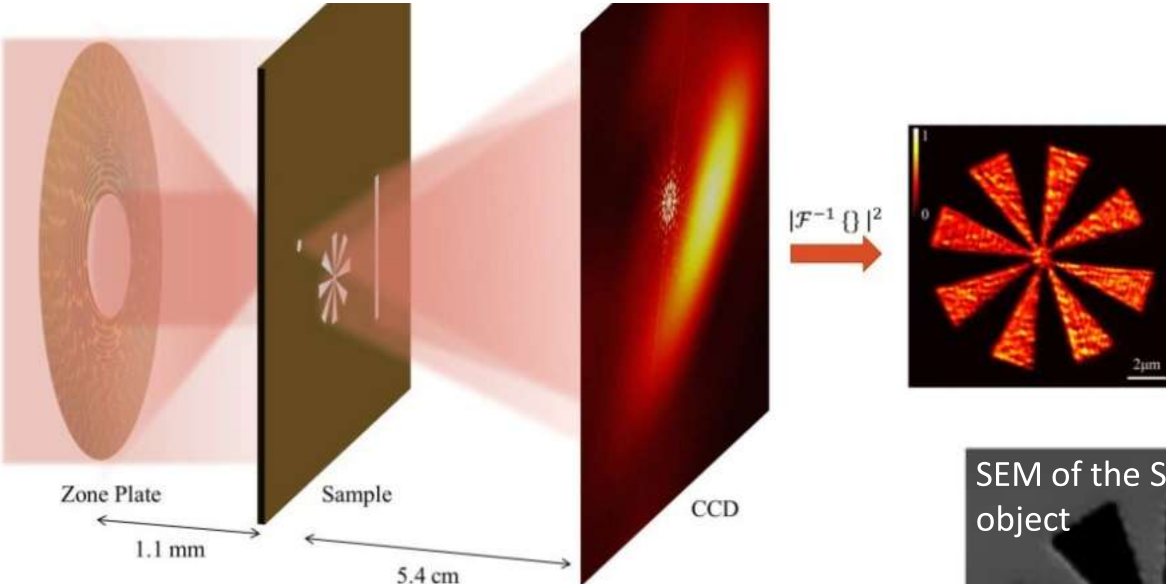

Schematic of the Fourier transform holography setup

- EUV beam is incident on the zone plate
-The central opening in the ZP passed the 0-order beam to illuminate the object
-1st order focus is the reference wave.
-The interference between the two beams was collected on a CCD and numerically reconstructed to obtain the final image

KE spatial resolution 120nm (multishot exposure, 167nm for a single shot exposure

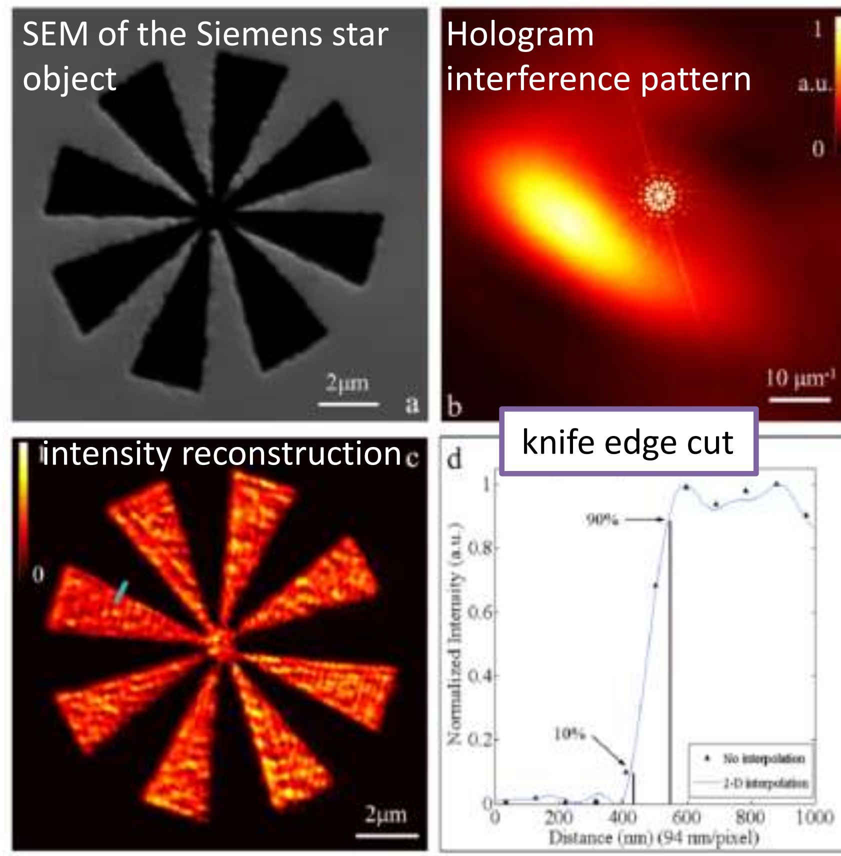

E. Malm,… P. Wachulak et al.,
Optics Express 21,8,9959 (2013)

Recording oscillations of sub-micron size cantilevers by EUV Fourier transform holography

Schematic of the Fourier transform holography setup

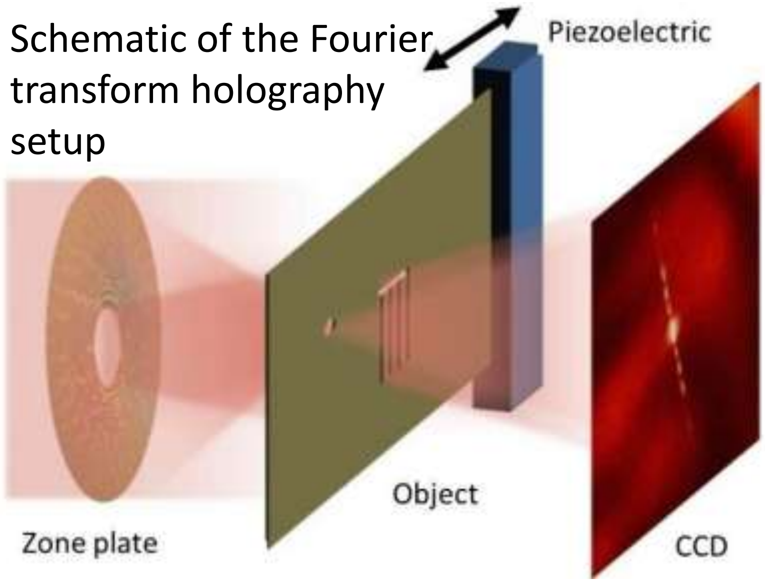

Examples of reconstructed frames of the oscillating pillars

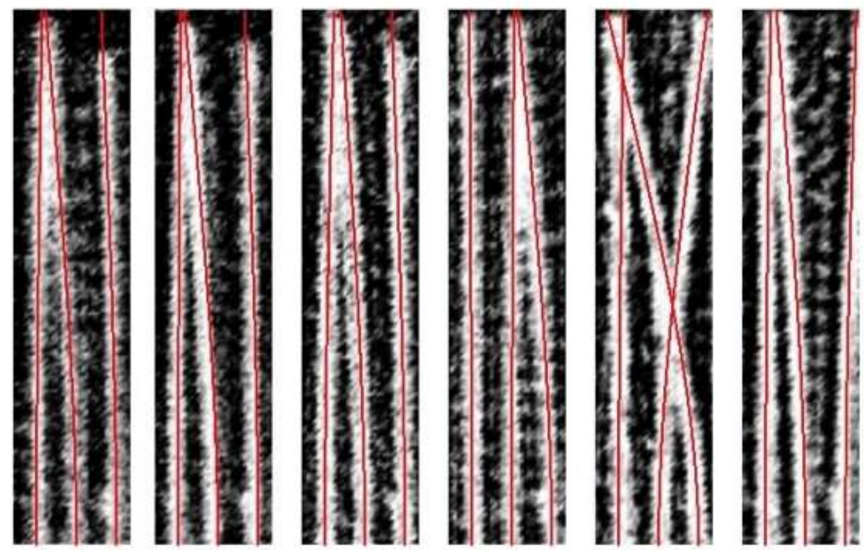

N. Monserud,… P. Wachulak et al., Optics Express 22,4,4161 (2014)

SEM of three nanopillars

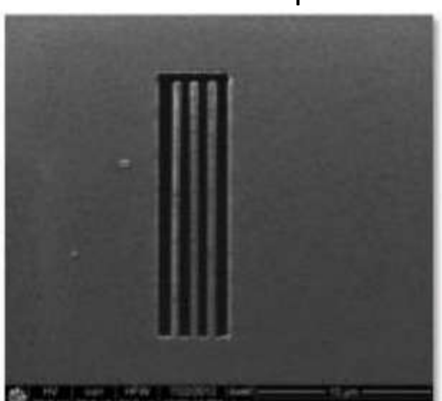

Central portion of the hologram

reconstruction of the pillars

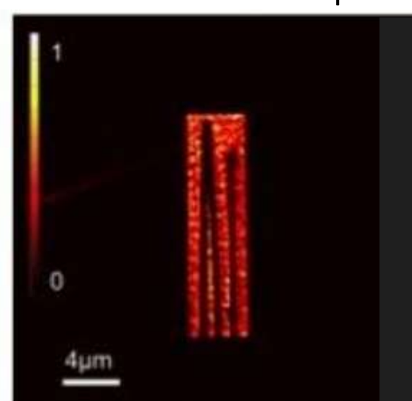

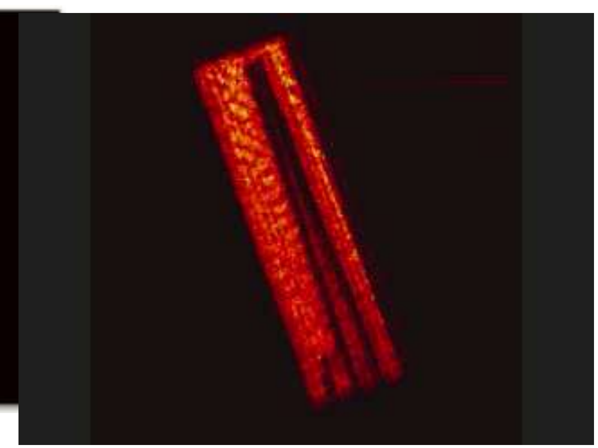

Single shot Fourier Hologram using Ni-Like Ag X-ray laser

apri ADVANCED PHOTONICS RESEARCH INSTITUTE

Fourier Transform Holography (FTH) experimental setup

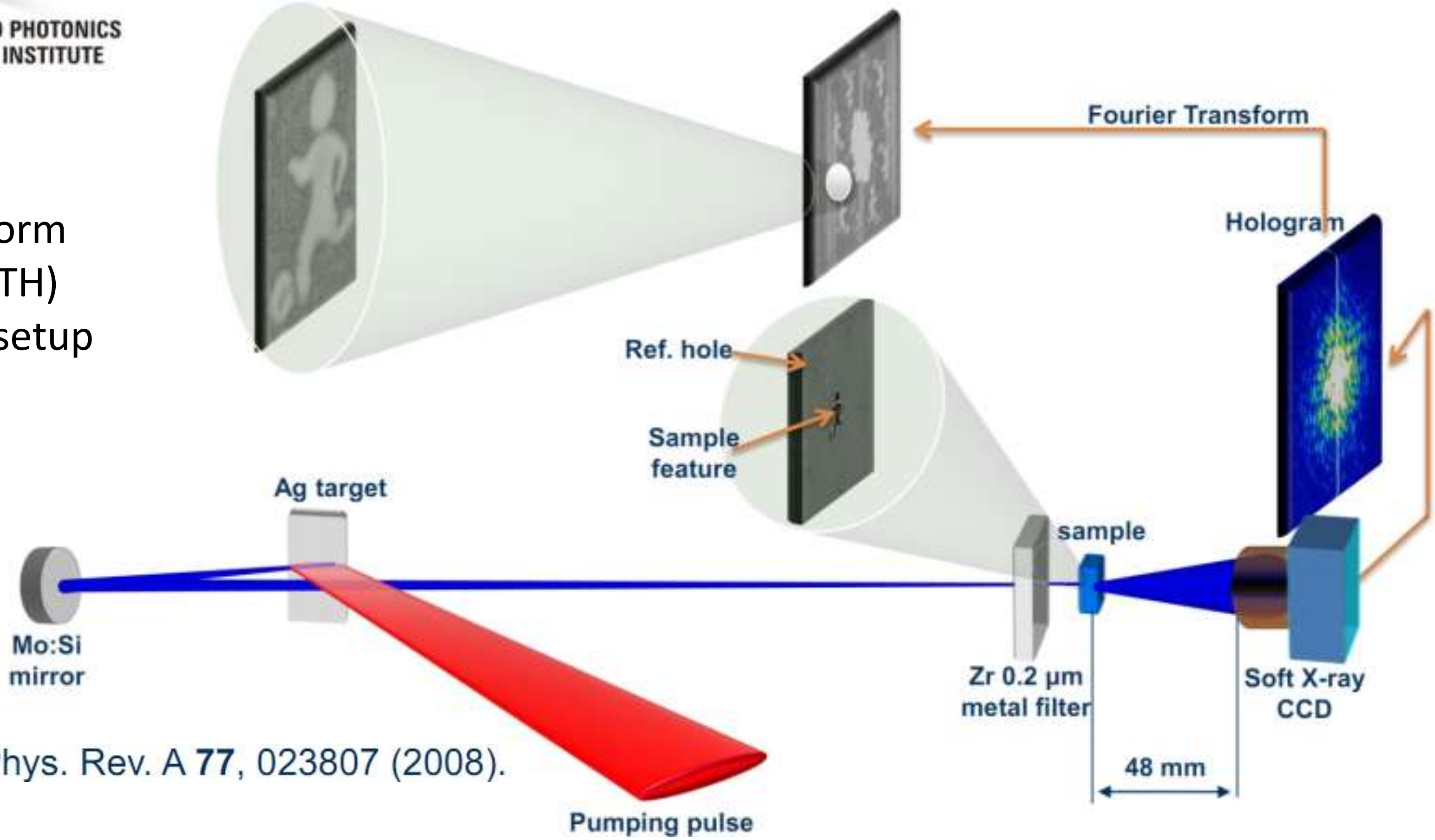

H. T. Kim et al., Phys. Rev. A **77**, 023807 (2008).

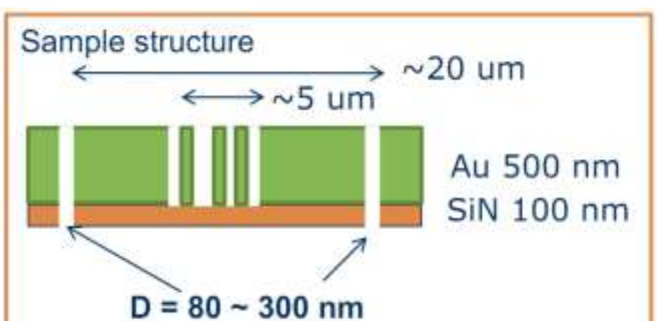

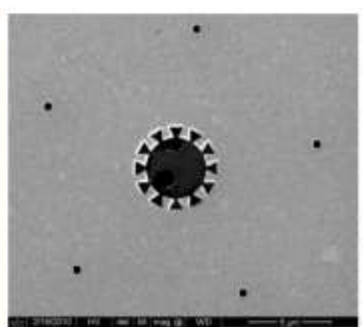

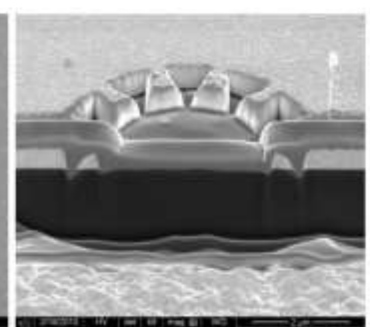

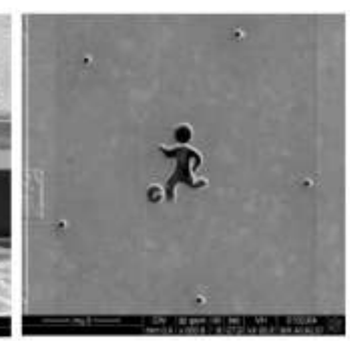

Single shot Fourier Hologram using Ni-Like Ar X-ray laser

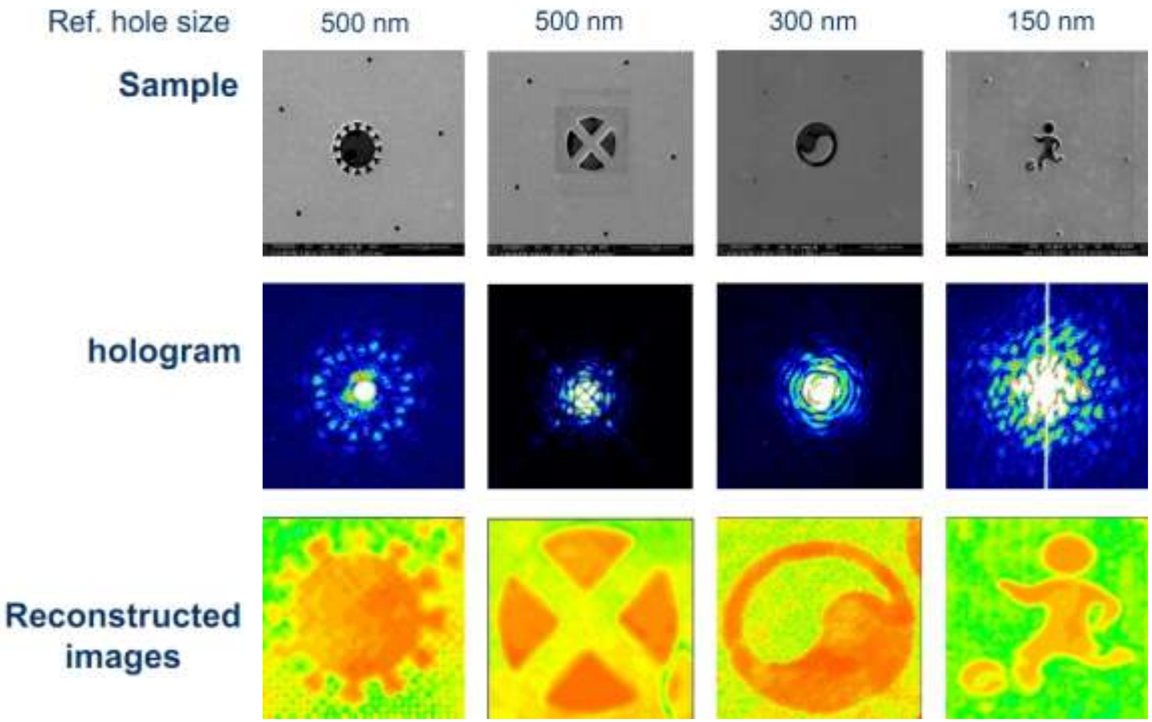

Various holograms and reconstructed images

Sample

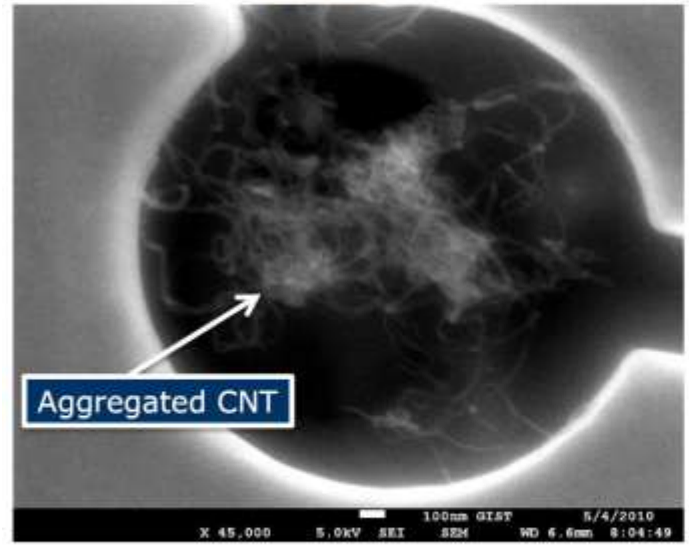

Carbon Nano Tube on the SiN membrane
(width : 20 – 30 nm)

Image

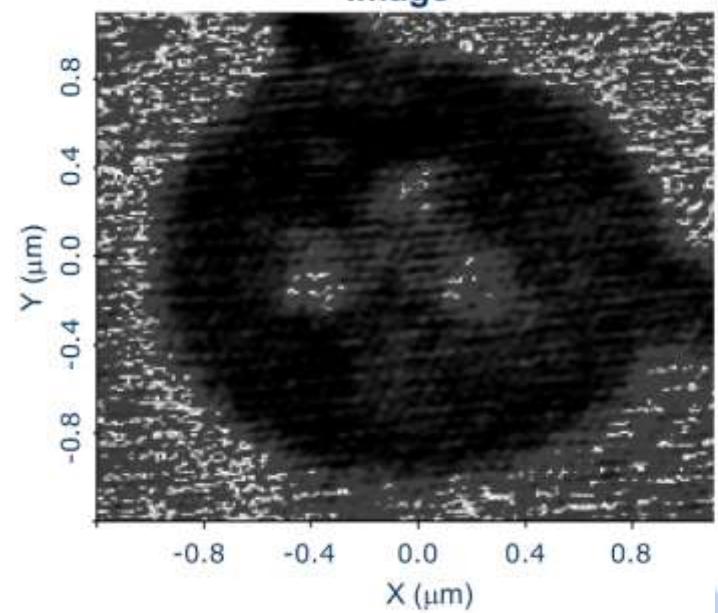

Single shot hologram and reconstruction of carbon nanotubes

Resolution of 94nm, single shot, λ=13.9nm

Images courtesy of Dr. H. T. Kim, GIST, Korea,

EUV reconstruction of computer generated holograms (CGH)

Experimental details:

Wavelength λ=46.9nm

Pixel Size=140nm

Line Width=1.54μm

Reconstruction distance Z=500μm

Field=$102.9 \times 102.9 \mu m^2$

NA=0.102, res. ~230nm

DOF=4.5μm

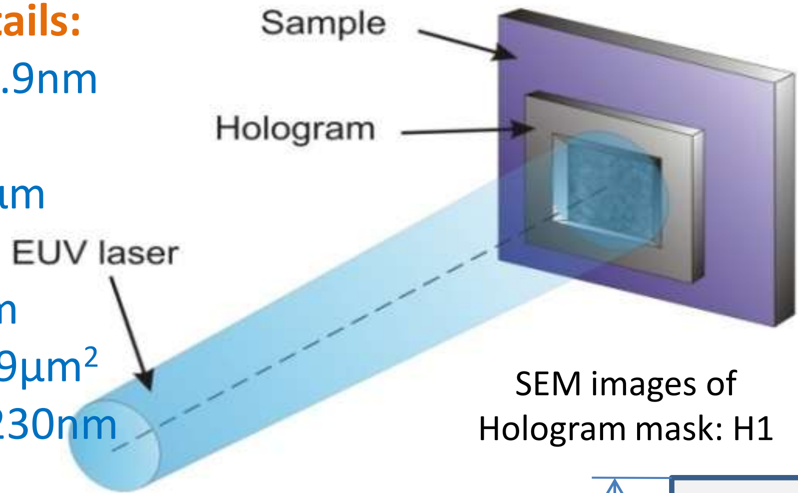

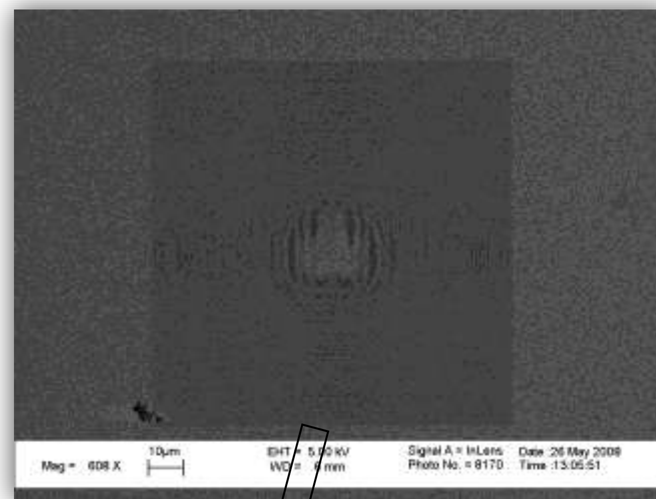

SEM images of Hologram mask: H1

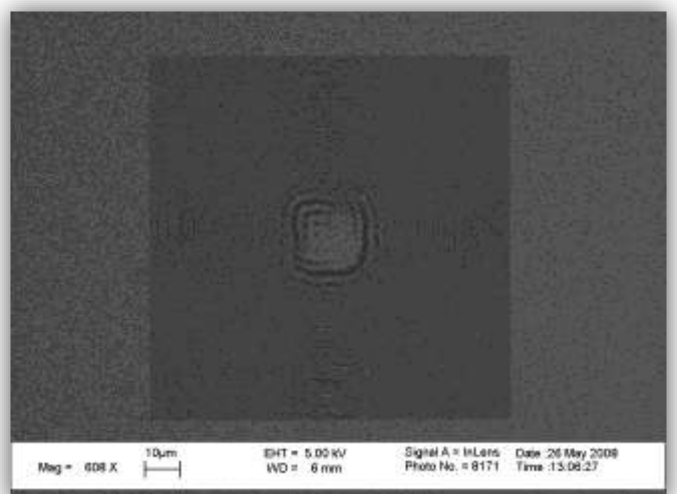

SEM images of Hologram mask: H2

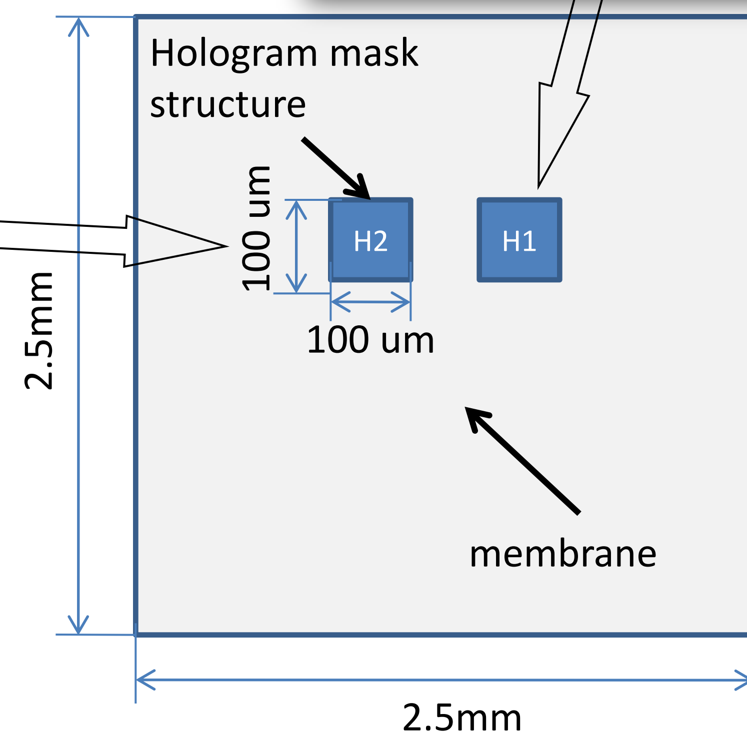

CGH EUV reconstruction results

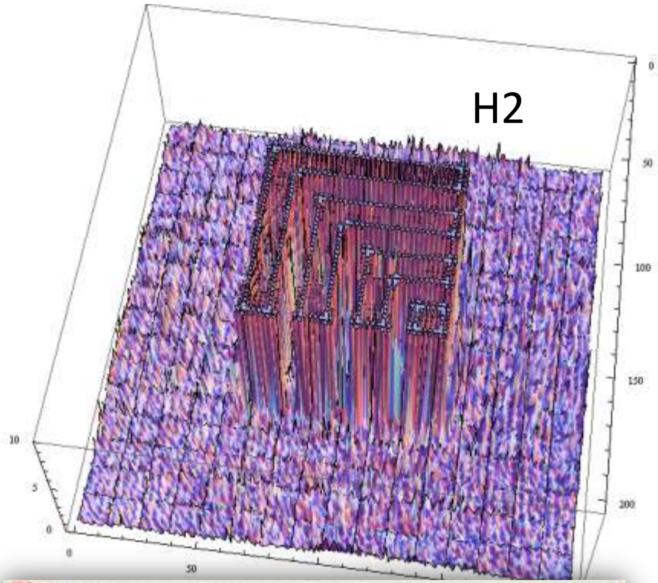

Simulated images of
reconstructed
holograms

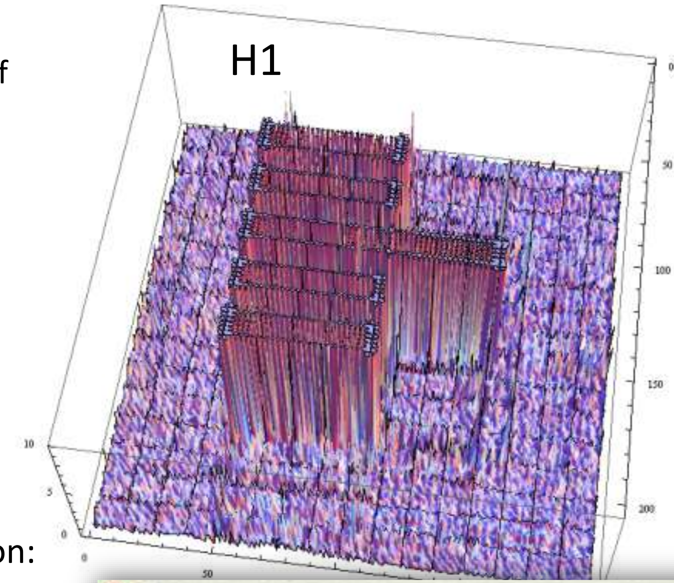

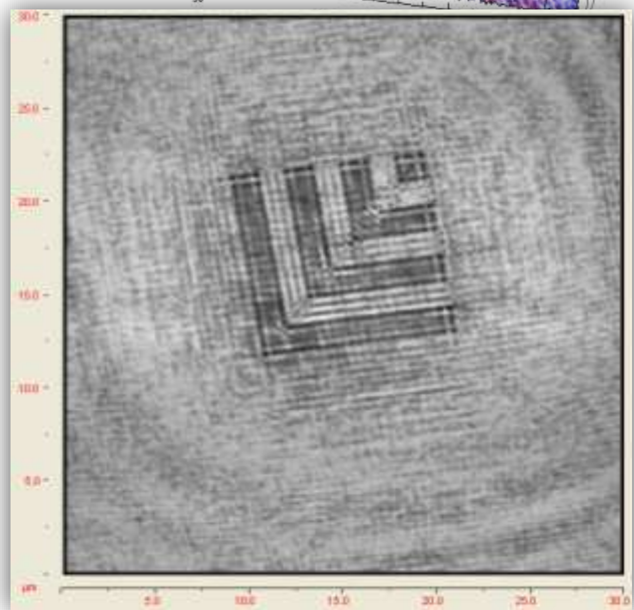

Hologram reconstruction:
AFM images
@ 500um gap (PMMA)

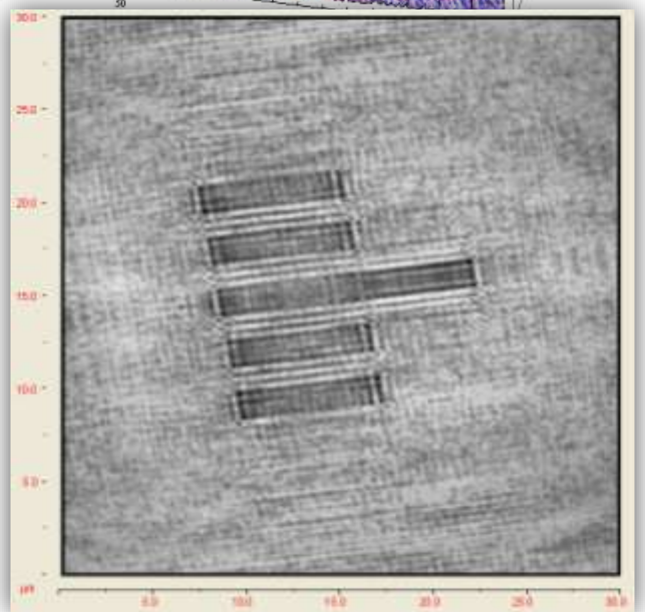

Advantage:
- your object does not need to exist
- Hologram might be partially damaged, your object will be reconstructed anyway.

A. Isoyan, …P. Wachulak, et al,., Journal of Vacuum Science & Technology B, 27, 6 , 2931-2937 (2009)

Talbot imaging at EUV wavelengths

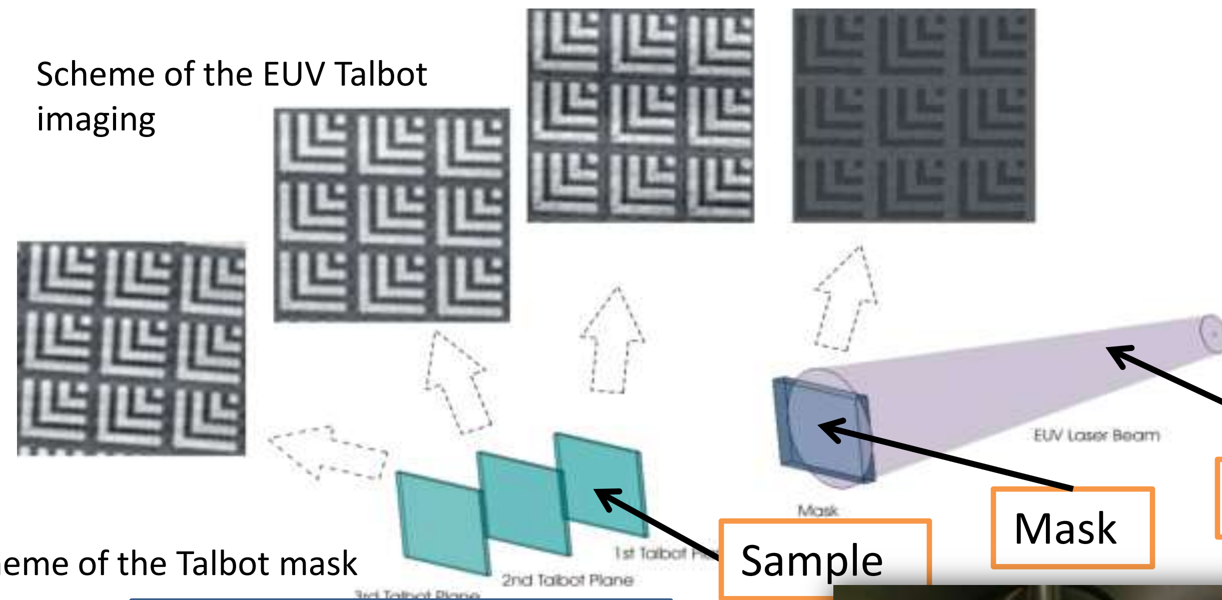

Experimental details:

Wavelength λ=46.9nm

Smallest features=140nm

Cell size p=4.842 μm (124x124)

Rec. distance z_T=1000μm

Field=600x600μm^2

NA=0.282, res.=83nm

DOF=0.6μm

$$z_T(n) = \frac{2p^2}{\lambda} n$$

Scheme of the Talbot mask

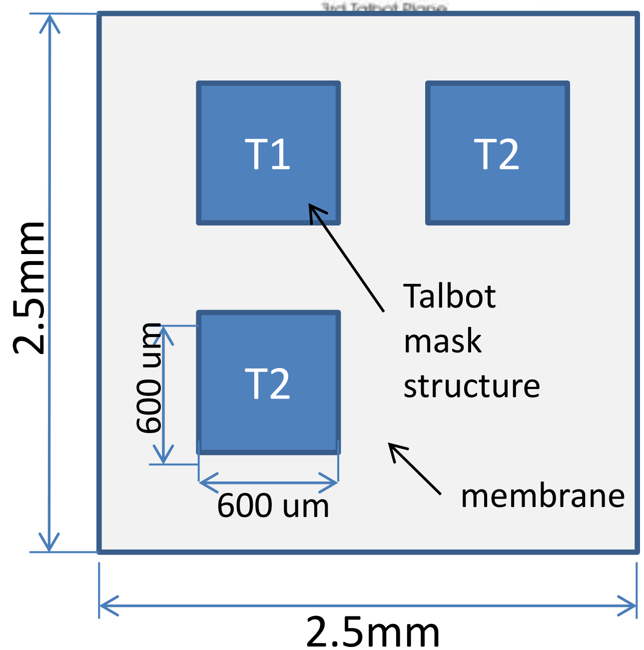

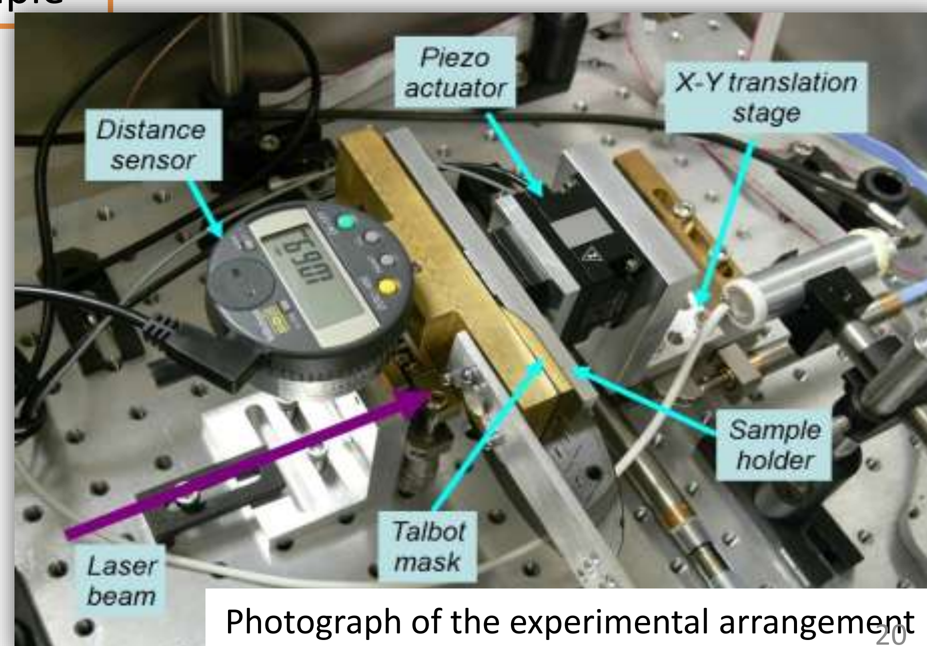

Photograph of the experimental arrangement

Talbot imaging results

SEM images of Talbot self-imaging mask: T1

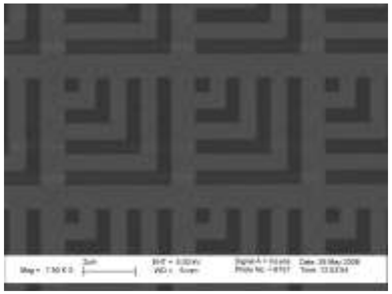

mask: T2

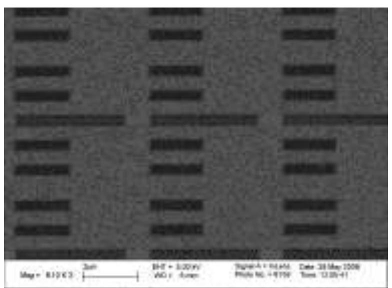

mask: T3

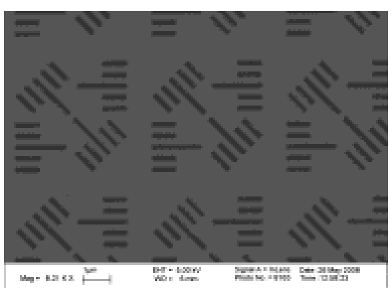

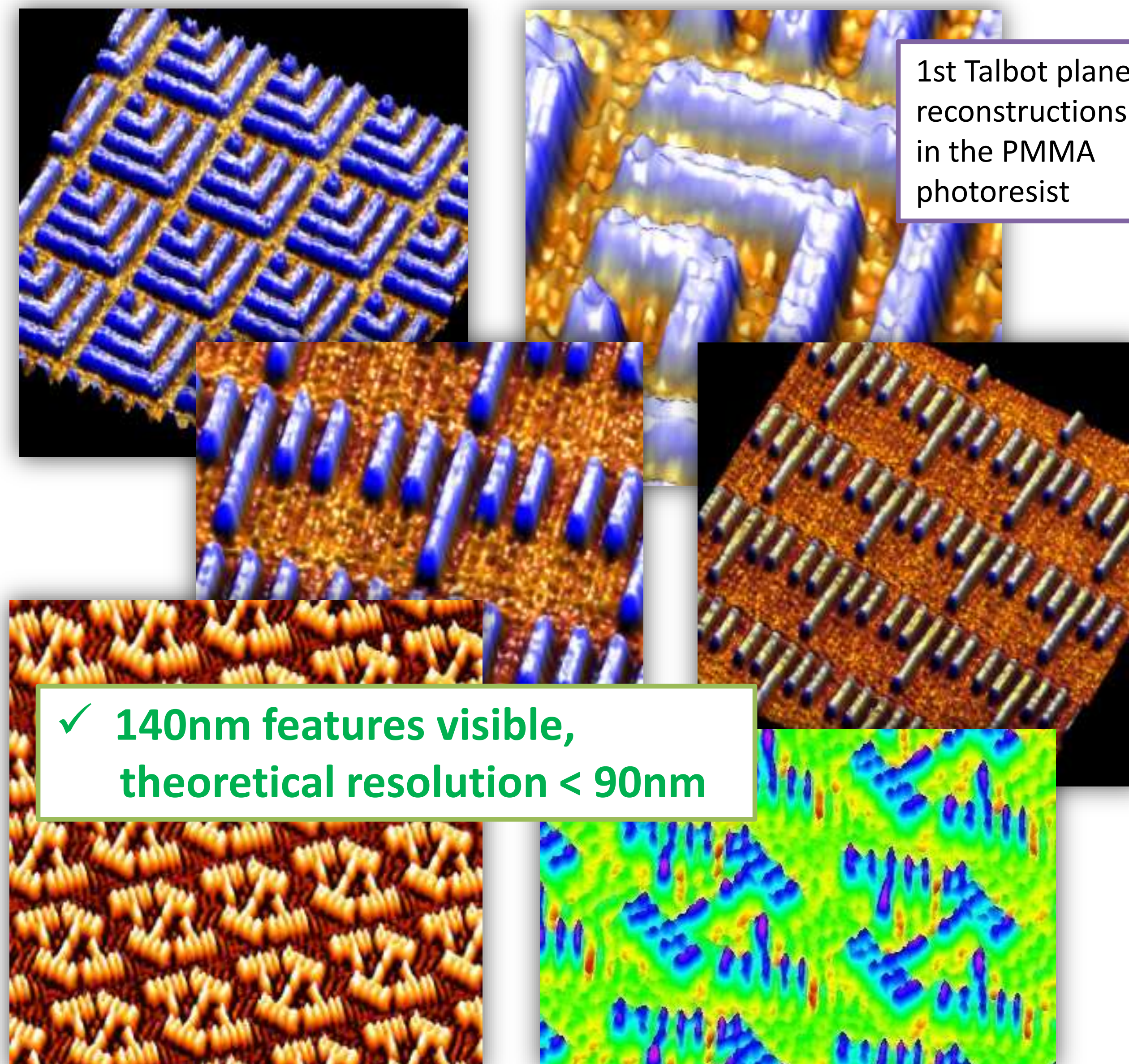

1st Talbot planes reconstructions in the PMMA photoresist

✓ **140nm features visible, theoretical resolution < 90nm**

A. Isoyan, …P. Wachulak, et al,., Journal of Vacuum Science & Technology B, 27, 6 , 2931-2937 (2009)

Different Talbot planes

Talbot image plane AFM images 20x20μm^2, z_T=1mm

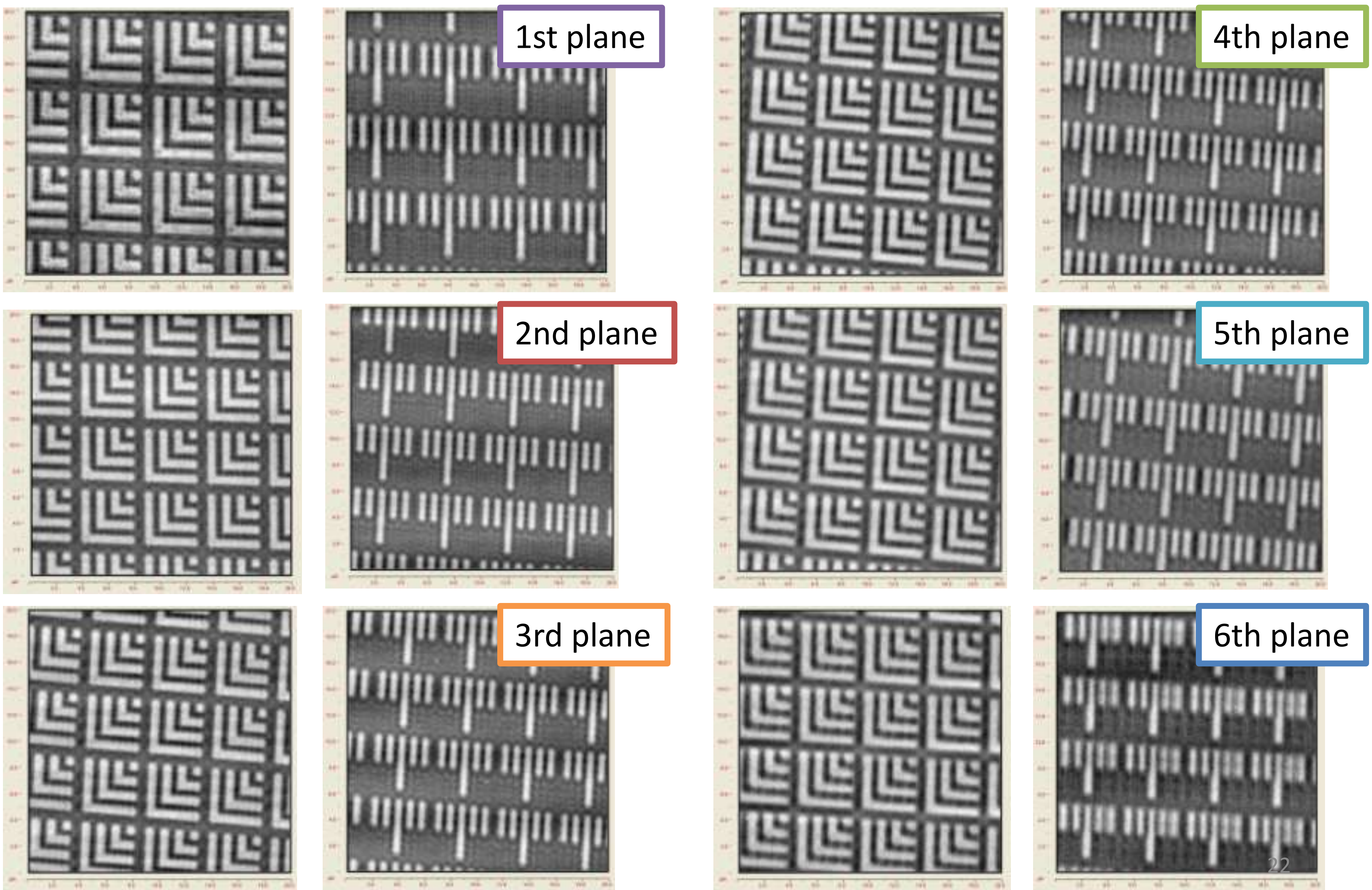

Coherent Diffractive (Lens-less) Imaging

No lens— Fourier relationship of diffraction

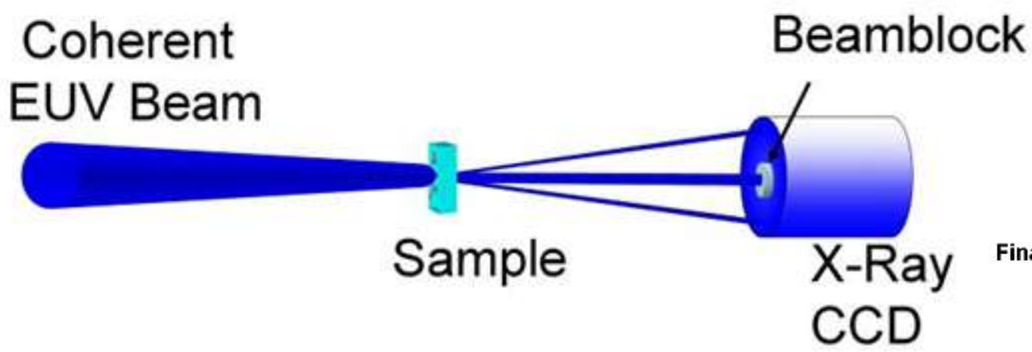

Reconstruction

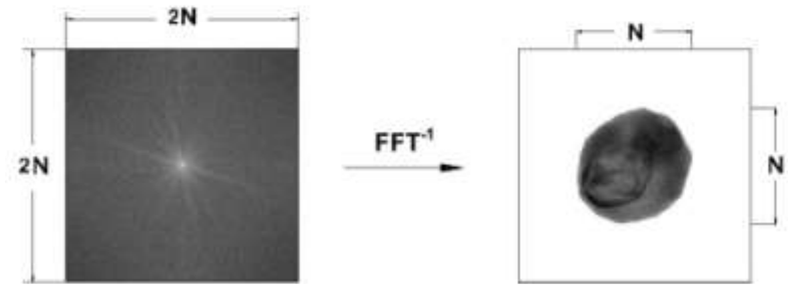

$$E(x, y, z = d) \propto \int E(x, y, z = 0) e^{-\frac{ik}{d}(xx' + yy')} dx' dy'$$

Far Field

$$z \gg \frac{D^2}{\lambda}$$

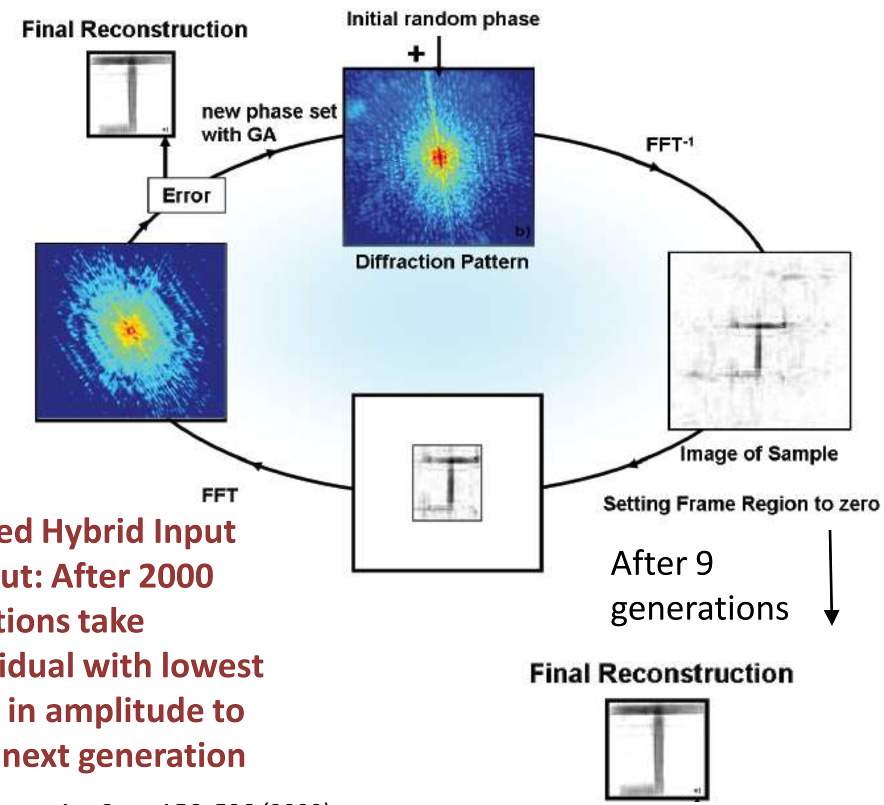

Far field diffraction is two dimensional Fourier transform of exit wave

Guided Hybrid Input Output: After 2000 iterations take individual with lowest error in amplitude to seed next generation

Peatross and Ware, Physics of Light and Optics (2008)
D. Sayre, Acta Cryst 5, 843 (1952)
J. Miao et al., Nature 400, 342 (1999)

Miao and Sayre, Act Cryst A56, 596 (2000)
C. Song et al., Phys. Rev. B 75, 012102 (2007)

Coherent Diffractive (Lens-less) Imaging code

O=4
512x512 pix

500 iteration per seed

$$|\Im\{f(-x)\}| = |\Im\{f(x)\}|$$

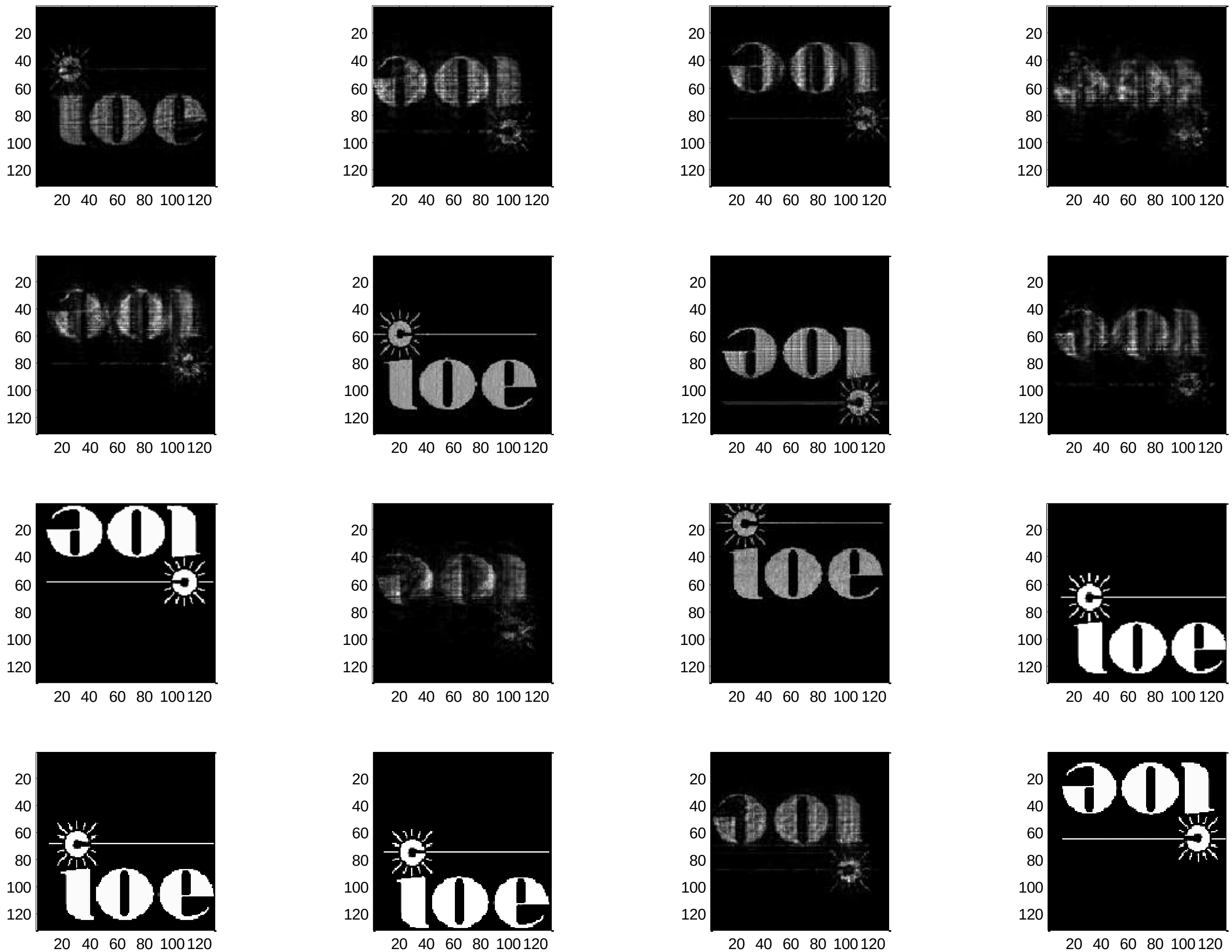

Initial, random phase seed is very important: 16 reconstructions with random phase start

Coherent Diffractive (Lens-less) Imaging code

Best reconstruction according to the rms error plot

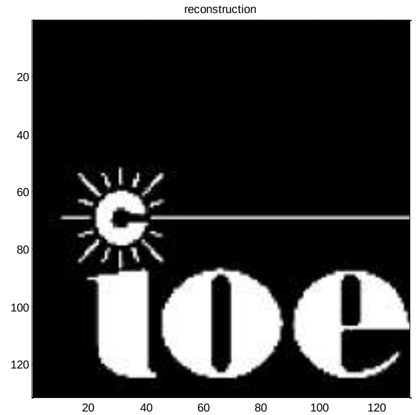

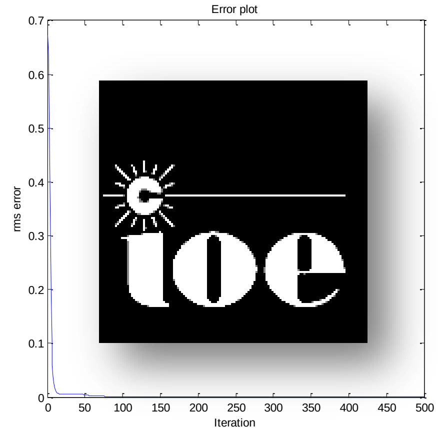

Fastest code convergence

$$Err = \frac{\int_{-\infty}^{\infty} \left[|G_k(u)| - |F(u)| \right]^2 du}{\int_{-\infty}^{\infty} |F(u)|^2 du}$$

Smaller Err -> images are more similar

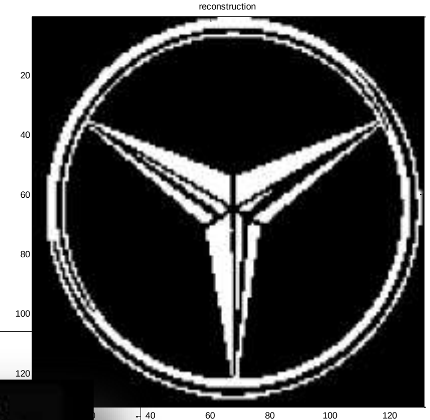

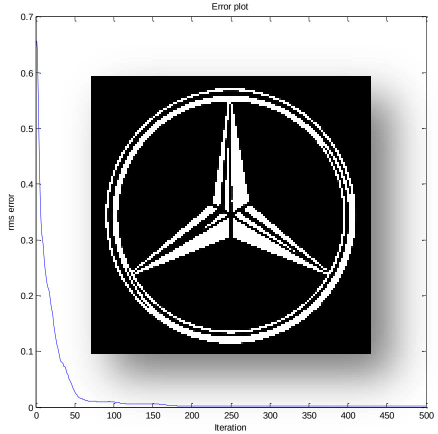

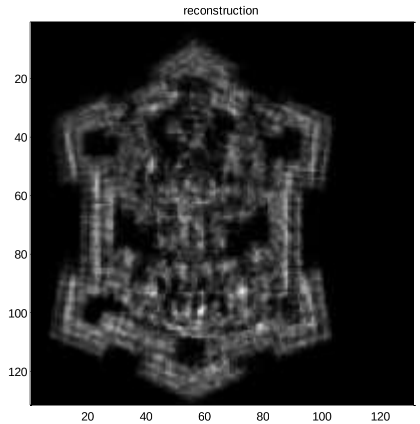

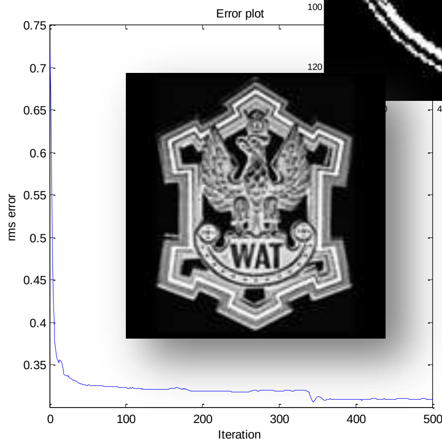

Gray-scaled images need more iterations, harder for the algorithm to converge

Lens-less, Diffraction Imaging
- Experimental Setup

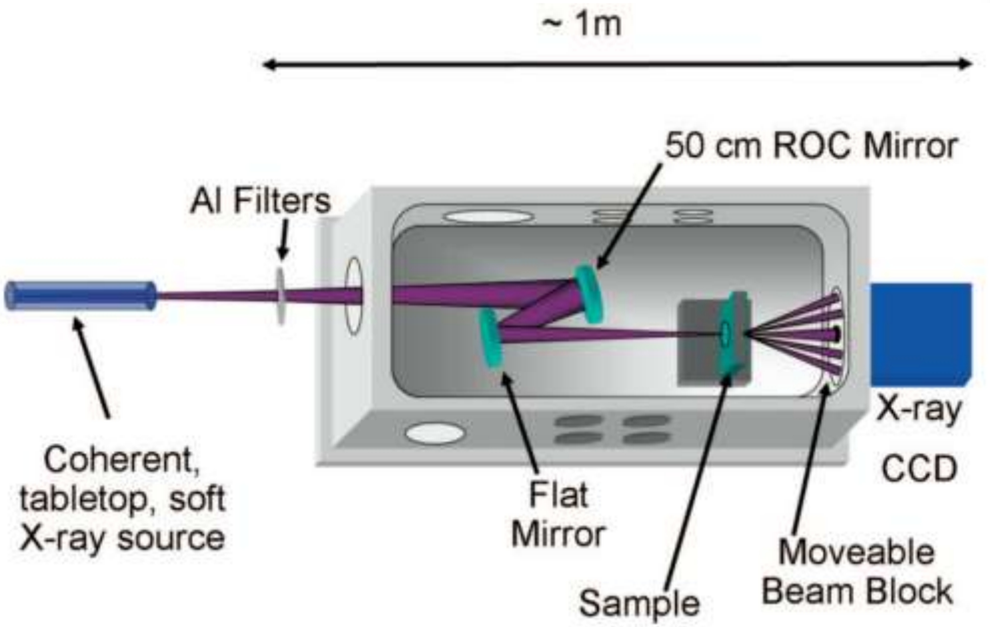

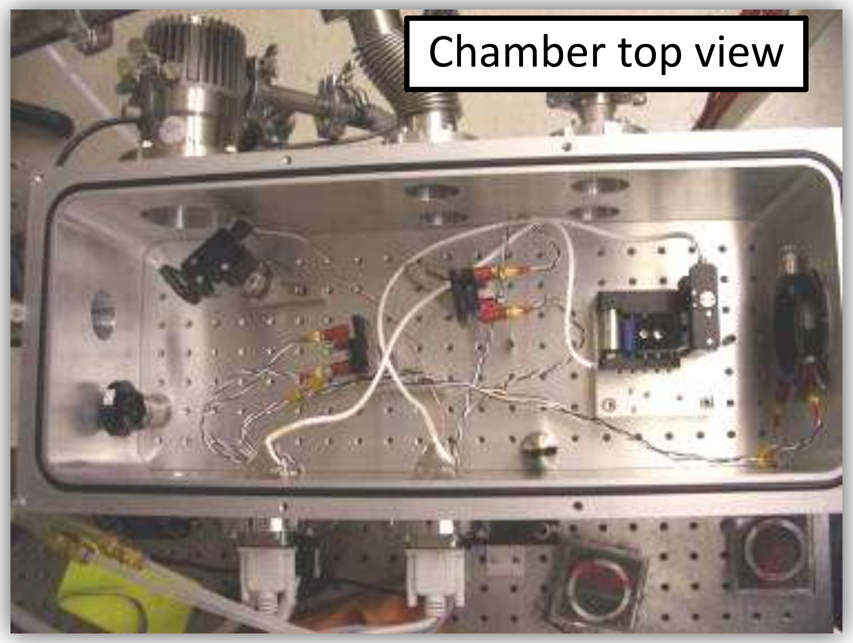

Experimental details:

Wavelength λ=46.9nm, energy per pulse = 0.2mJ, divergence half angle ~4.5mrad, $\lambda/\Delta\lambda=10^4$

Spatially filtered by 1.5mm diameter pinhole at 1.5m from the laser to improve the spatial coherence

100nm Al filter to block a visible light, two Sc/Si multilayer mirrors R~40% at λ =46.9nm

CCD camera: Andor 2048x2048 pix, p=13.5μm pixel size

Object: D= 7μm tall „stick-figure” etched in 100nm thick SiN membrane

Sample-CCD distance z= 17mm, O=8.4

NA=0.63, res.=~40nm

$$O = \frac{z\lambda}{pD}$$

EUV tabletop lens-less imaging at 72 nm resolution (λ=47 nm)

SEM Image

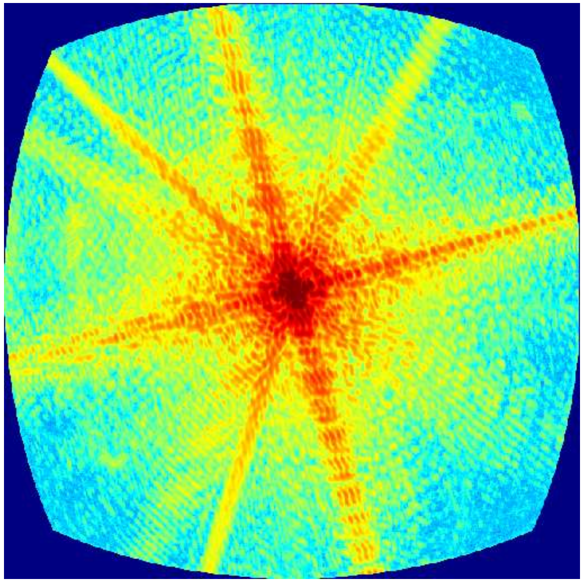

Reconstruction

K-E resolution measurements

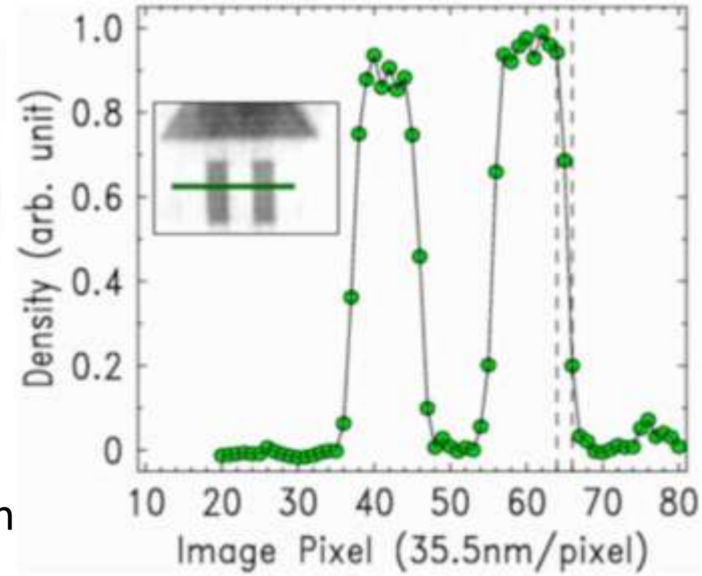

Curvatur
Diffracti

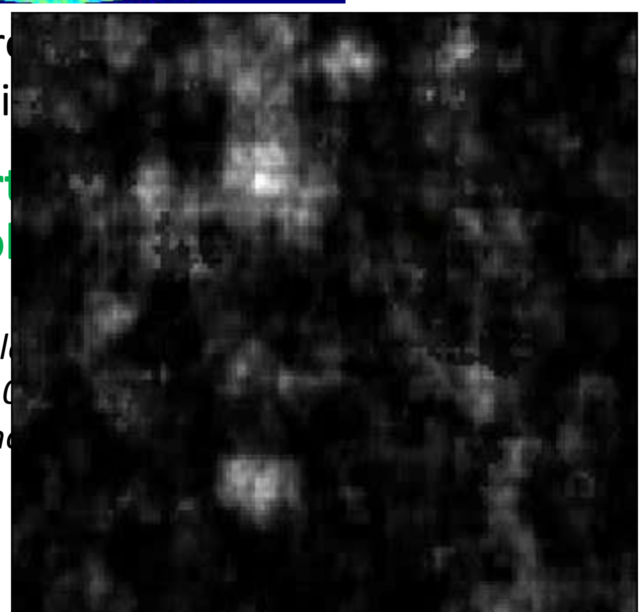

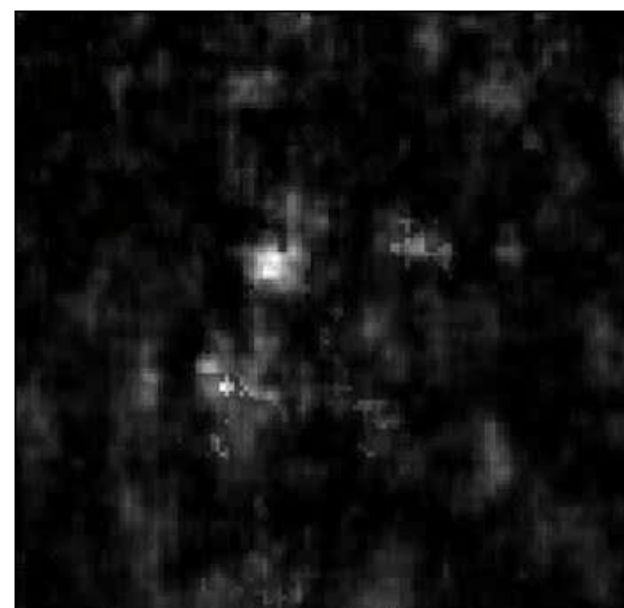

- ✓ **High numerical apert achieves 72 nm resol**

R.L. Sandberg, C. Song, P.W. Wachul the National Academy of Science, 1(and Research Highlights, Nature Ph

High-order Harmonic Generation (HHG)

typically nJ/pulse, kHz rep. rate, EUV/SXR photons
100’ as-fs time duration of each pulse

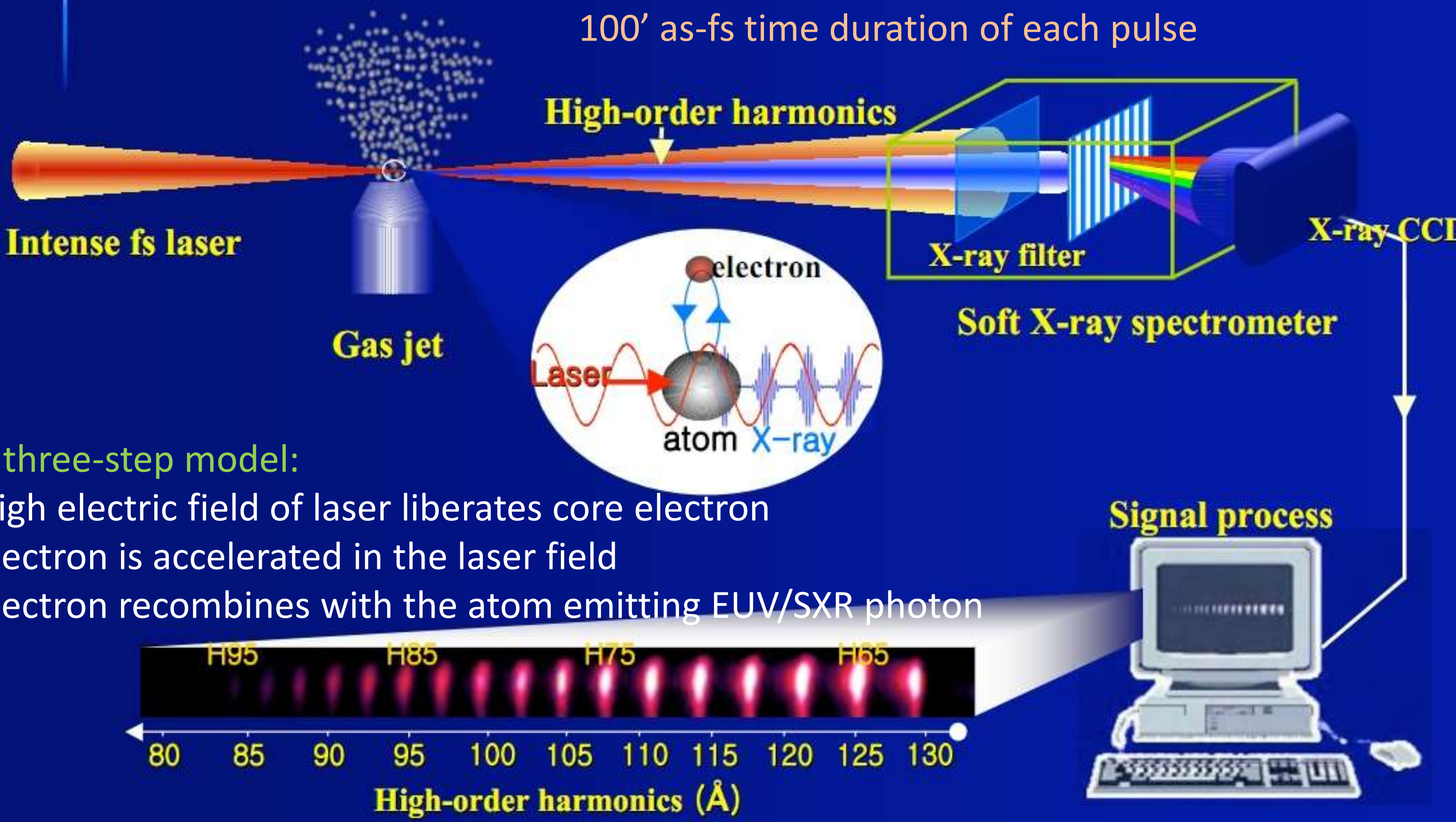

The three-step model:

1. High electric field of laser liberates core electron
2. Electron is accelerated in the laser field
3. Electron recombines with the atom emitting EUV/SXR photon

Courtesy of Professor Chang Hee Nam, KAIST University, Daejeon, Korea

22nm resolution diffraction imaging with HHG

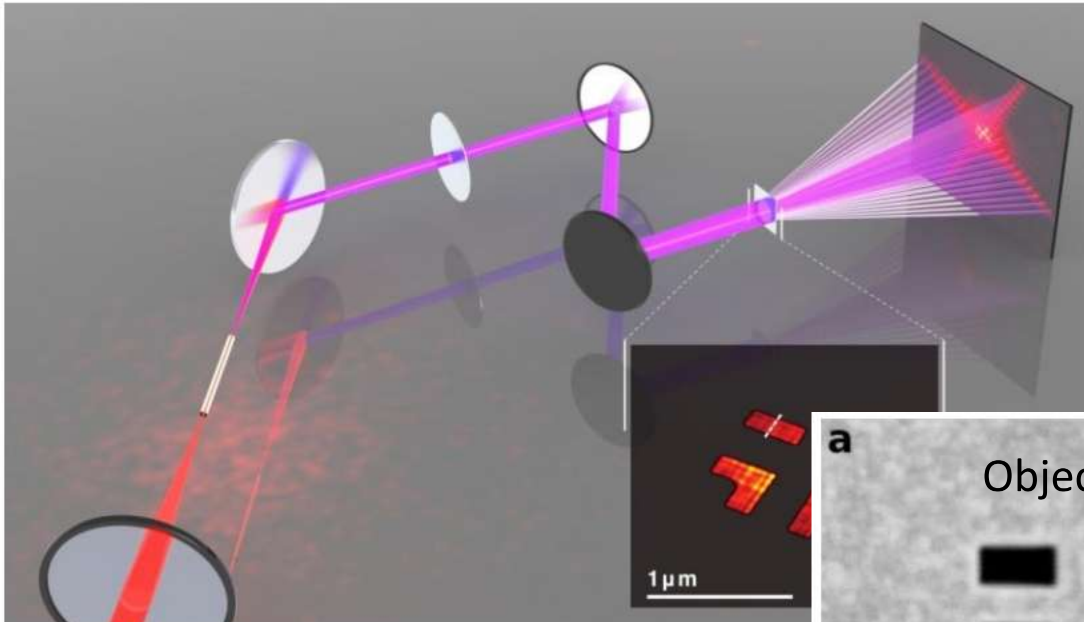

JILA science

University of Colorado Boulder

Rayleigh resolution = 22nm @ λ=13nm

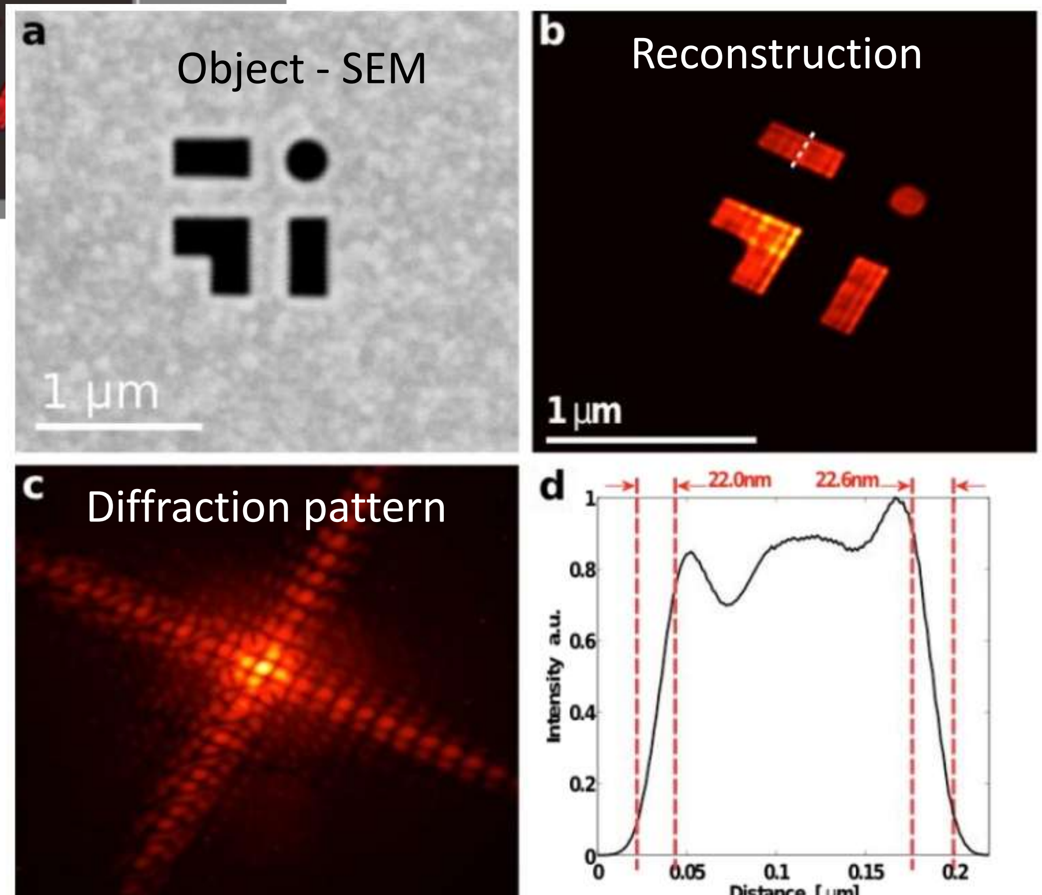

-A femtosecond laser is focused into a gas-filled waveguide.

- Bright, coherent 13 nm HHG beam is produced and focused into the sample.
- the diffraction pattern is captured on a CCD camera
- the image is retrieved using an iterative phase retrieval algorithm.

M. D. Seaberg Optics Express, 19, 23, 22470

Coherent diffraction imaging with focused hard x-rays achieves sub-10nm resolution

high-resolution coherent x-ray diffraction pattern measurements of gold/silver (Au/Ag) nanoboxes

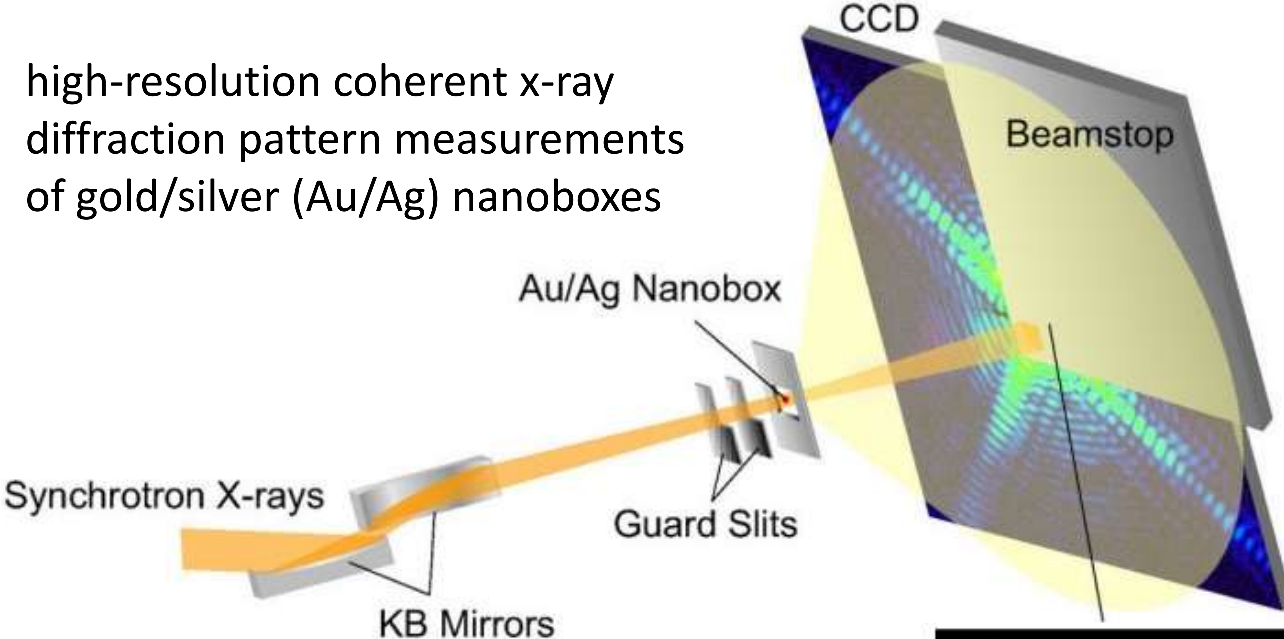

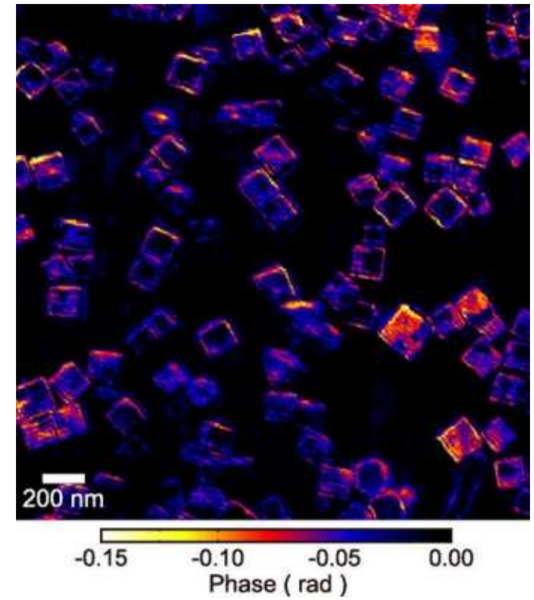

Isosurface rendering of a 3D reconstruction of a single Au/Ag nanobox viewed from two directions, showing small pits (blue arrows) and a depression (green arrow)

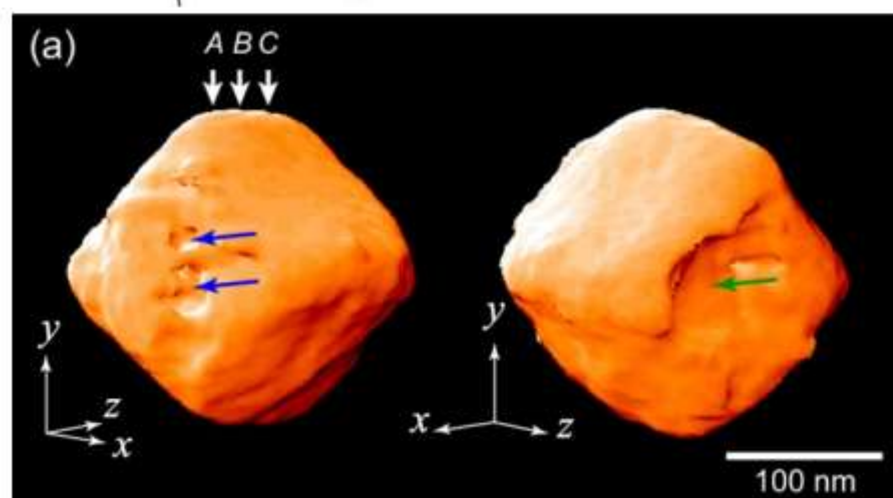

Yukio Takahashi, SPIE Newsroom, 10.1117/2.1201309.005099

Femtosecond diffractive imaging with a soft-X-ray free-electron laser

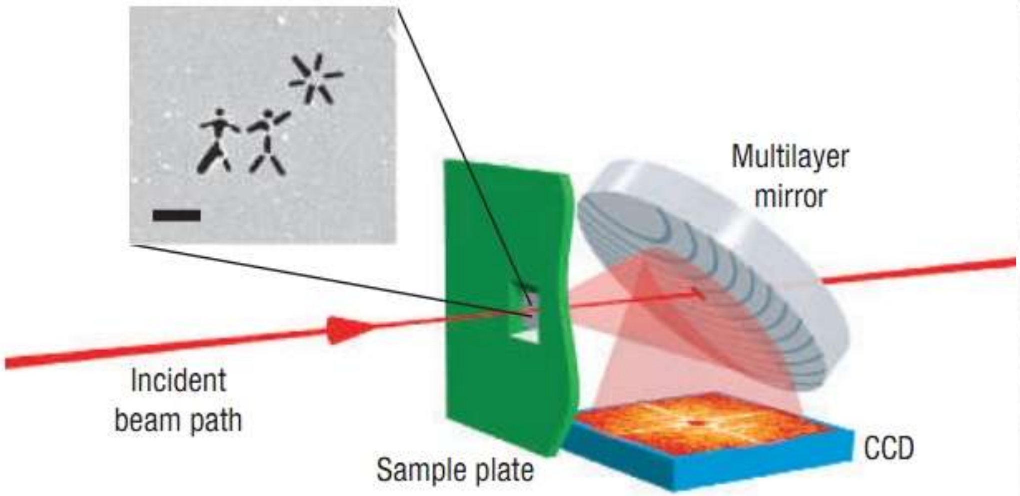

Schematic diagram of the experimental apparatus

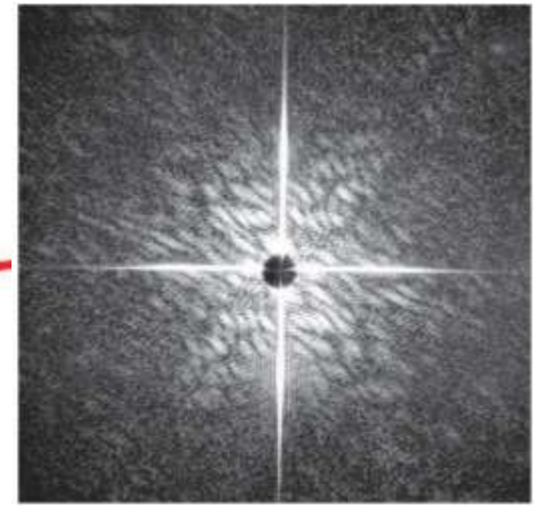

Coherent diffraction pattern recorded for a single $(4\pm2)\times10^{14}$ Wcm^{-2},25±5 fs pulse

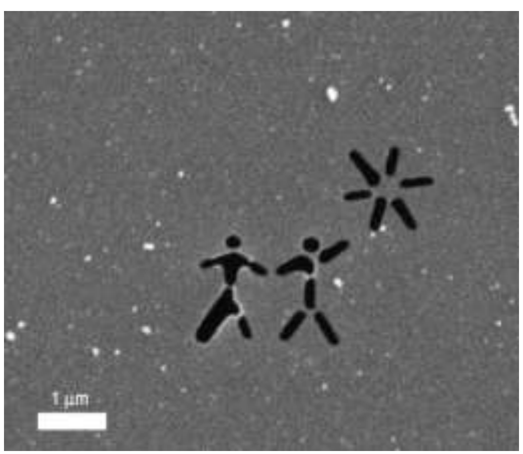

SEM image of the sample before exposure to the FEL beam

Image reconstructed, from the ultrafast coherent diffraction pattern

Resolution ~62nm
@ λ=32nm

H. N. Chapman et al., Nature Physics, 2, 839 (2006)

Ptychography – High resolution Scanning Diffraction Microscopy

ptychographic imaging method bridges the gap between CDI and STXM by measuring a set of diffraction patterns at each point of a STXM scan.

Advantages:
-Very high resolution (for HXR ~10-20nm) for test samples. Resolution limited by geometry,
- lack of optics allows for such high resolution
- contrast for phase samples

Disadvantages:
- Challenging to reconstruct

scheme

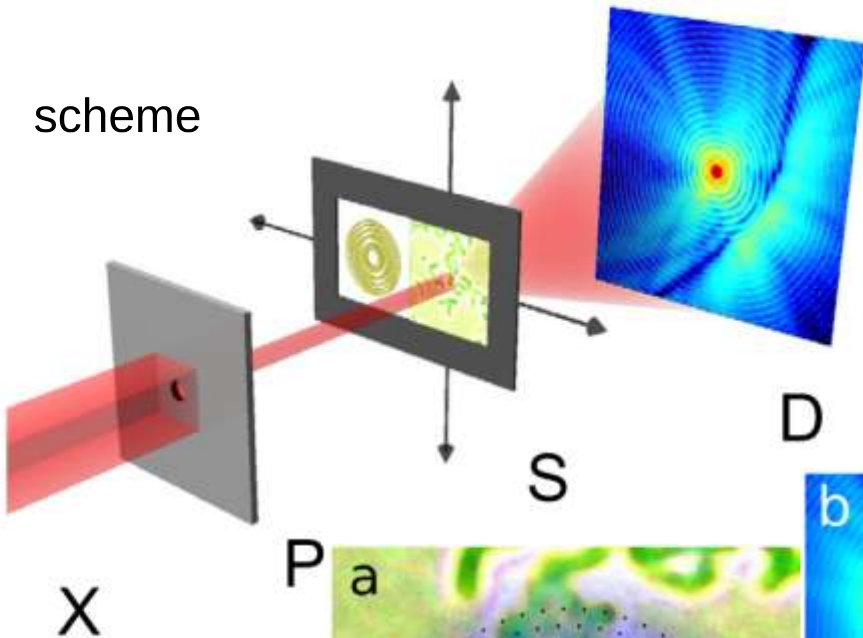

Typical scanning positions

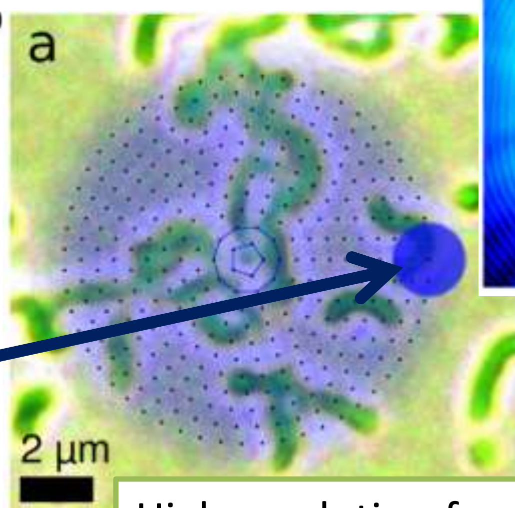

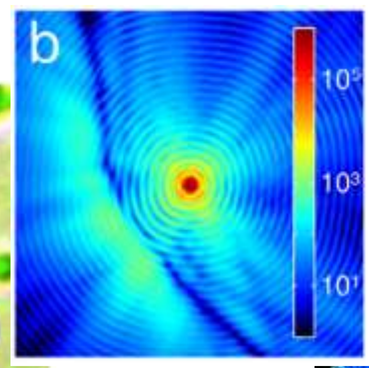

X-ray sopt much larger than resolution

High resolution from heavily dversampled set of data

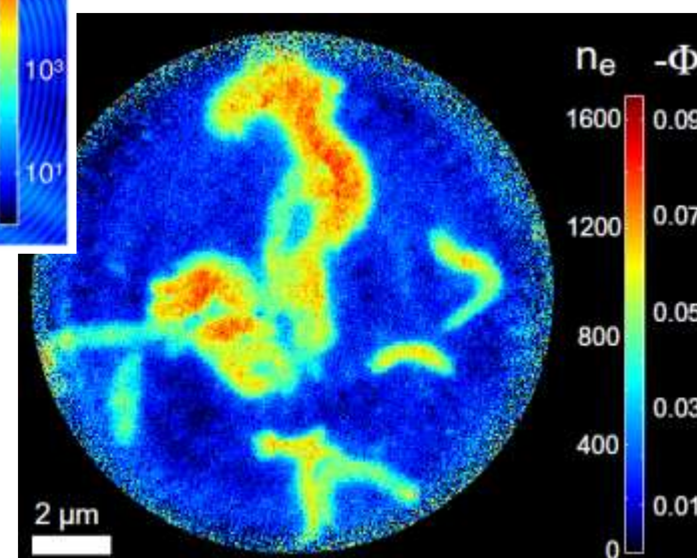

Martin Dierolf *et al. New J. Phys.* **12,** 035017 (2010)

Reconstruction results

X-ray ptychographic computed tomography at 16 nm isotropic 3D resolution

scheme

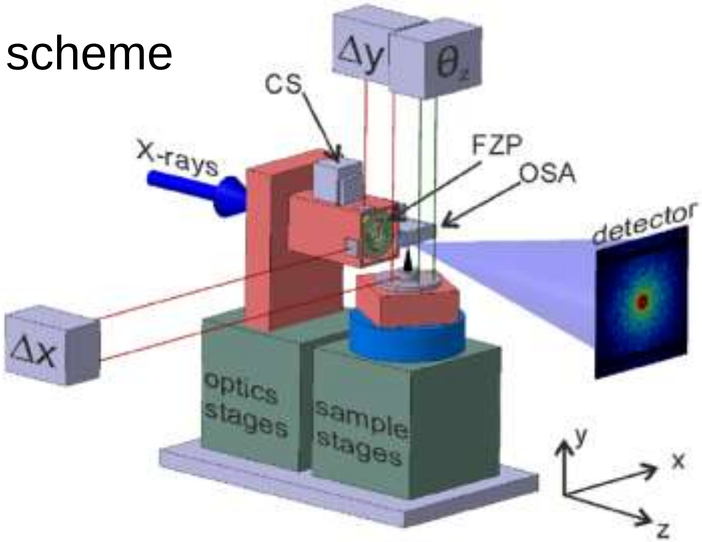

Test pattern

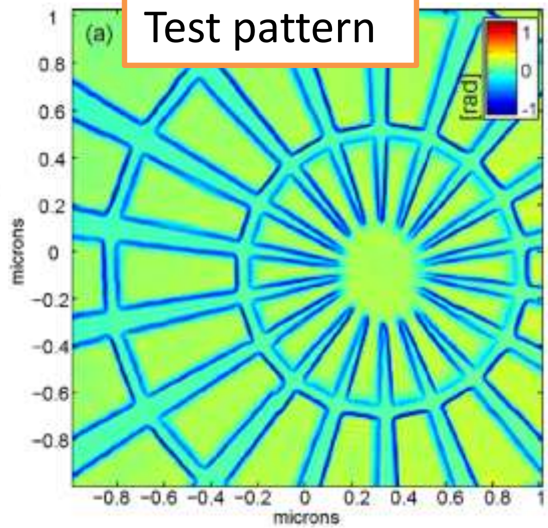

Part of 3-D reconstr.

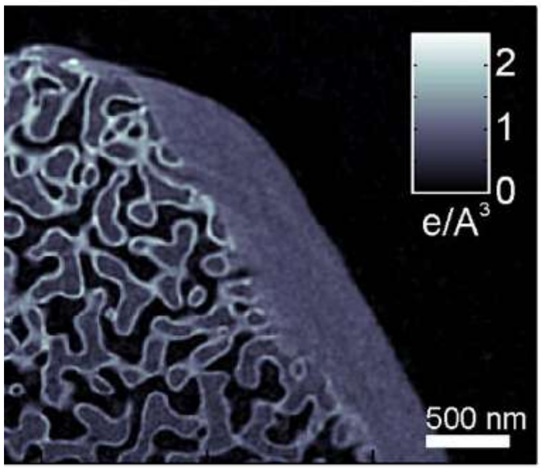

Holler et al., Scientific Reports, 4, 3857 (2014)

scheme

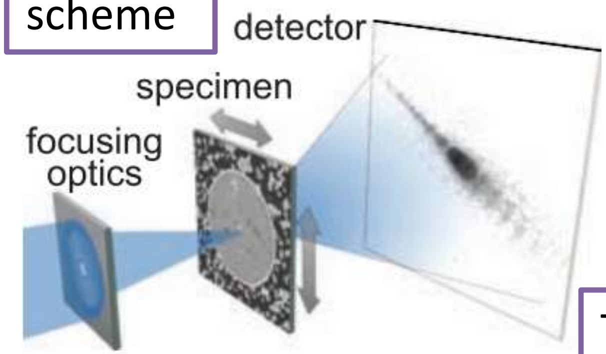

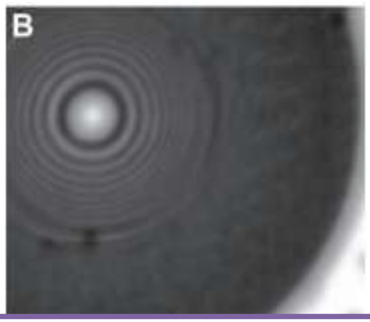

Transmission image

FZP
dr=70nm

Ptychography image

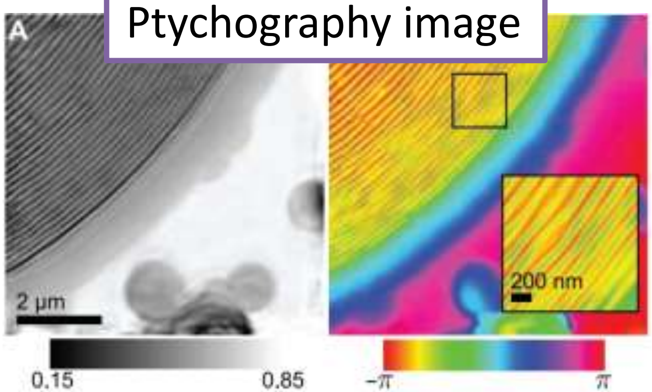

Thibault et al., Science **321**, 5887, 379-382 (2008)

Algorithms:

- „ePIE" (Maiden and Rodenburg, Ultramicroscopy 109, 1256 (2009)
- Difference Map (Thibault et al., Science 321, 379 (2008)
- Conjugate gradient (Guizar-Sicairos et al., Opt. Expr. 16, 7264 (2008)

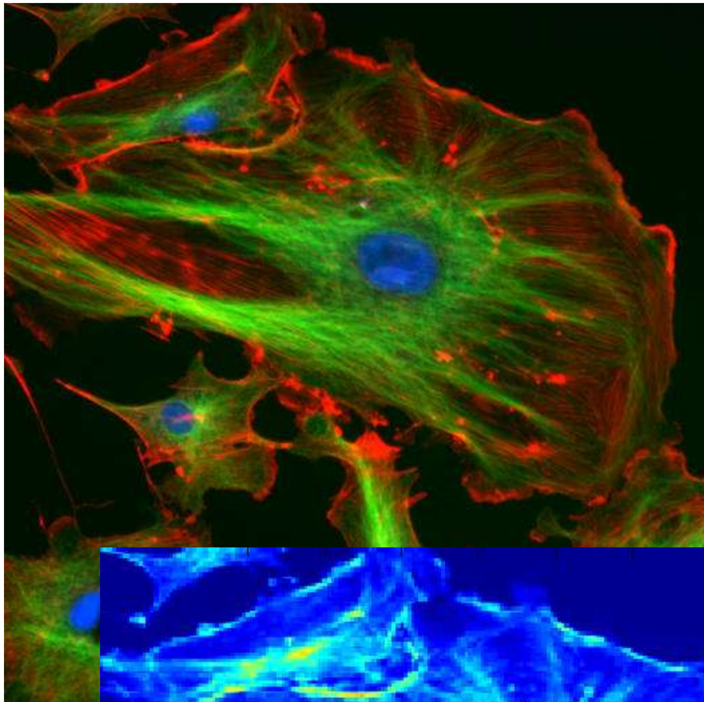

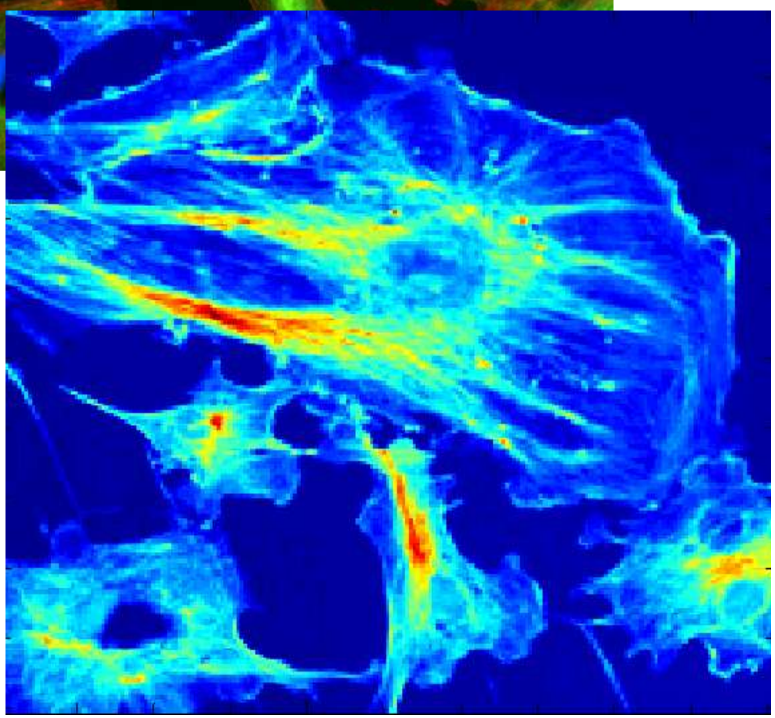

e-PIE algorithm

Diff patterns on a 6x6 grid, beam size D=80 pix, 8 iterations.

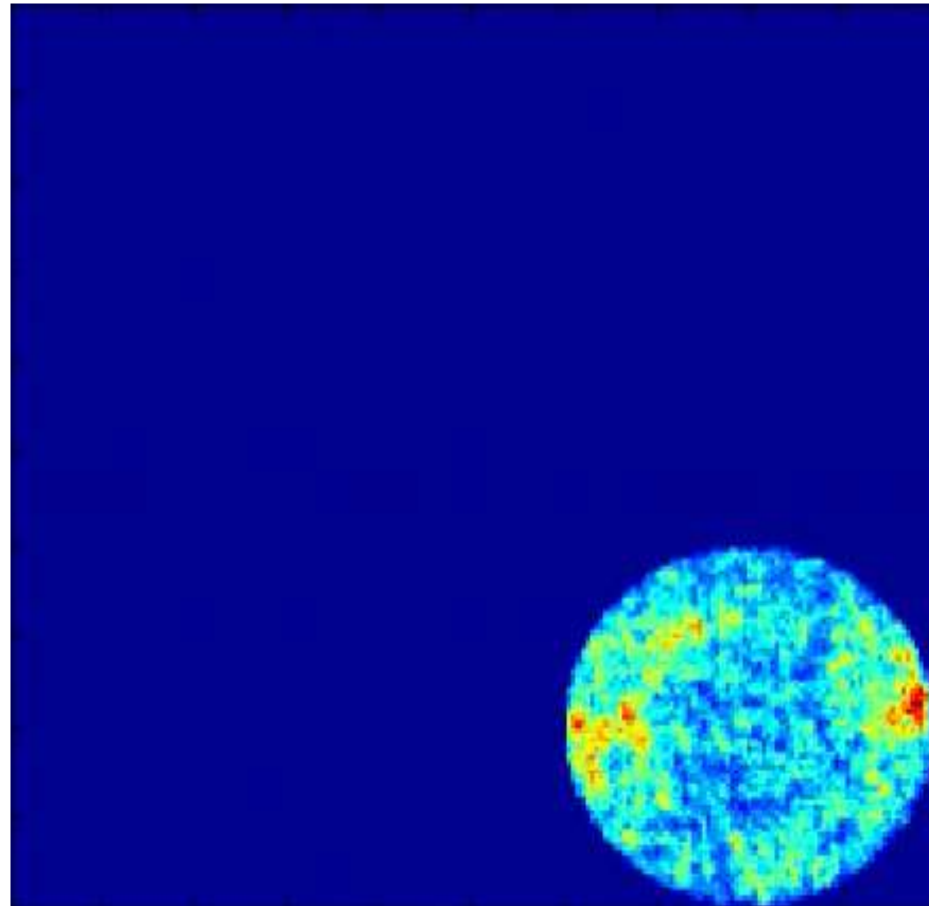

Hard X-ray imaging of bacterial cells using ptychography

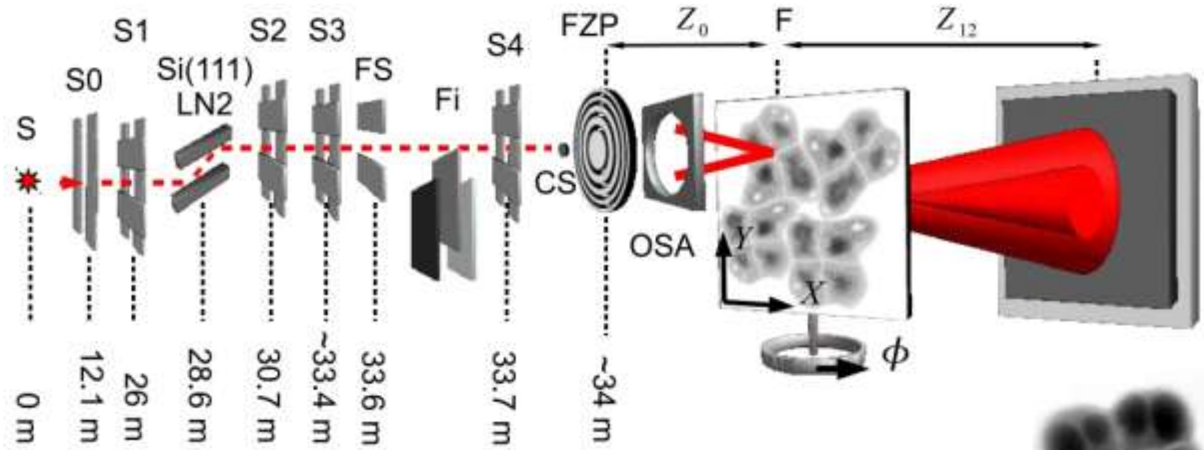

PAUL SCHERRER INSTITUT

cSAXS - X12SA:
Coherent Small-Angle X-ray Scattering Beamline

Probe size: 0.75x1.5um^2
Spatial resolution ~90nm @ 6.2keV
Au on Si_3N_4 FZP, dr=100nm

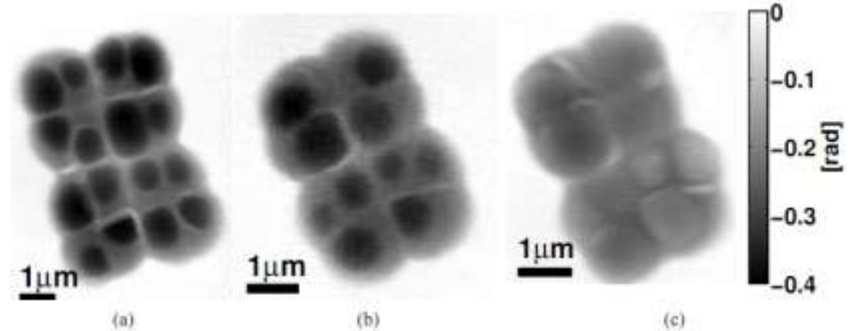

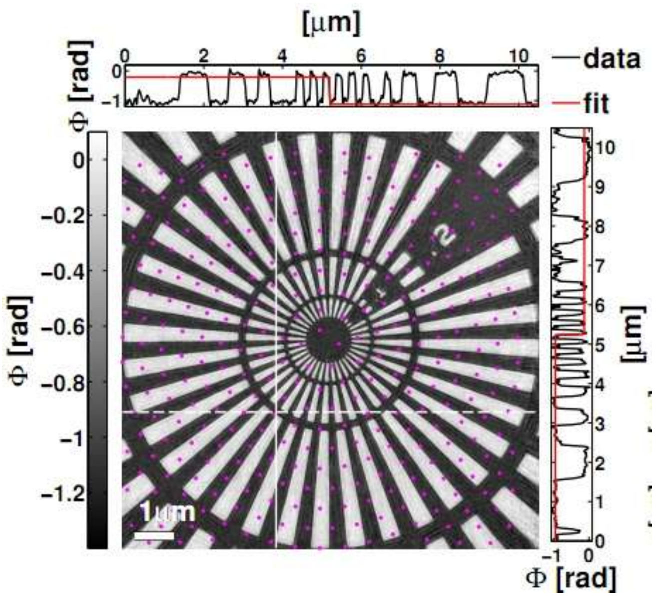

Phase reconstructions of D. radiodurans

- Multiple diffraction patterns enhance **resolution beyond the probe size**

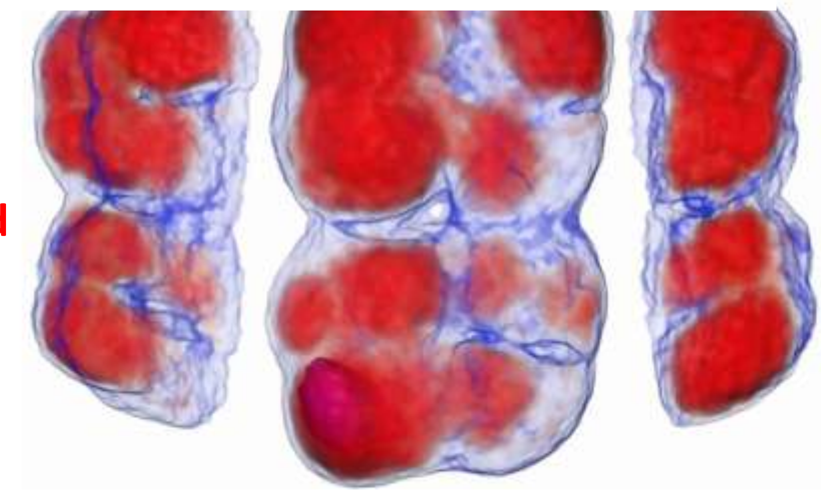

R. N. Wilke, et al., Optics Express 20,17, 19232 (2012)

Zone plates

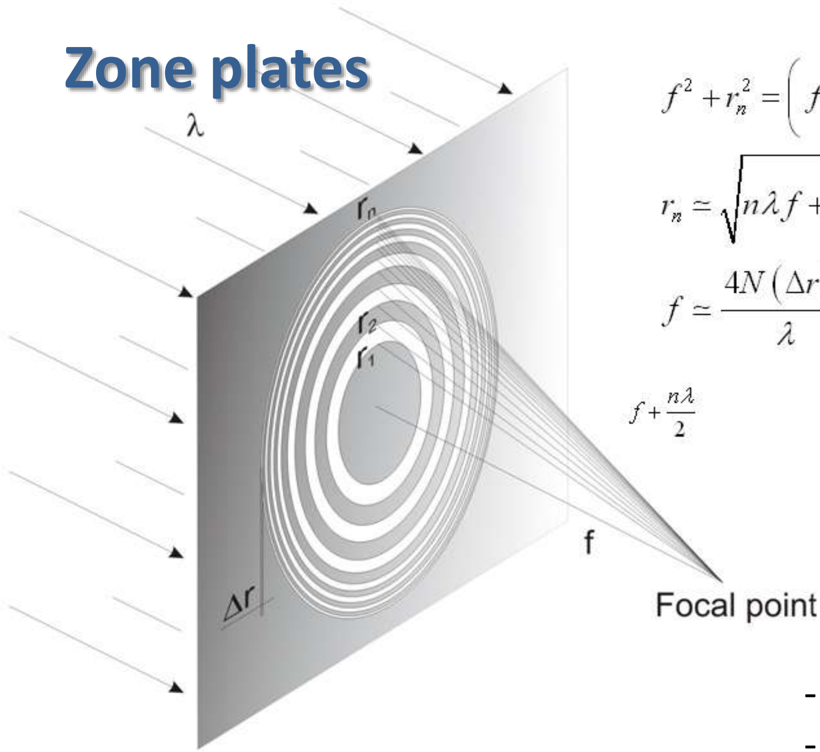

$$f^2 + r_n^2 = \left(f + \frac{n\lambda}{2}\right)^2$$

$$r_n \simeq \sqrt{n\lambda f + \frac{n^2\lambda^2}{4}}$$

$$f \simeq \frac{4N(\Delta r)^2}{\lambda}$$

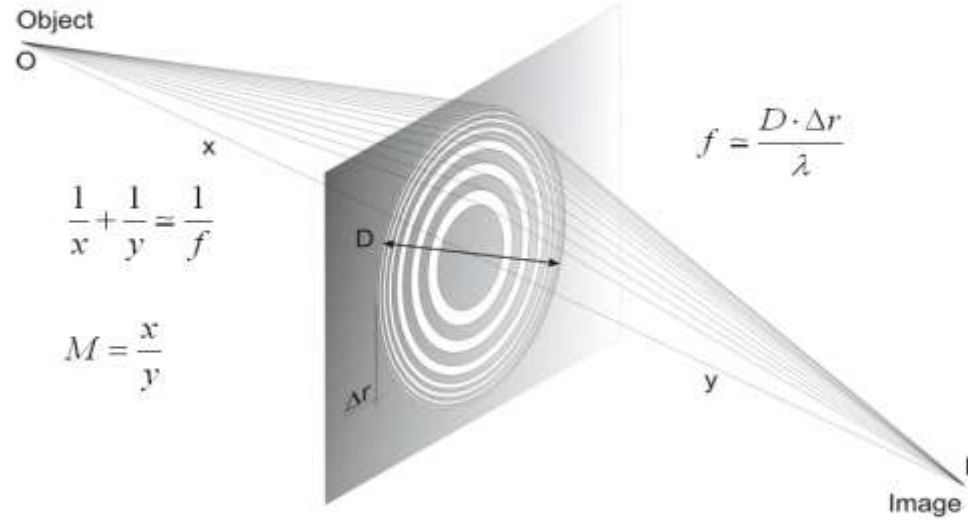

$$\frac{1}{x} + \frac{1}{y} = \frac{1}{f}$$

$$M = \frac{x}{y}$$

$$f = \frac{D \cdot \Delta r}{\lambda}$$

- use diffraction of light
- highly chromatic devices
- used typically to focus light and in the imaging scheme
- very small, thin and fragile

MATLAB + Image J

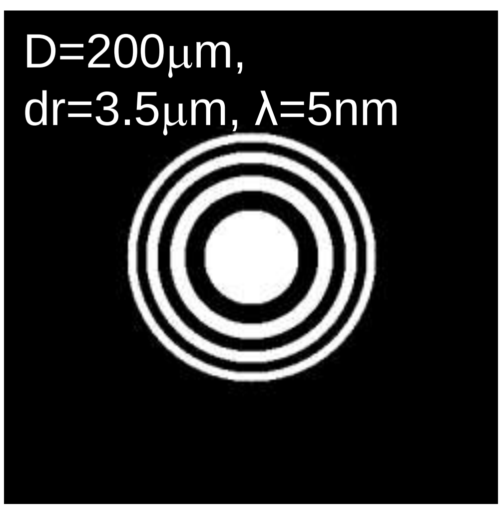

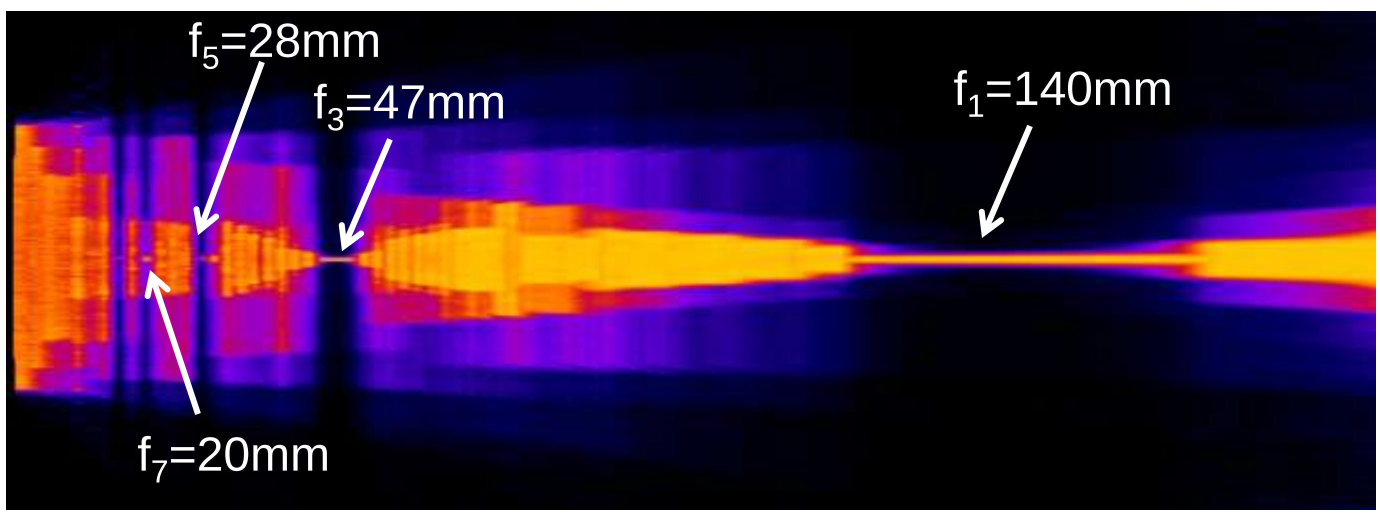

Various Zone Plates

Free standing

www.cxro.lbl.gov

orthogonal linear ZP -
orthogonal Fresnel array

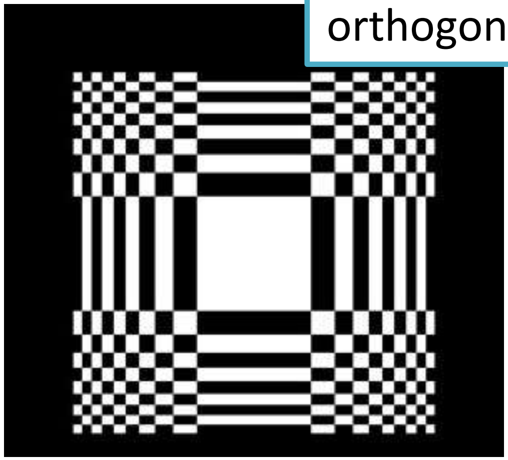

http://bonryu.com/atelier_bonryu_e/ZP_Salon_5.html

J. Metje, et al., Optics Express 22, 9, 10747-10760 (2014)

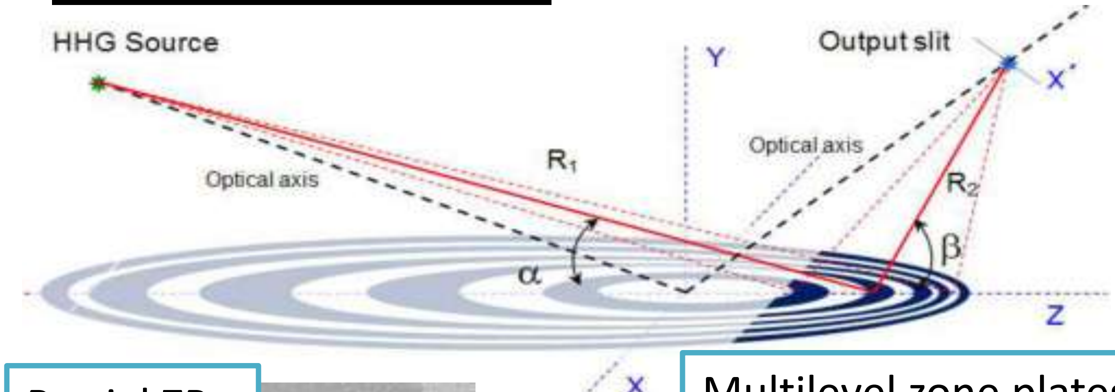

Photon Sieve

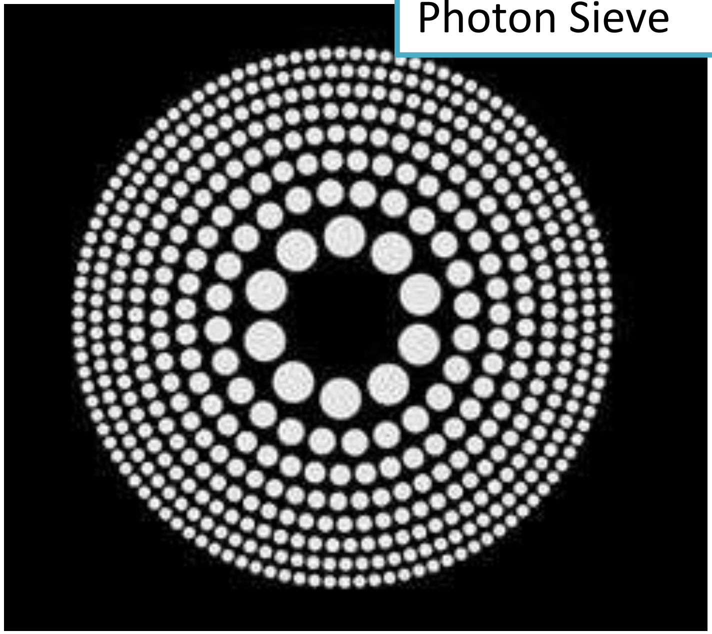

http://www.oocities.org/penate@rogers.com/sieve/photonsieve.html

Partial ZP

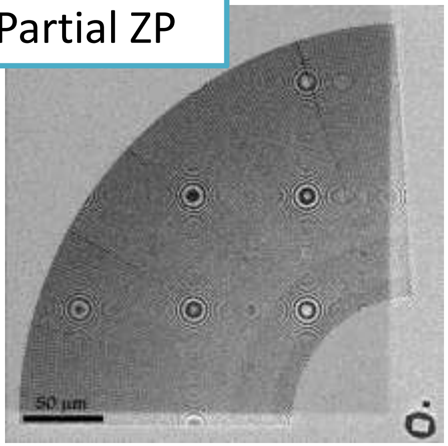

www.zoneplates.ltd

Multilevel zone plates

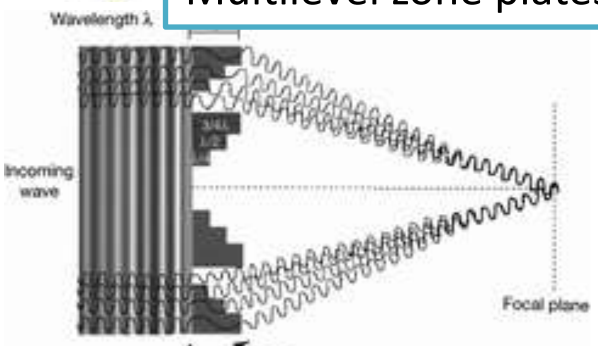

E. Di Fabrizio et al., Nature 401, 895-898,1999

Zone plates
- Fabrication for 46.9nm

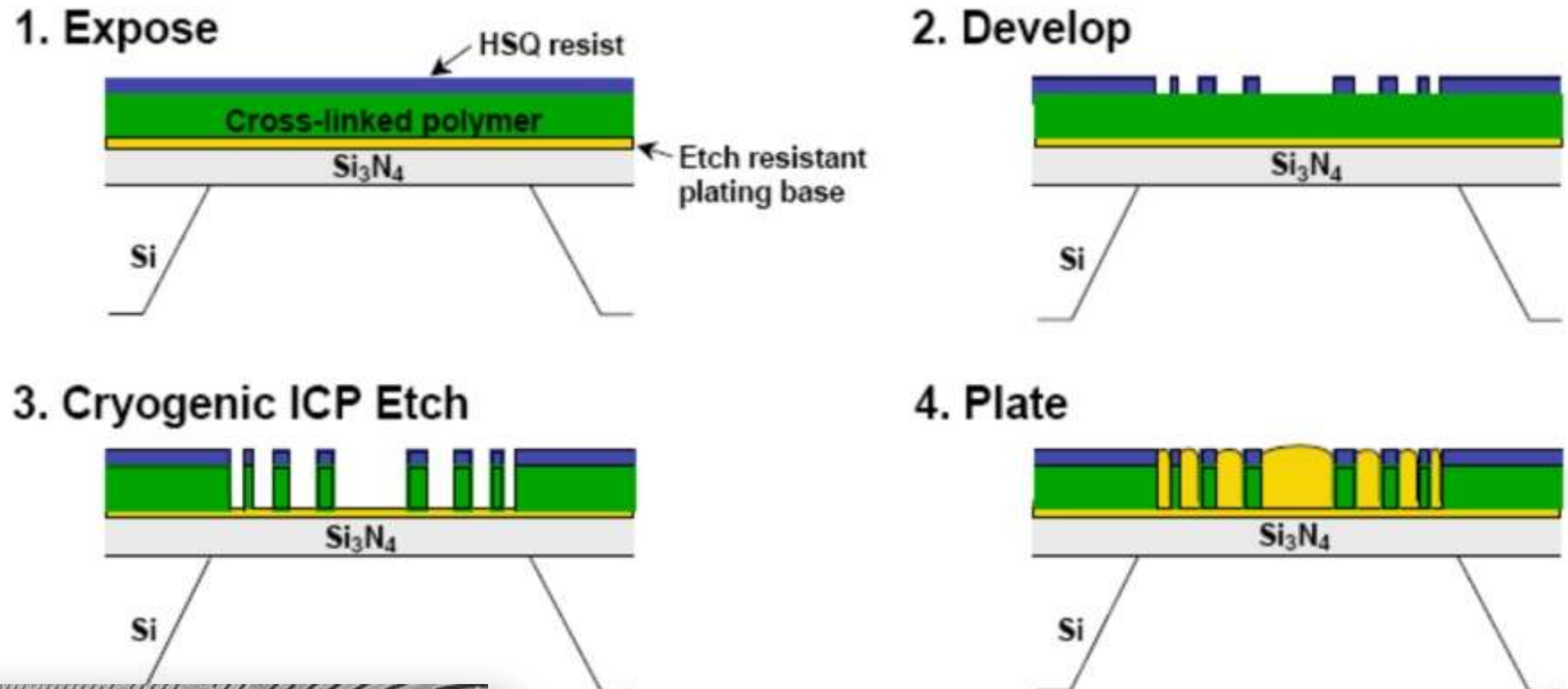

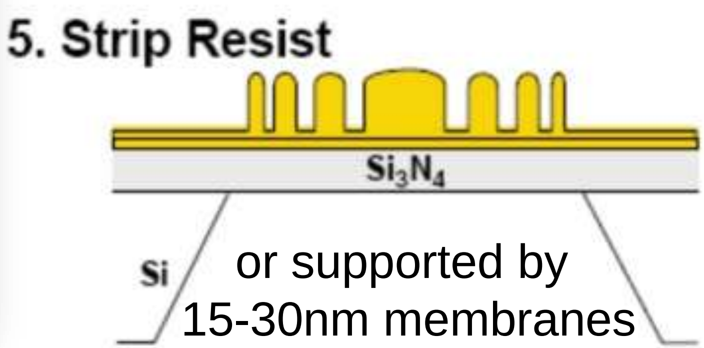

or supported by
15-30nm membranes

E. H. Anderson, IEEE JQE ***42****, 27 (2006)*

Free-standing design

Zone plates for λ=13.8nm

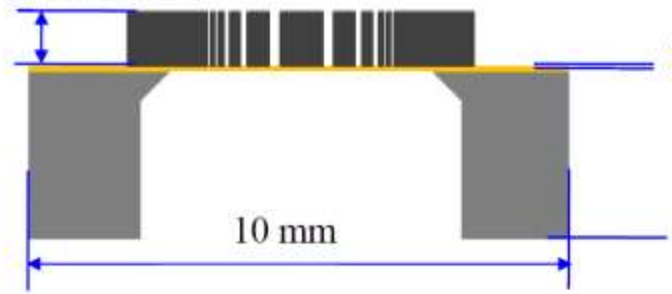

나노종합팹센터
NATIONAL NANOFAB CENTER

$$r_n^2 = n\lambda f + \frac{n^2\lambda^2}{4}$$

$$NA \ll 1$$

$$r_n \simeq \sqrt{n\lambda f}$$

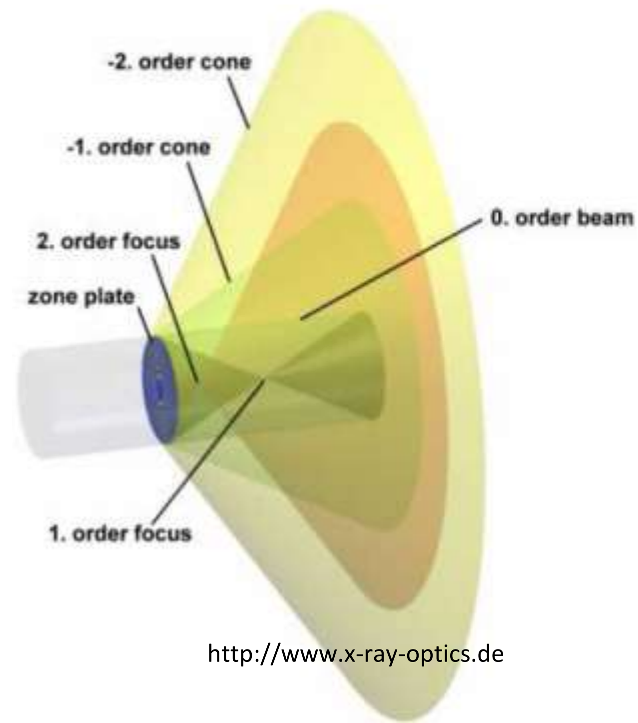

http://www.x-ray-optics.de

Dr. H. T. Kim and
Dr. S. Ch. Jeon
Korea

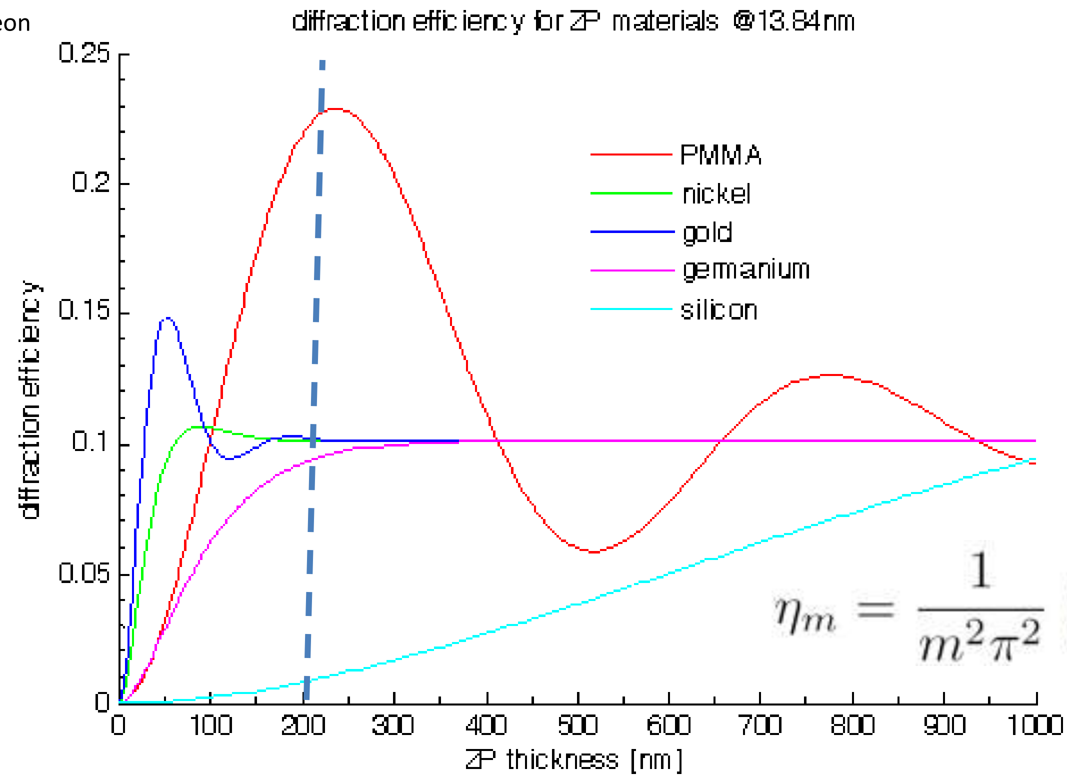

$$\eta_m = \frac{1}{m^2\pi^2}\left(1 + e^{-2\phi\beta/\delta} - 2e^{-\phi\beta/\delta}\cos\phi\right)$$

$$\phi = 2\pi t\delta/\lambda$$

J. Kirz, ***JOSA 64, 301 (1974)***

Zone plates for „water window”

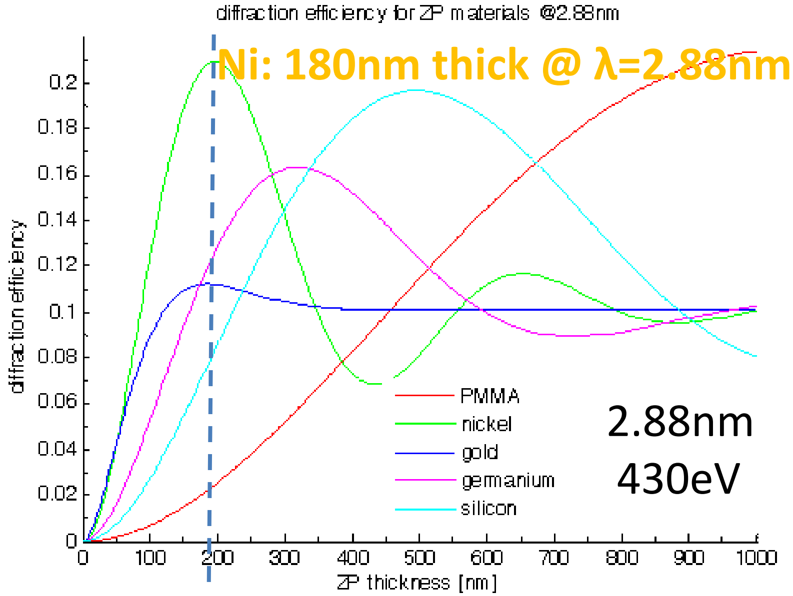

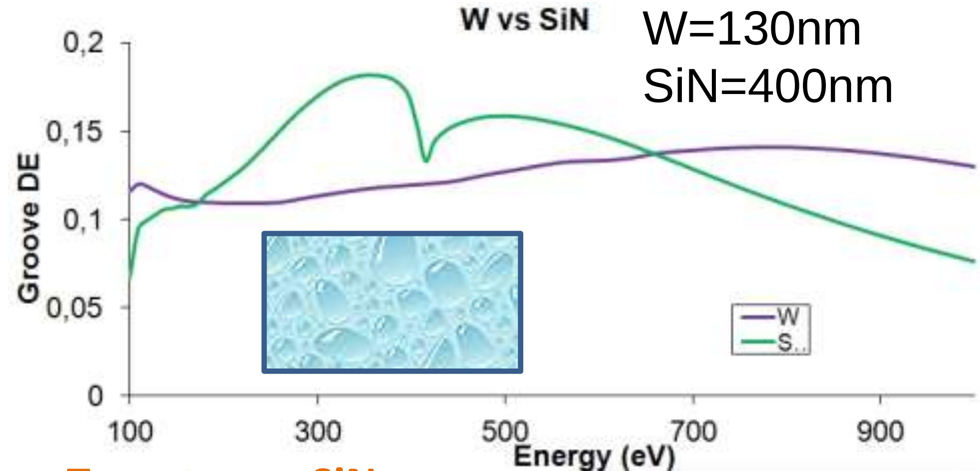

Thickness:
W=130nm
SiN=400nm

Tungsten or SiN

http://www.zoneplates.com/index.html

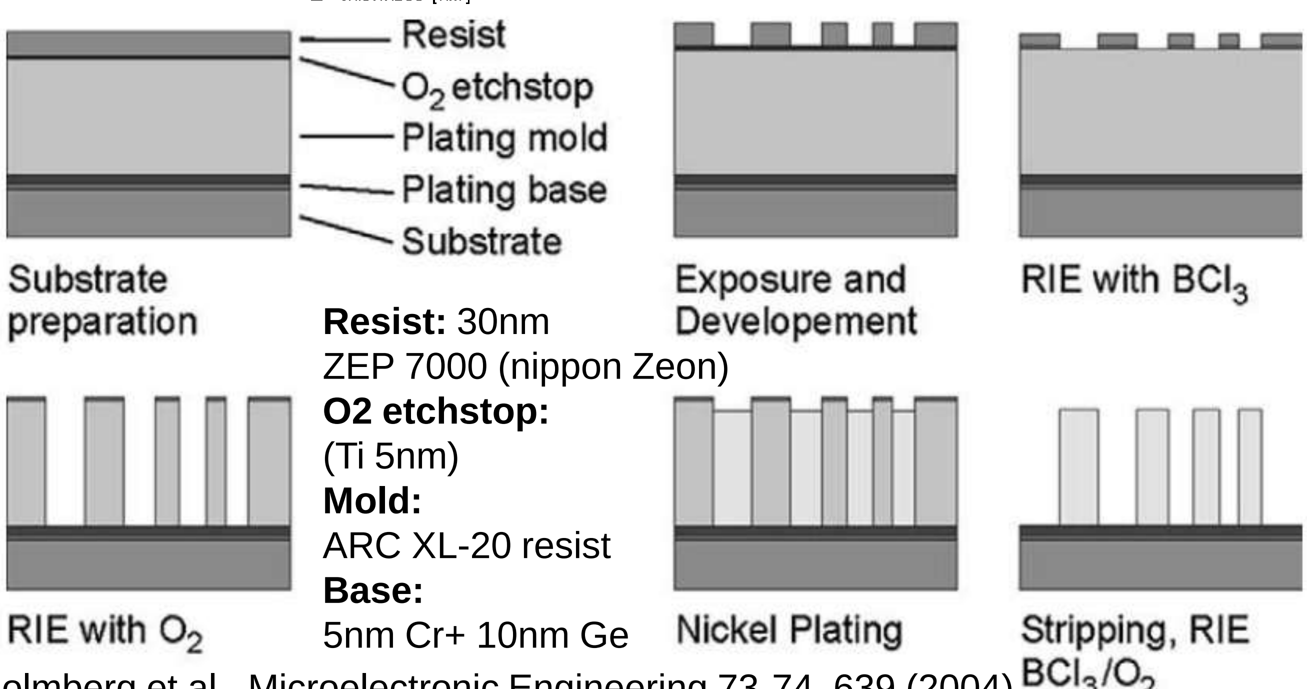

Resist: 30nm
ZEP 7000 (nippon Zeon)
O2 etchstop:
(Ti 5nm)
Mold:
ARC XL-20 resist
Base:
5nm Cr+ 10nm Ge

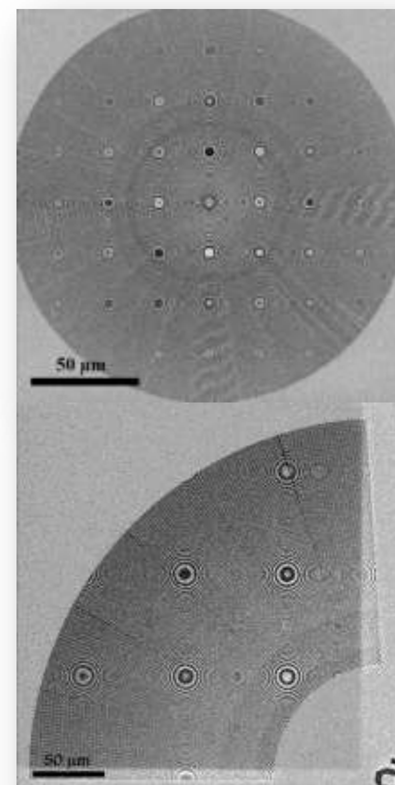

A. Holmberg et al., Microelectronic Engineering 73-74, 639 (2004)

Desktop-size capillary discharge λ=46.9 nm EUV laser

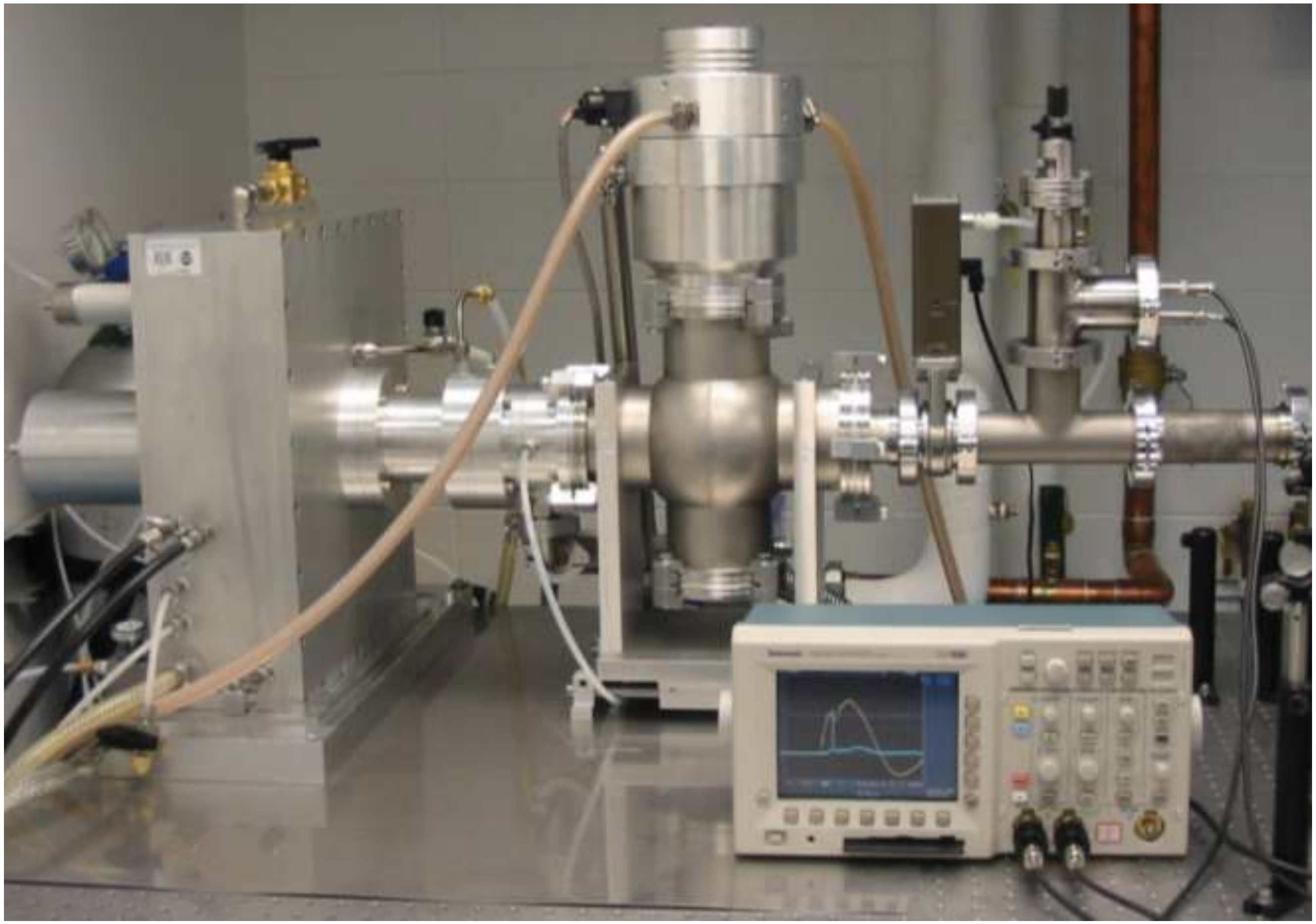

Laser Output Characteristics:

- Output Energy: > 10 µJ/pulse
- Average power: 0.15 mW
- Repetition rate: up to 12 Hz
- Pulse duration: ~1.5 ns
- Bandwidth: $\Delta\lambda/\lambda < 1 \times 10^{-4}$

S. Heinbuch , et al., Opt. Exp. 13, 4050 (2005)

Courtesy of Courtney Brewer, Colorado State University

Single-shot EUV laser imaging of nanostructures with wavelength resolution

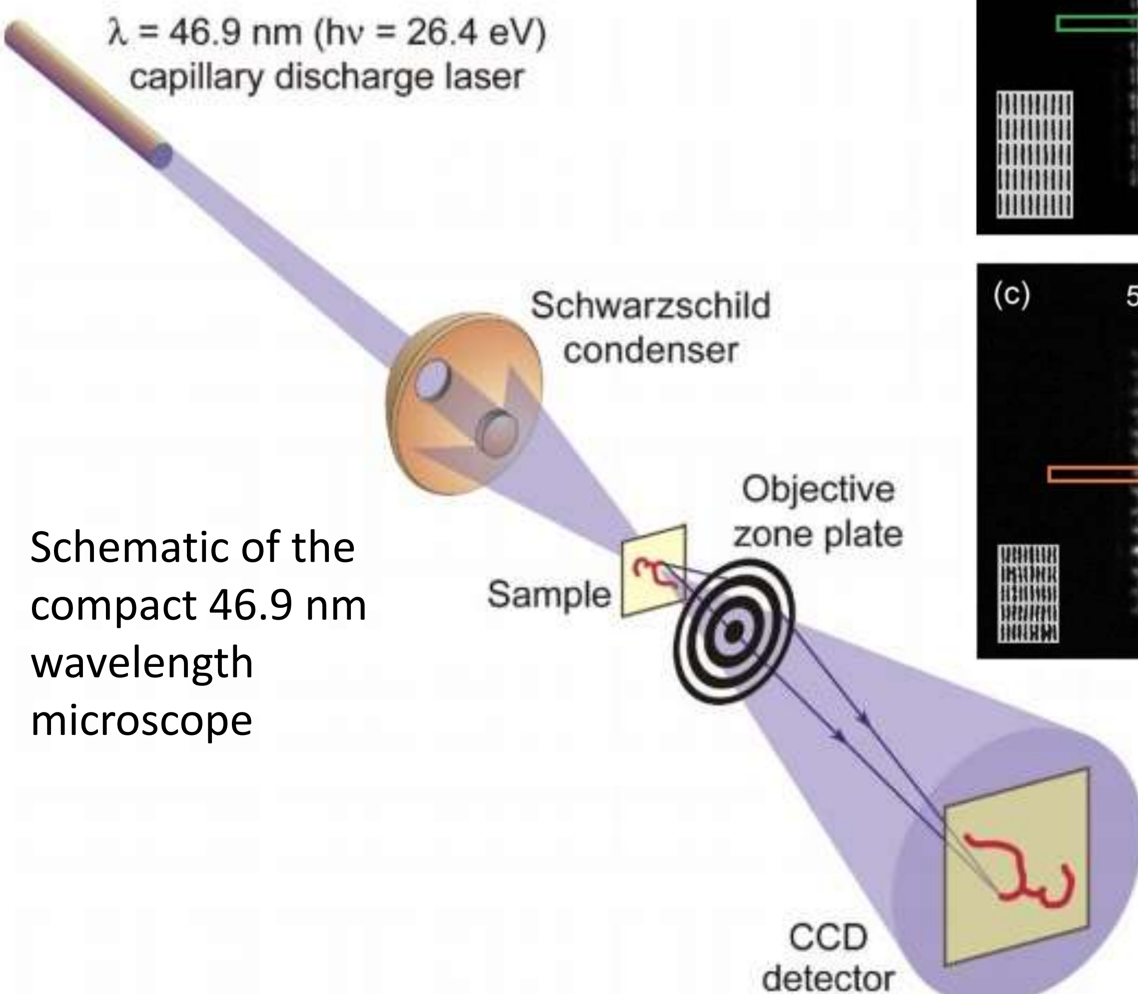

Schematic of the compact 46.9 nm wavelength microscope

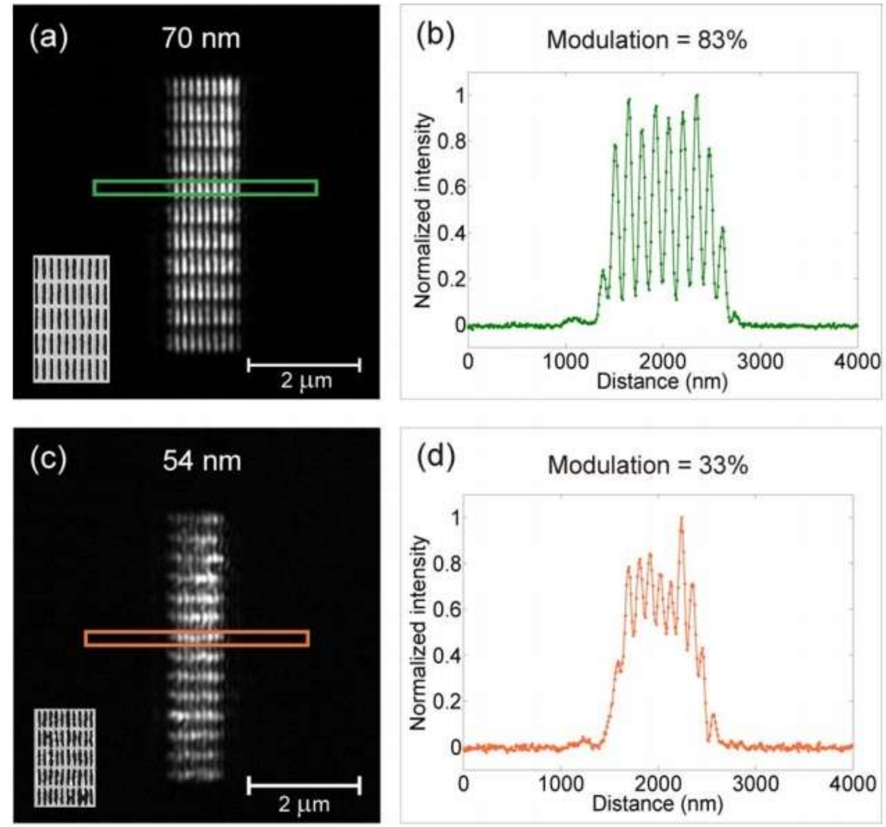

Single-shot EUV images

Brizuela et al., OPTICS LETTERS / Vol. 33, No. 5 / March 1, 2008

Single-shot EUV laser imaging of nanostructures with wavelength resolution

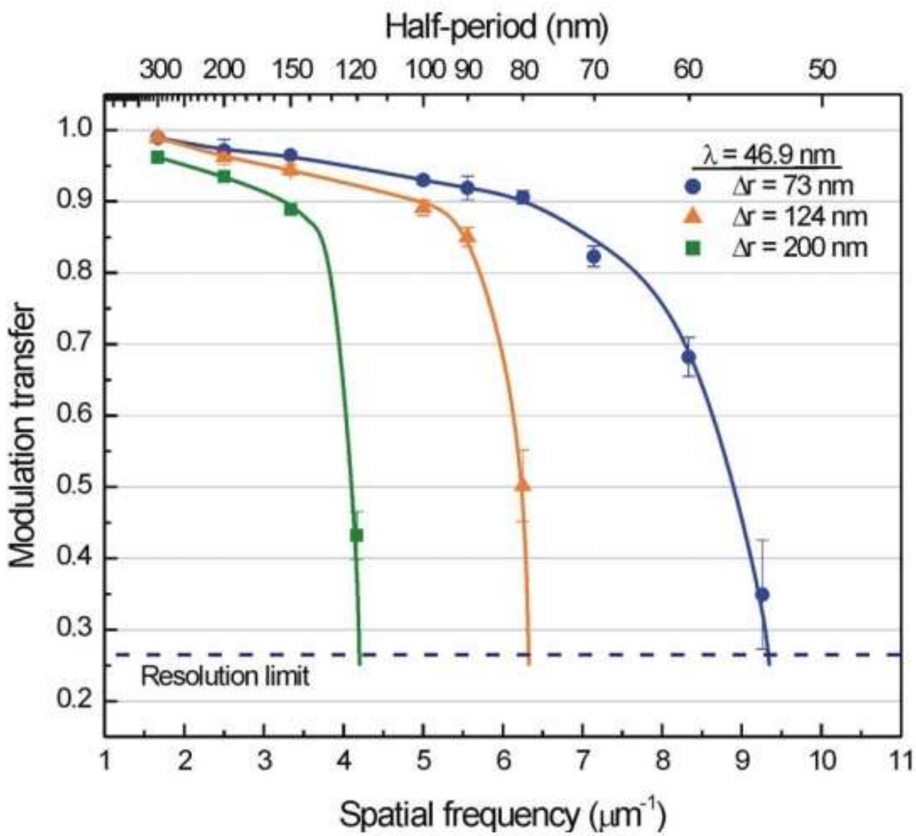

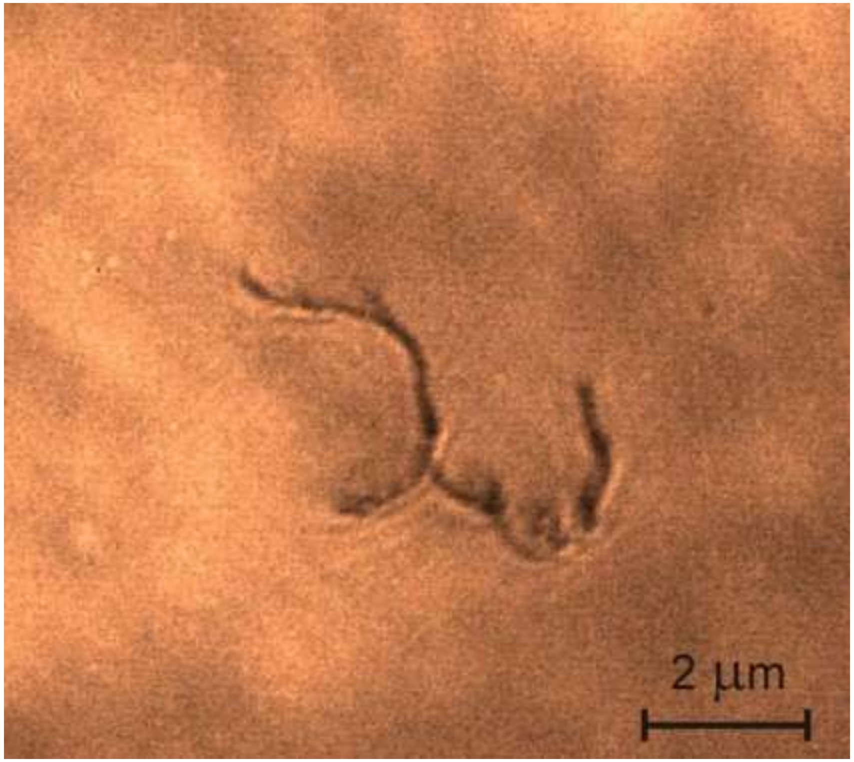

Measured MTFs for objective zone plates with outer zone widths of Δr=200, 124, and 73 nm (NA=0.12, 0.19, and 0.32, respectively).

Single-shot image of an entanglement of 50 nm diameter carbon nanotubes. This image was obtained using the Δr=73 nm objective lens and a wavelength of 46.9 nm.

Rayleigh-like resolution values of 120, 80, and 54 nm

C. A. Brewer, F. Brizuela, P. Wachulak, et al., Optics Letters, 33, 5, 518-520 (2008)

Water – window CDL microscope (CTU Prague)

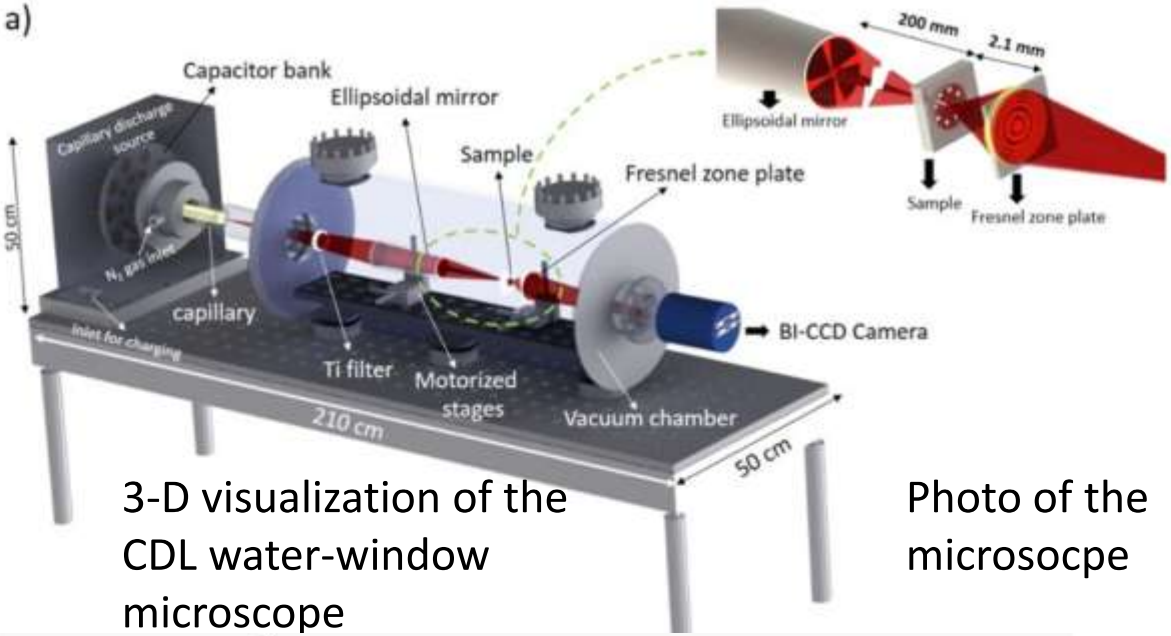

3-D visualization of the CDL water-window microscope

Photo of the microsocpe

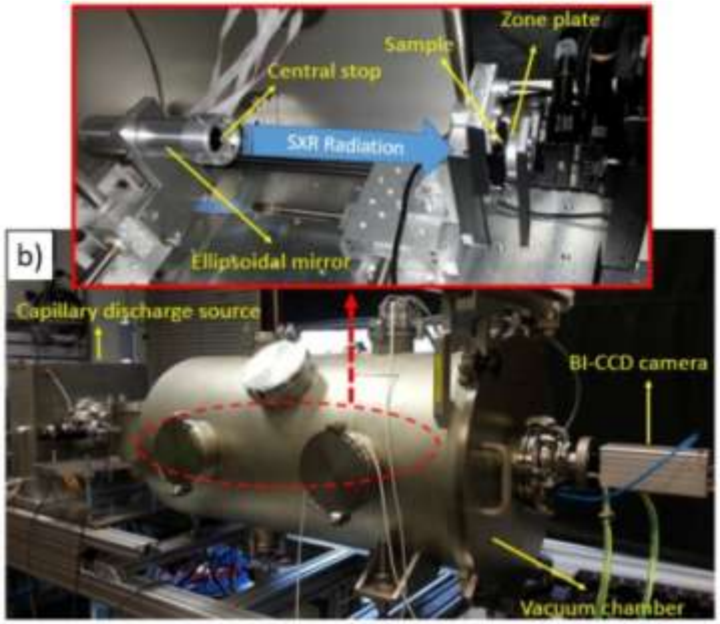

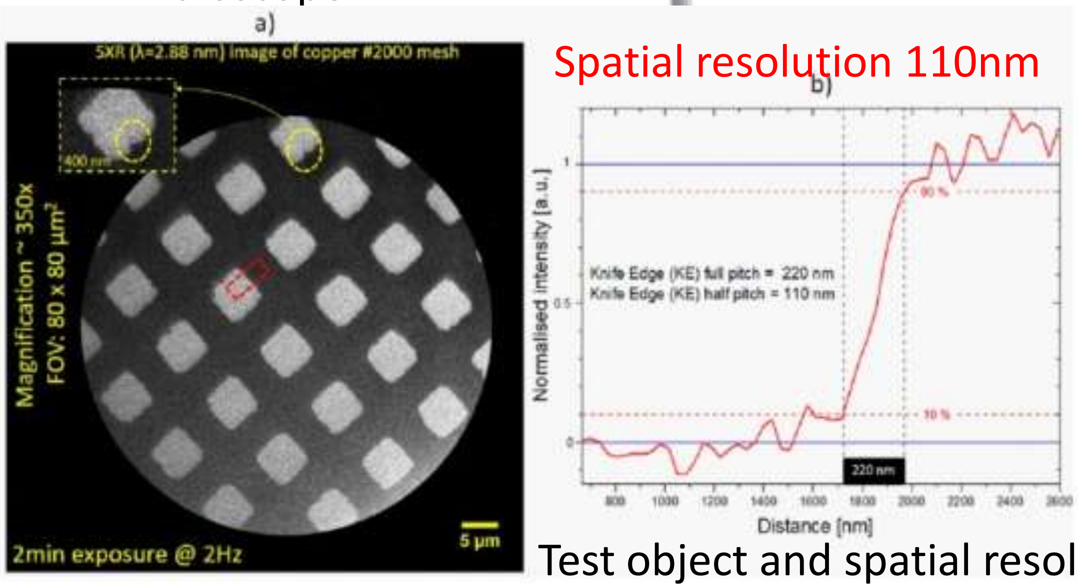

Spatial resolution 110nm

Test object and spatial resolution

Number of photons: **~1.2x10⁹** /pulse @ λ=**2.88nm**

Energy: **83nJ/pulse** and at 3-Hz repetition rate

FZP objective
- tungsten zoneplate **130nm** thick
- D=**180µm**, Δr=**33nm**,
- f=**2.1mm**, λ=**2.88nm**, NA_{O_in}=**0.043**
- magnification: **350x**

Nawaz et al., Journal Instrumentation 11, 07, P07002, 1-12 (2016),

A 50nm spatial resolution EUV imaging with FZP and gas puff target based source

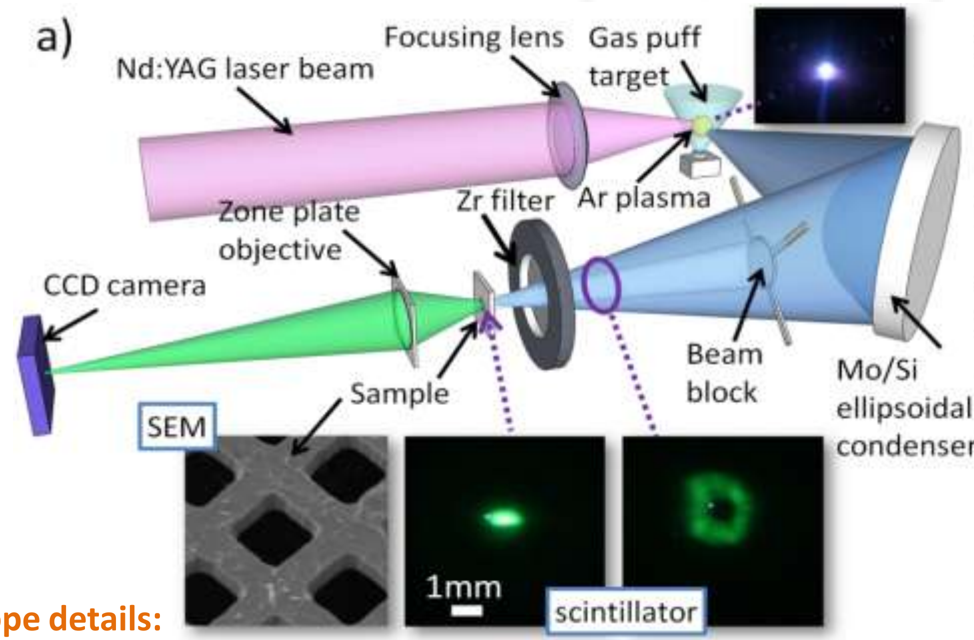

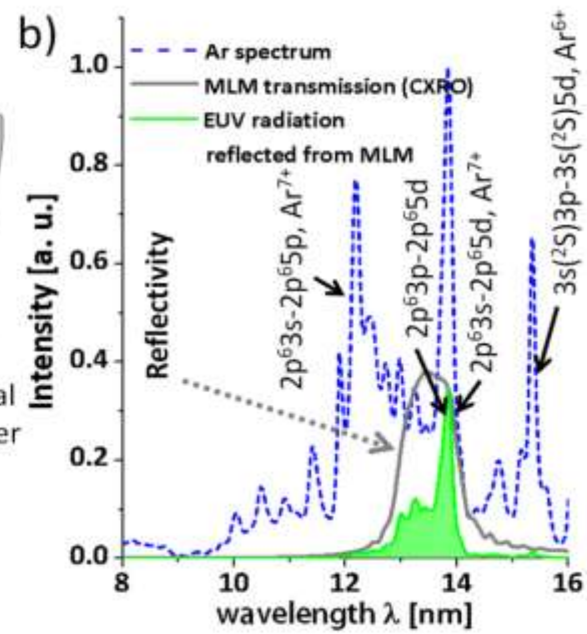

Microscope details:

CCD camera: iKon-M (Andor) with 1k x 1k pix, 13x13 μm^2

Condenser NA: H= 0.11, V=0.15

Objective NA: 0.137

Magnification: (min) 470x

Pixel size: (max) 27.7nm

Acquisition time: 10-100sec/2Hz

Zone plate objective parameters:

D: 200 μm, Δr: 50 nm, f: 0.724 mm, N: 1000 zones, NA: 0.137, Rayleigh resolution: 1.22Δr=61 nm, DOF: +/-0.5λ/NA^2 +/- 385 nm

LIDER 2012 Mikroskop EUV

Realizacja projektu została sfinansowana przez

LIDER

Narodowe Centrum Badań i Rozwoju

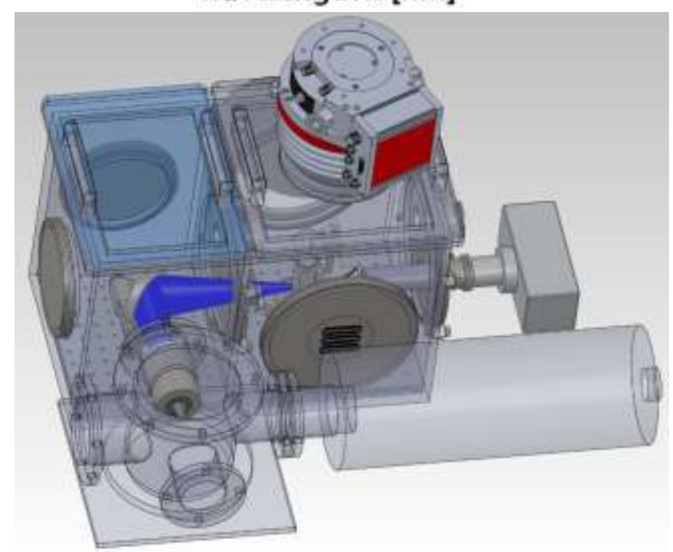

P. W. Wachulak, et al., Applied Physics B 123:25, 1-5 (2017)

http://www.ztl.wat.edu.pl/zoplzm/lider/

Developed EUV microscope system

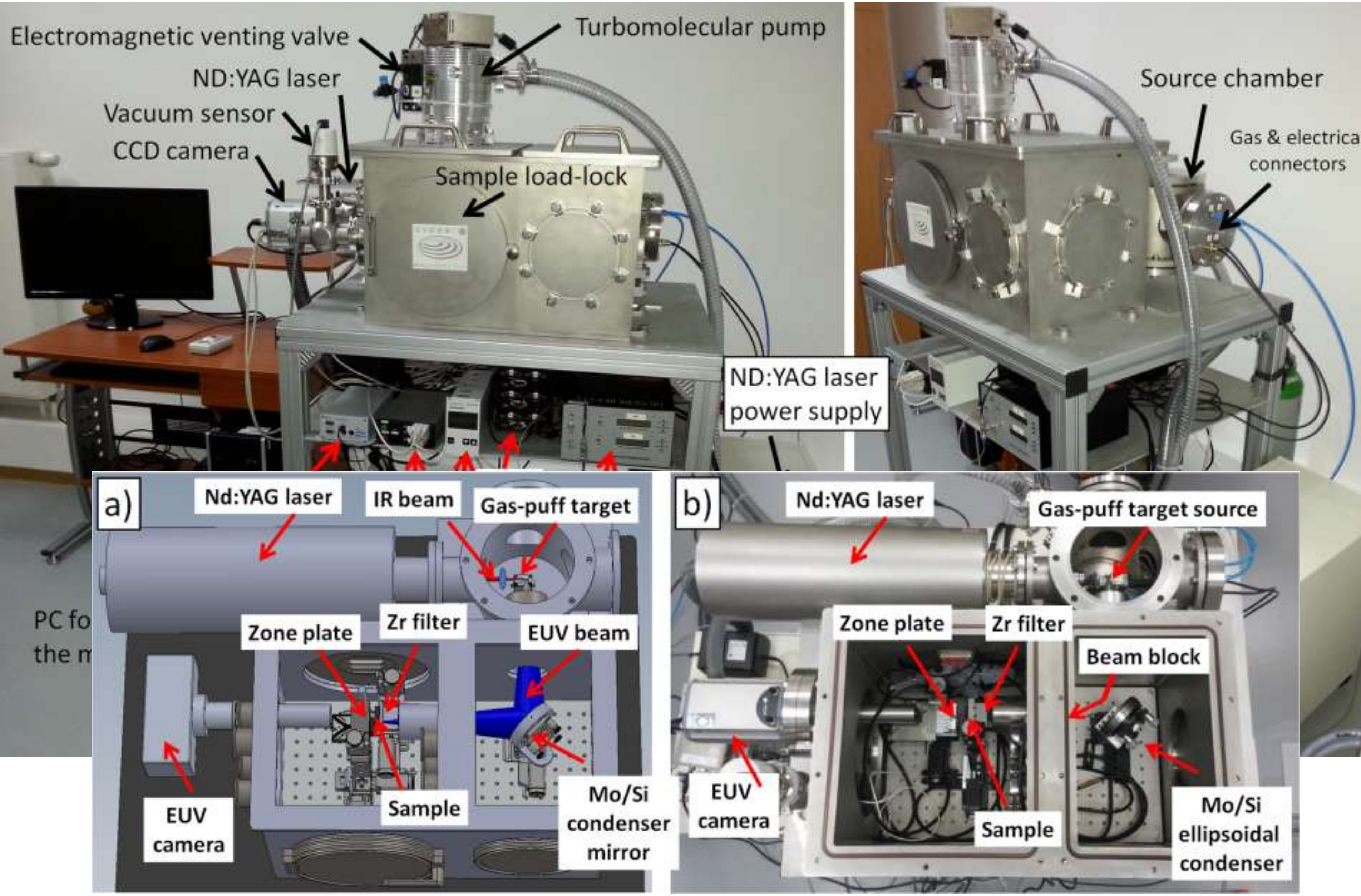

…studying thin films

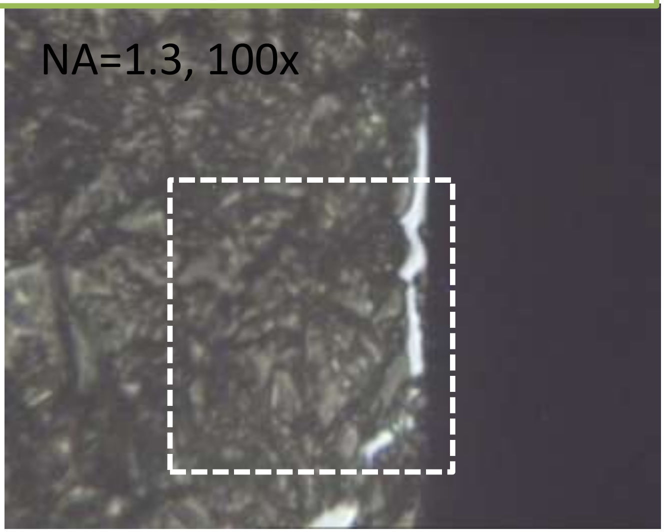

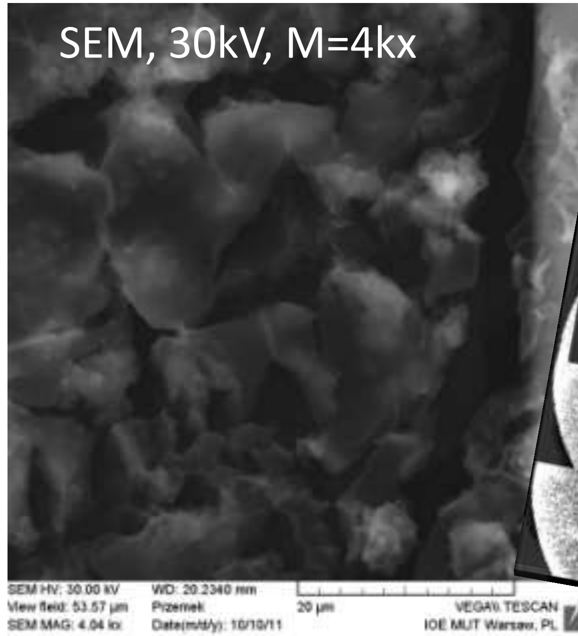

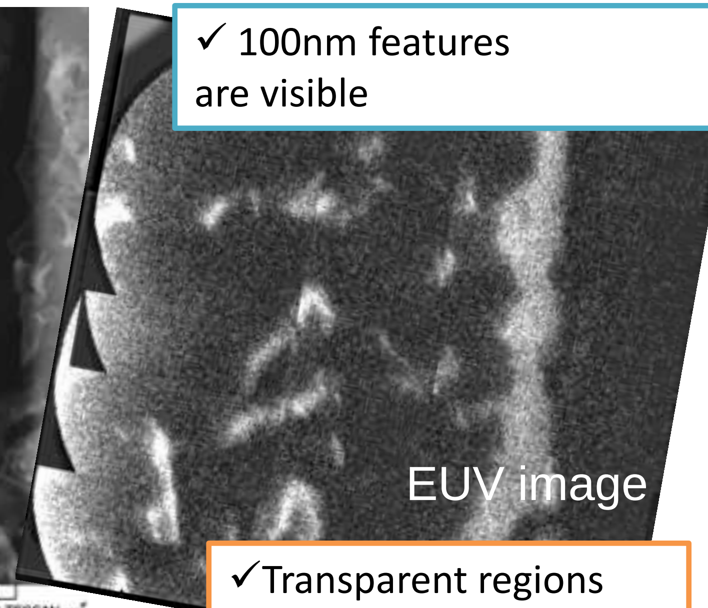

✓ 100nm features are visible

✓Transparent regions with thickness <100nm (cracks, holes, etc.)

…imaging of nanostructures: ZnO nanowires

P. Wachulak et al., Radiation Physics and Chemistry 93 (2013) 54–58

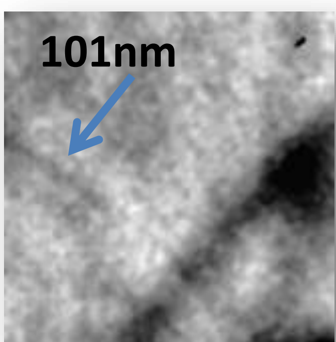

EUV microscope image, 100 EUV pulses exposure

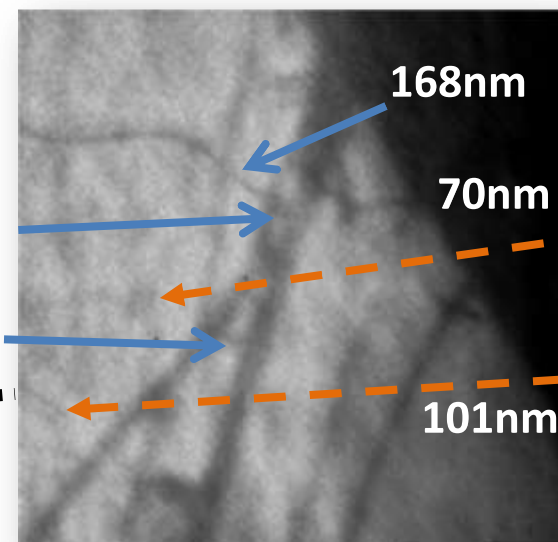

SEM micrograph at accelaration voltage of 30kV

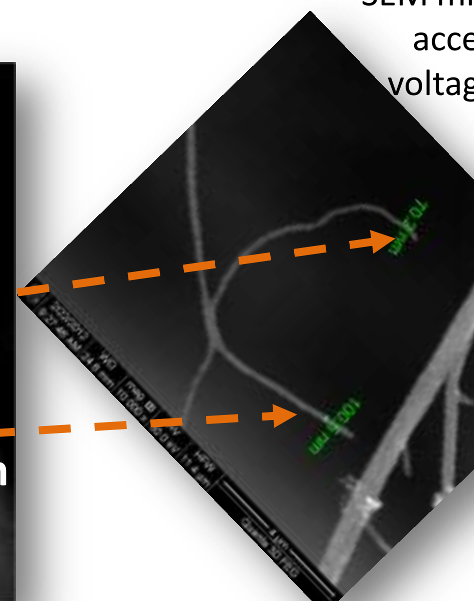

Optical micrograph of ZnO nanofibers

Resolution and applications

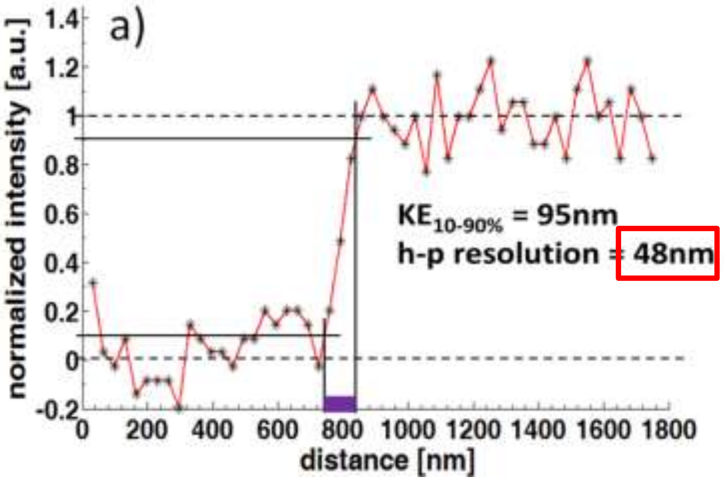

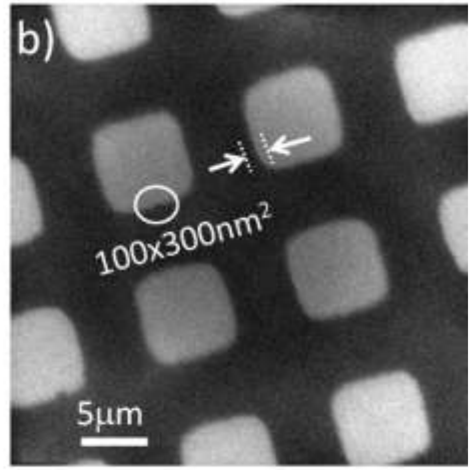

Spatial resolution estimation based on knife-edge test

A. Torrisi, et al., Journal of Microscopy 265, 2, 251-260 (2017)

EUV image of CT 26 fibroblast cells...

...obtained with exposure of 200 EUV pulses (22 seconds), with visible features as small as 60 nm.

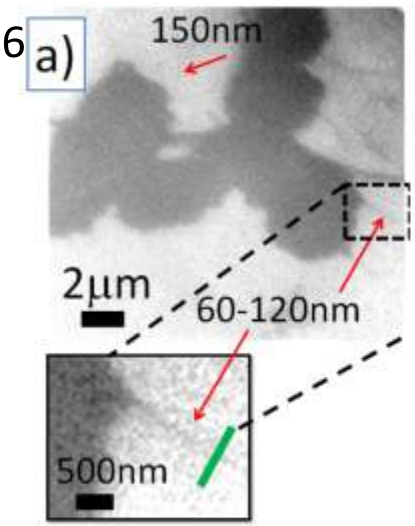

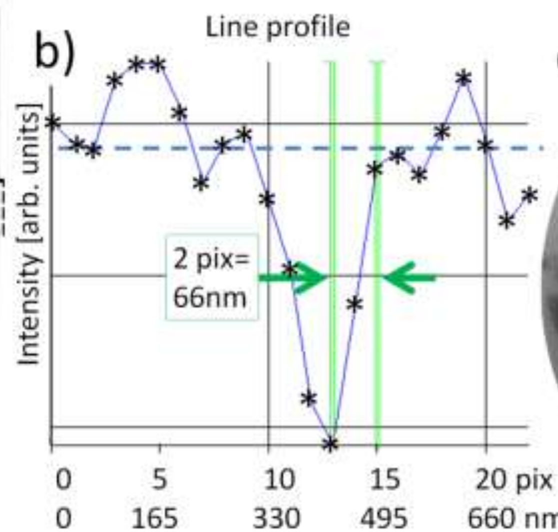

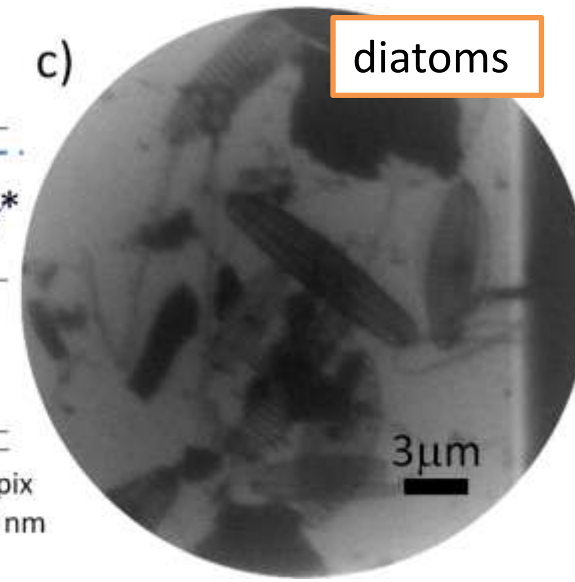

Microscope details:

CCD camera: iKon-M (Andor) with 1k x 1k pix, 13x13 μm^2

Condenser NA: H= 0.11, V=0.15, Objective NA: 0.137

Magnification: (min) 410x, Pixel size: (max) 33nm

Acquisition time: 10-100sec/10Hz

Sub-38 nm resolution tabletop microscopy with 13 nm wavelength laser light

Schematic diagram of the 13 nm wavelength imaging system.

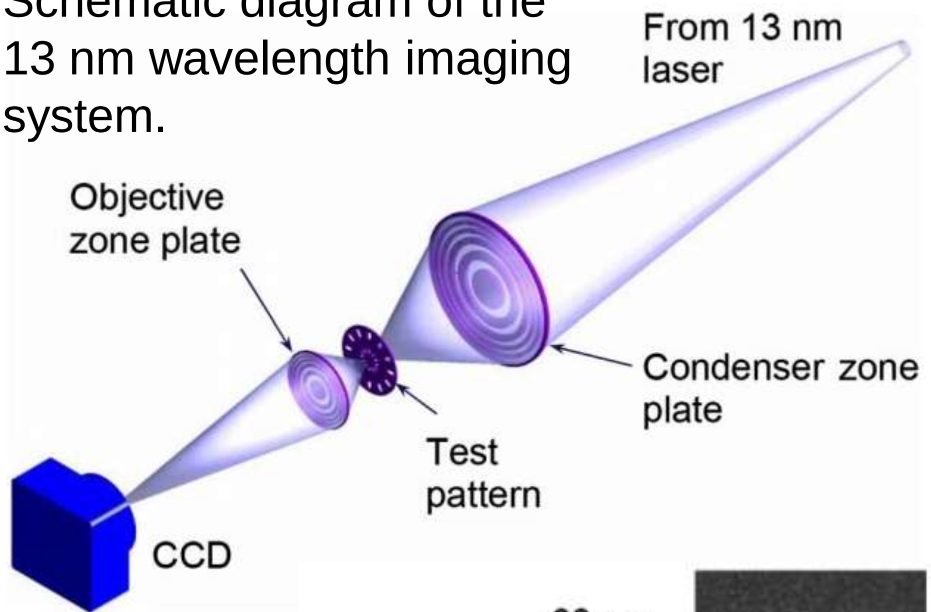

Ni-like Ag, pumped by 1J/8ps Ti:Sa laser
λ=13.9nm, E=1-2uJ/pulse

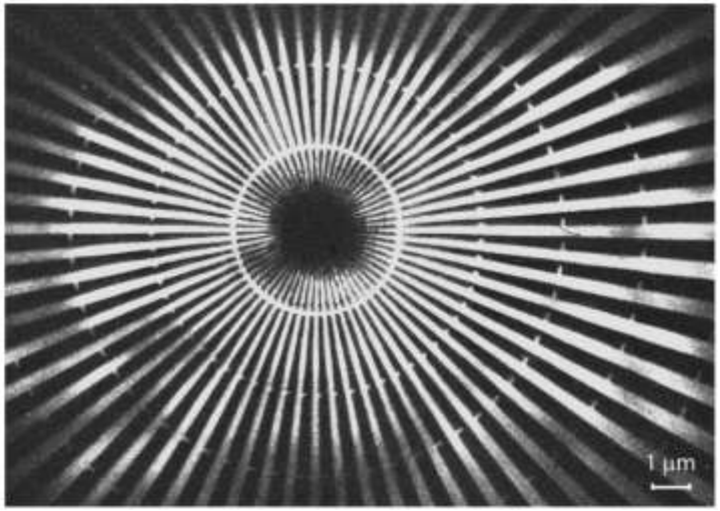

Ni-like Cd
λ=13.2nm
dr=50nm ZP
20 sec exp.
38nm lines resolved

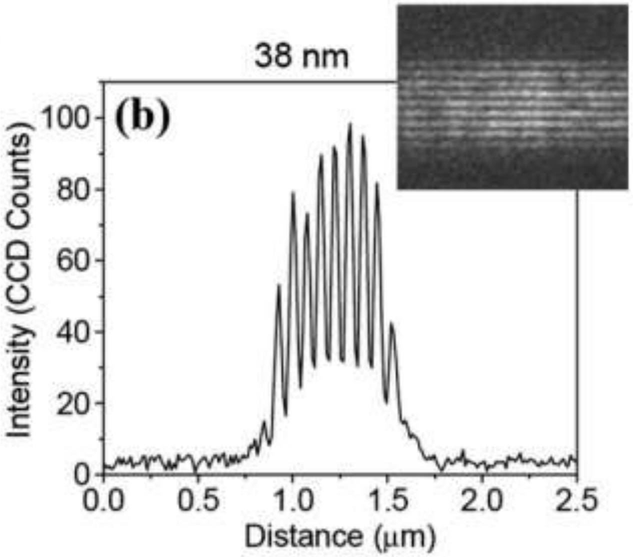

Condensor: D=5mm, 12500 zones, dr=100nm, NA=0.07, f=38mm
Objective 1: D=0.2mm, 625 zones dr=80nm, NA=0.0825
Objective 2: D=0.1mm, dr=50nm, NA=0.132

Large-field-of-view image of a set of radial spokes
- dr=80 nm zone plate
- 20 s exposure.
- 60 nm half-period resolution

G. Vaschenko, Optics Letters, 31, 9 (2006)

EUV scanning transmission microscope operating with high-harmonic and laser plasma radiation

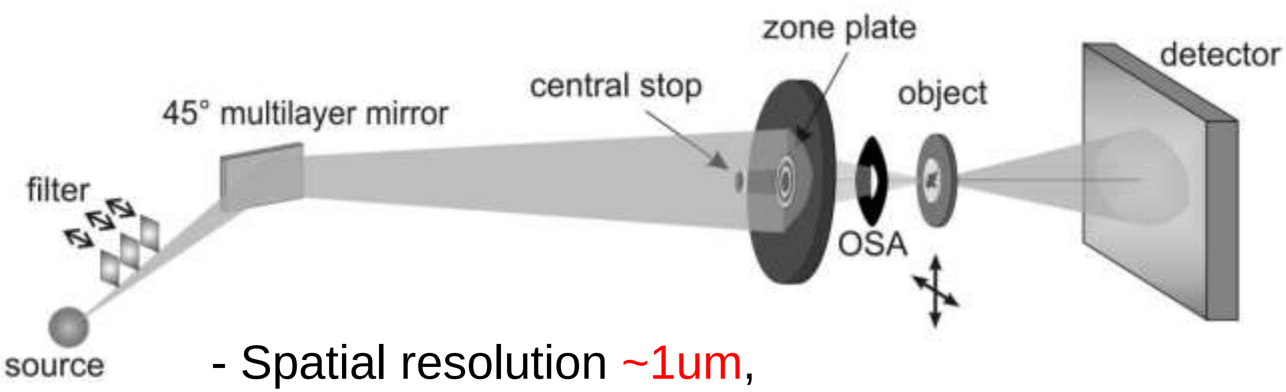

scanning transmission EUV microscope set-up

- Spatial resolution ~1um,
- Ti:Sa pumping laser, 1kHz, 800nm/30fs pulses, 1mJ focused onto a SS tube,

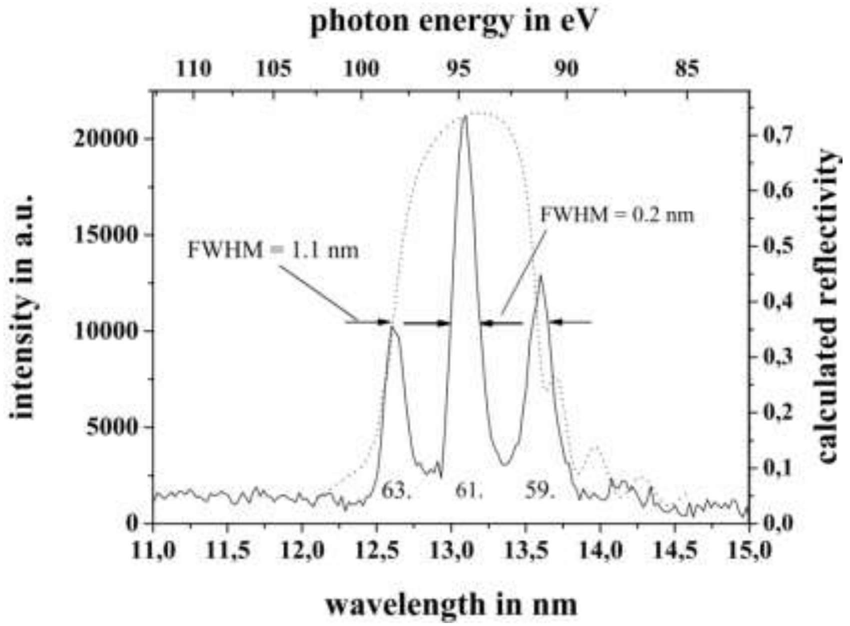

Spectrum extracted from the HH source using a Mo/Si multilayer mirror

- Zr filters and Mo/Si mirror λ/Δλ~13
-

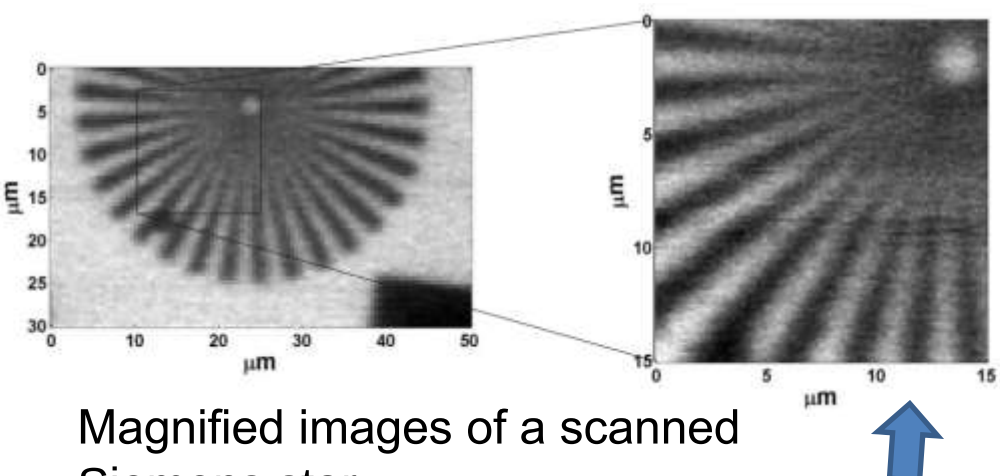

Magnified images of a scanned Siemens star

100 × 100 pixel image a scan step size of 150 nm

R. Fruke et al., Europhys. Lett., 72 (6), 915–921 (2005)

EUV microscopy for defect inspection by dark-field mapping and zone plate zooming

EUV microscope scheme

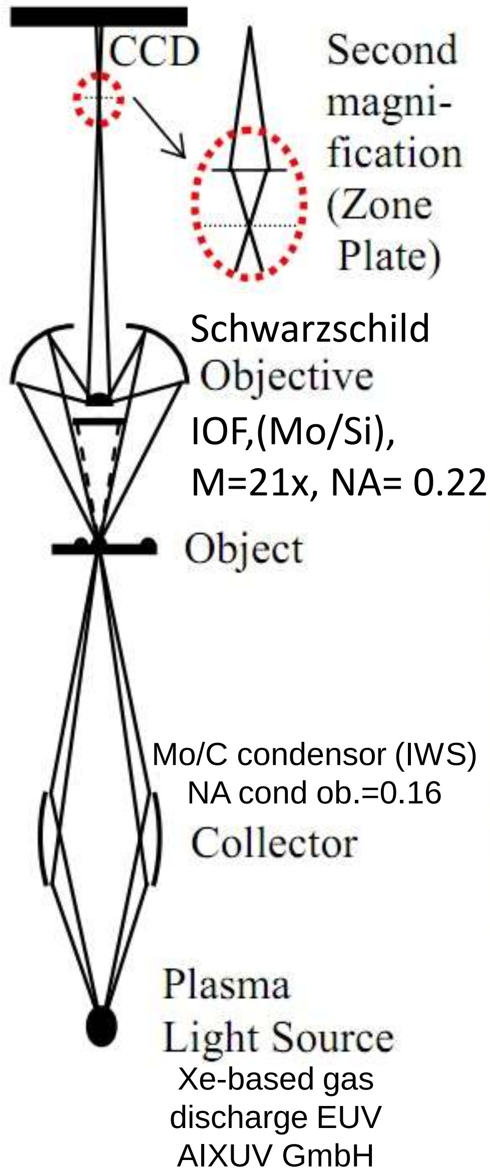

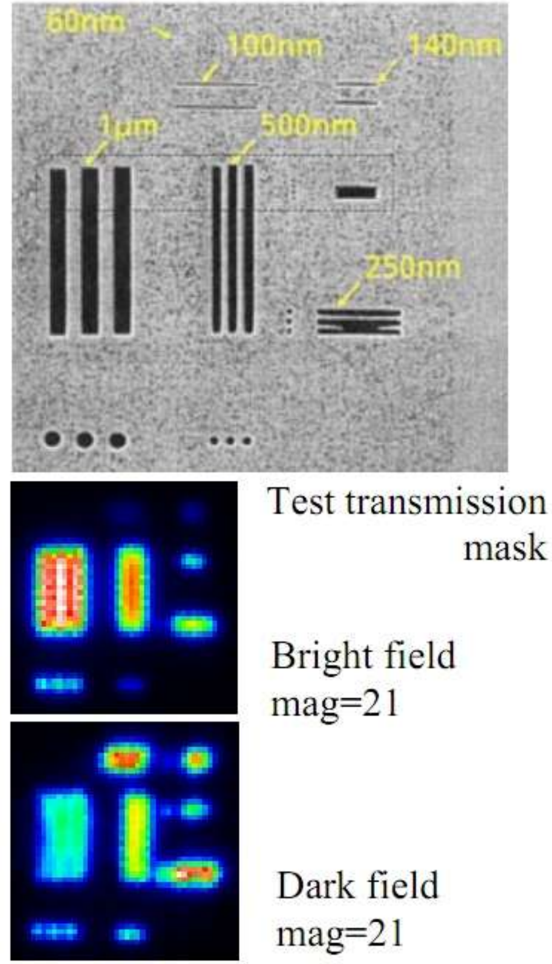

100nm holes,
Dist. 100nm

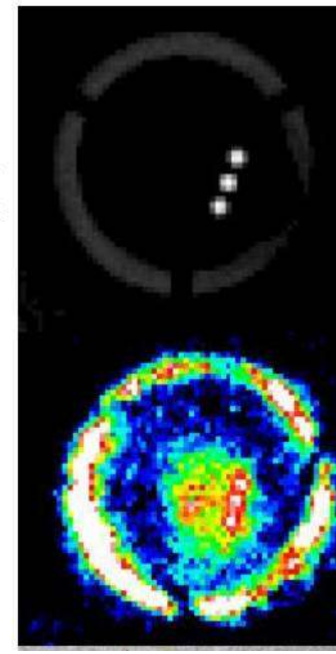

NASSO,det = 0.01, Mag = 10
NA ZP=0.011 (30 zones), res ~1um
Combined resolution ~100nm

L. Juschkin, Journal of Physics: Conference Series 186 (2009) 012030

Compact water-window transmission X-ray microscopy

- 100Hz/3ns/100mJ pulses, Nd:YAG (Coherent Infinity)
- ethanol droplet target, W/B_4C condensor mirror, λ=3.37nm,
- ZP: D=56um, 468 zones, dr=30nm, f=498um.
- magnification: 650x-1000x

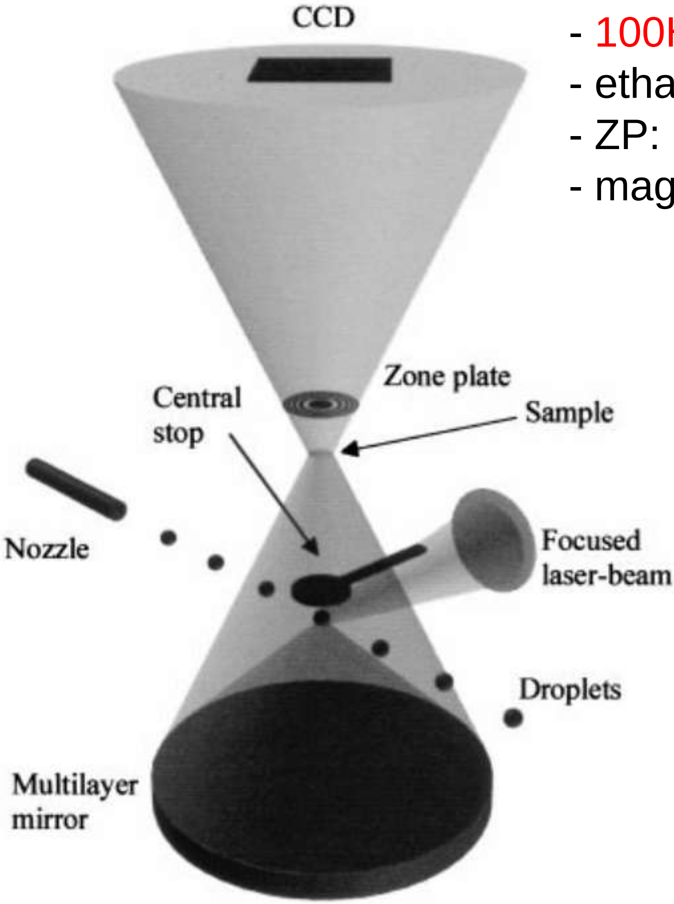

Table-top water-window X-ray microscopy arrangement

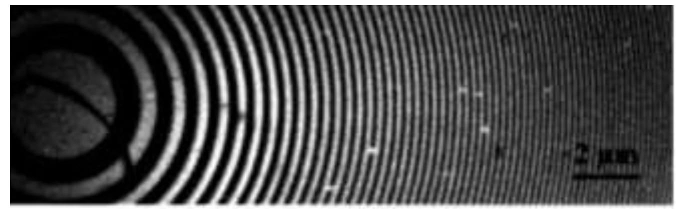

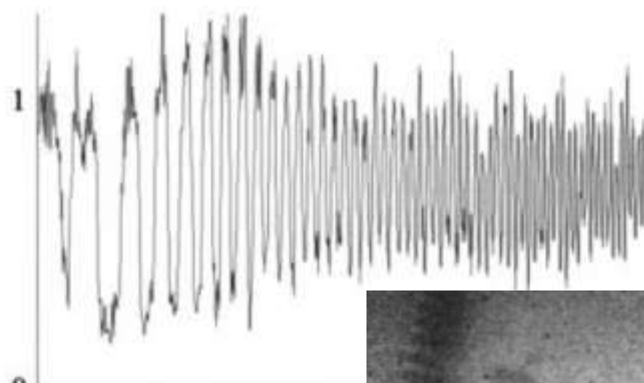

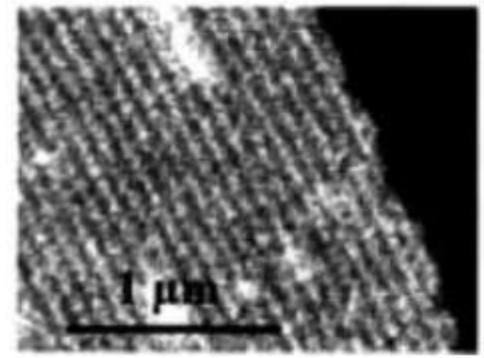

1000x magnification
60nm features visible

Image of diatom with M=650x

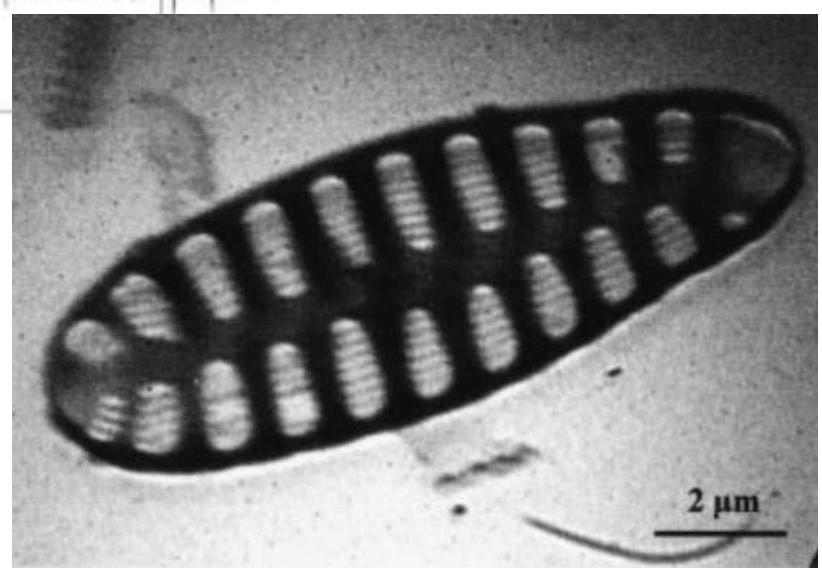

M. Berglund, et al., Journal of Microscopy 197, 3, 268-273 (2000)

High-resolution compact X-ray microscopy

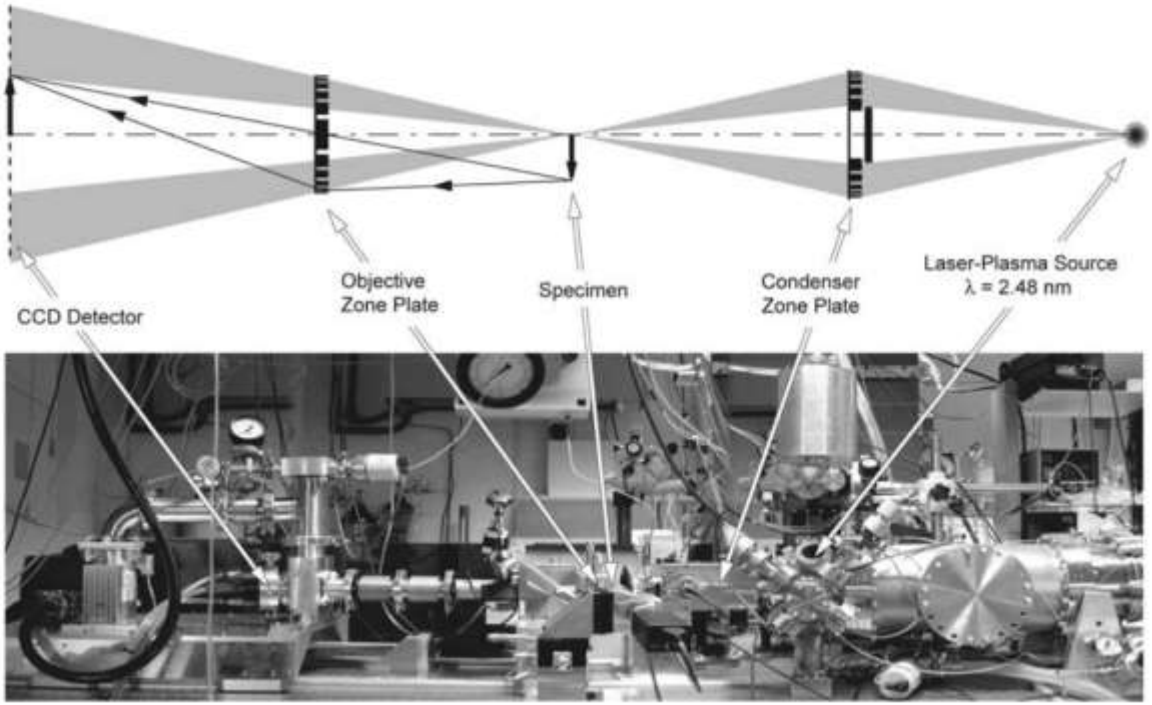

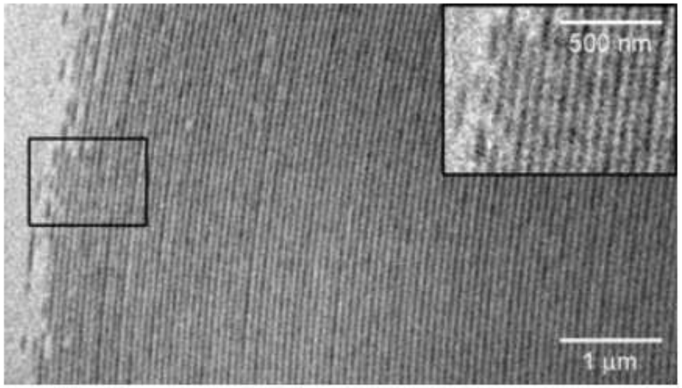

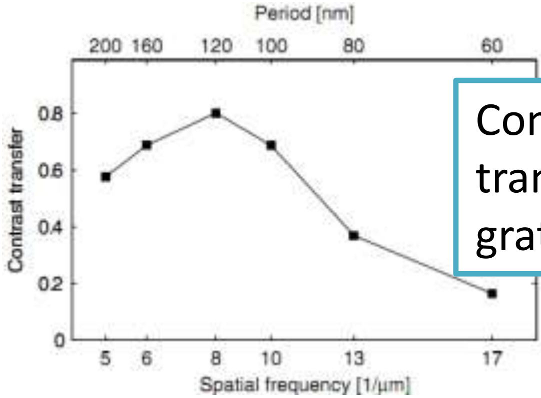

Contrast transfer for gratings

- $100Hz/3ns/100mJ$ pulses, Nd:YAG (Coherent Infinity)
- 100-Hz regenerative liquid-nitrogen-jet laser-plasma source , $\lambda=2.48+2.49nm$
- sub-60-nm resolution
- exposure: 5 min

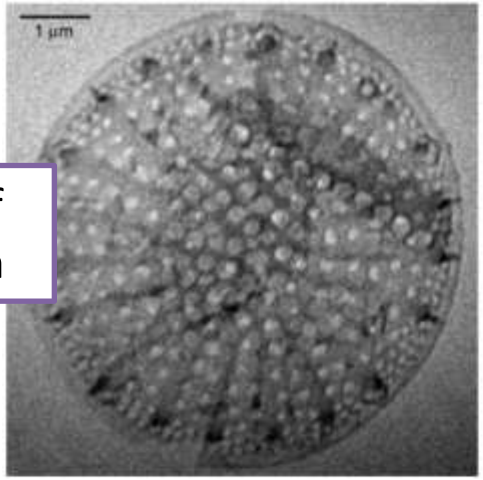

Image of a diatom

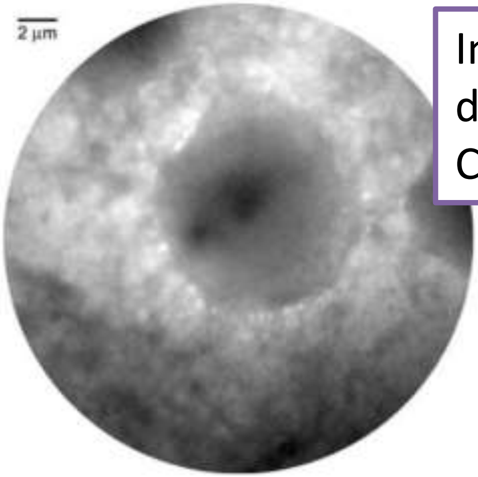

Image of a dehydrated COS-7 cell

P.A.C. Takman et al., Journal of Microscopy, 226, 175–181 (2007)

Compact x-ray microscope for the water window based on a high brightness laser plasma source

a few optical tables

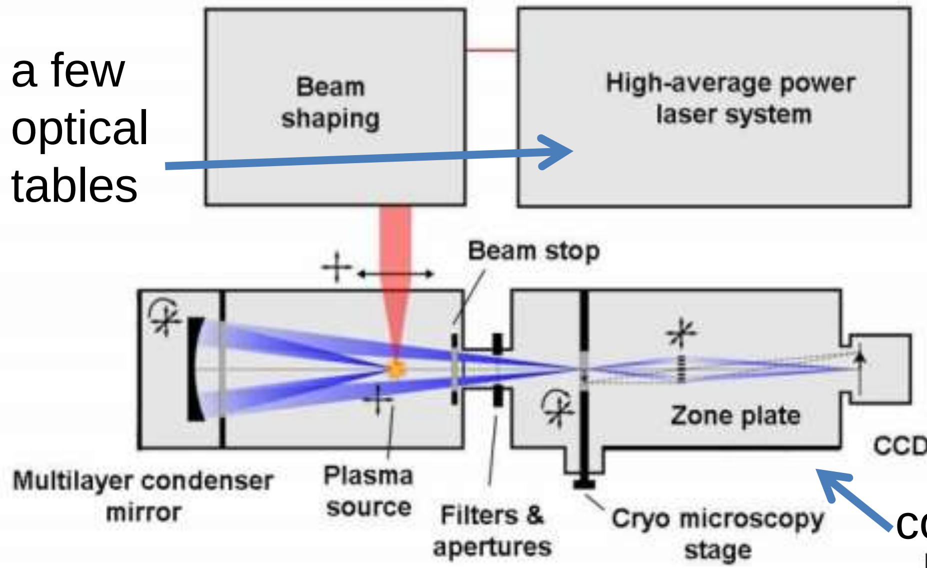

compact

The arrangement and optical layout of the table top water window x-ray microscope

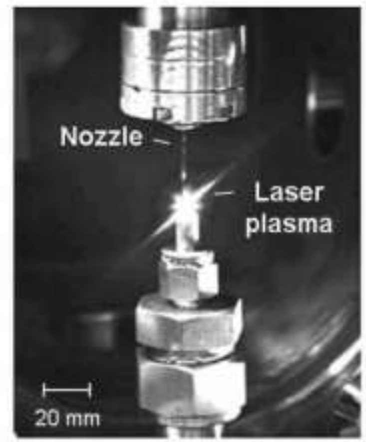

Pumping source: λ=1064nm (Nd:YAG), 450ps/1.3kHz
-Target L-N_2, λ=2.48nm
- Cr/V multilayer condenser mirror (FhG-IOF Jena), NA=0.05
- ZP: dr=25nm, NA=0.05,
- half-pitch resolution: **40-50nm**

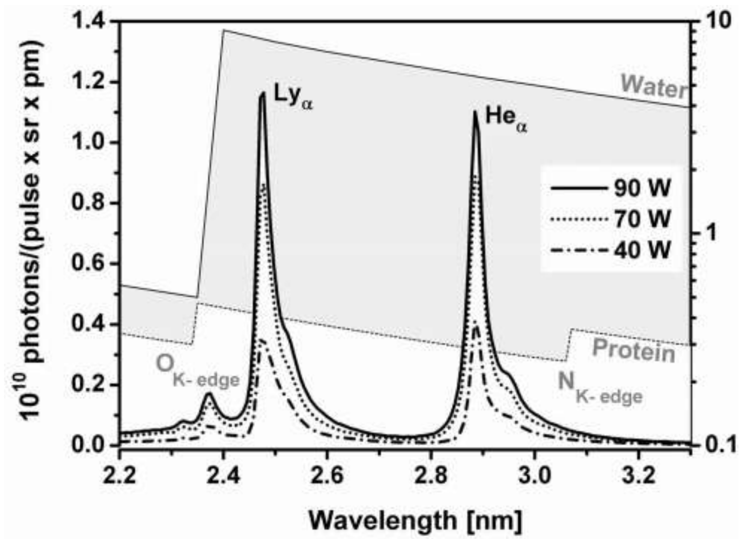

Images of the diatoms and ZP

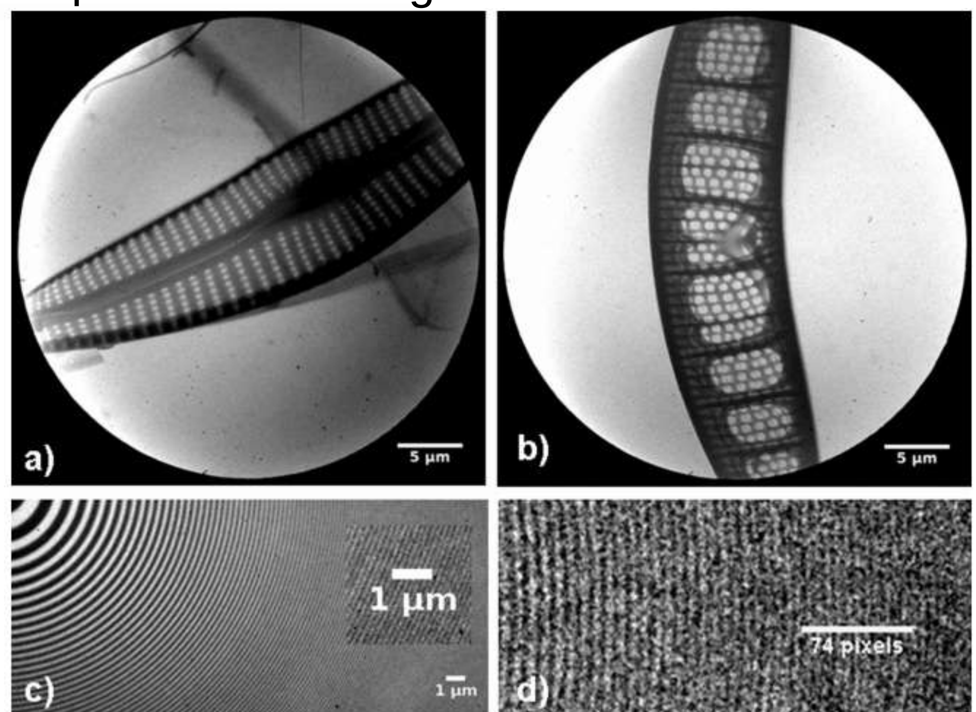

H. Legall et al., Optics Express 20, 16, 18362 (2012)

Compact soft x-ray microscope using a gas-discharge light source

λ=2.88nm (He-line N_2), 1kHz, electrical discharge
Grazing incidence condensor
ZP: 468 zones dr=30nm, D=56um , f=0.585mm,
NA=0.048
spatial resolution: **40nm**
exposure: 20sec
photons: **2.9E6/um²/s, aim 1E7**

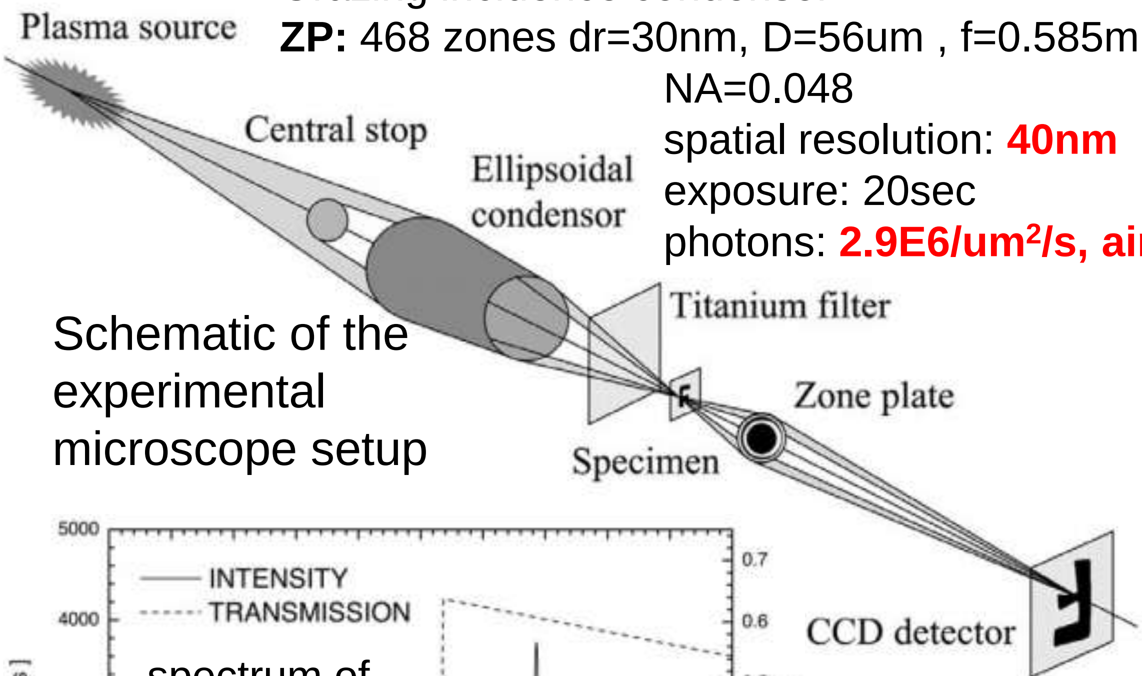

Schematic of the experimental microscope setup

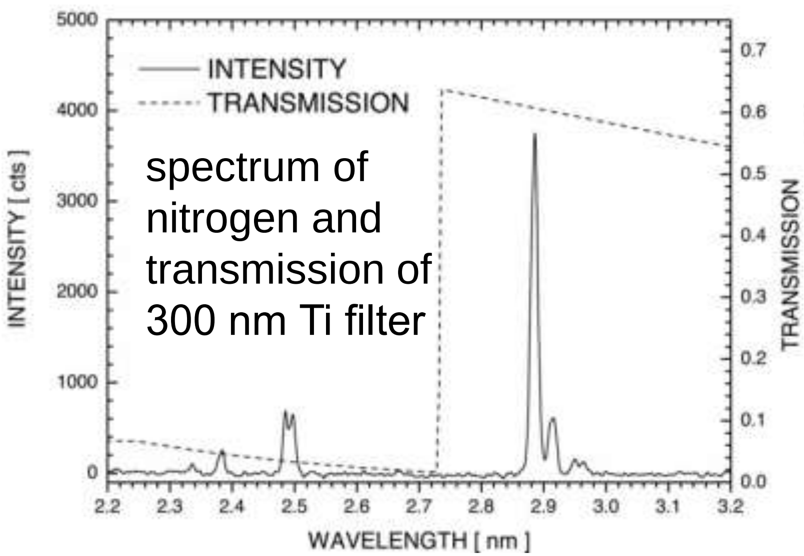

spectrum of nitrogen and transmission of 300 nm Ti filter

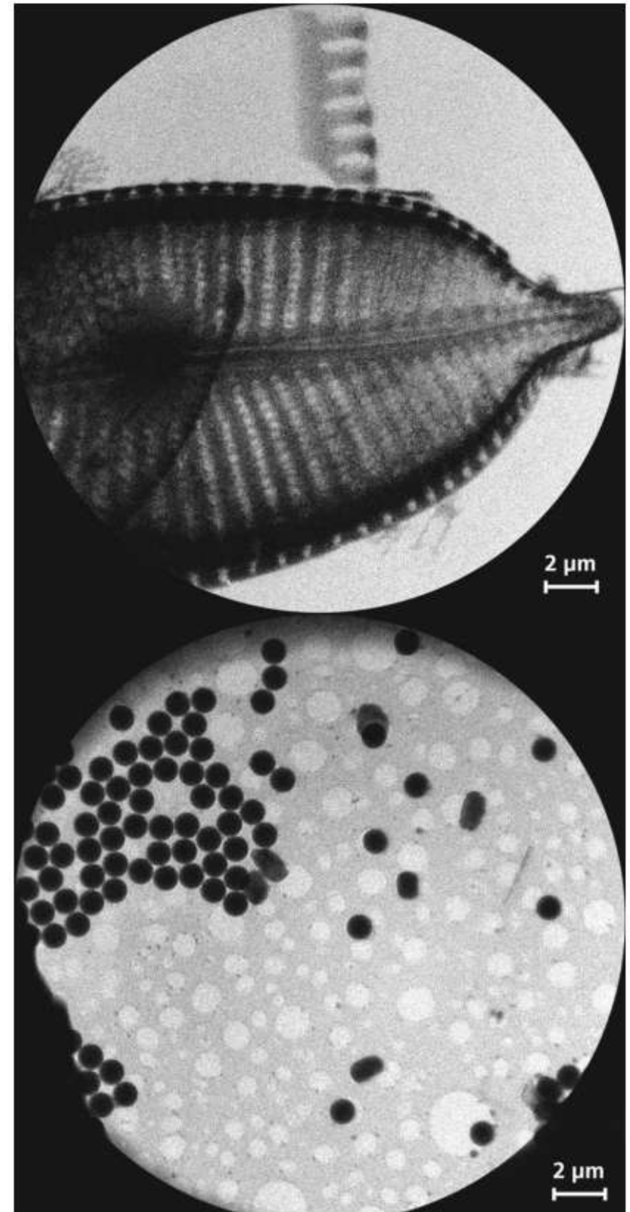

Microscopic images of diatoms and latex spheres

M. Benk et al., Optics Letters 33, 20, 2359 (2008)

Compact SXR transmission microscope using double stream gas puff target with 60 nm spatial resolution

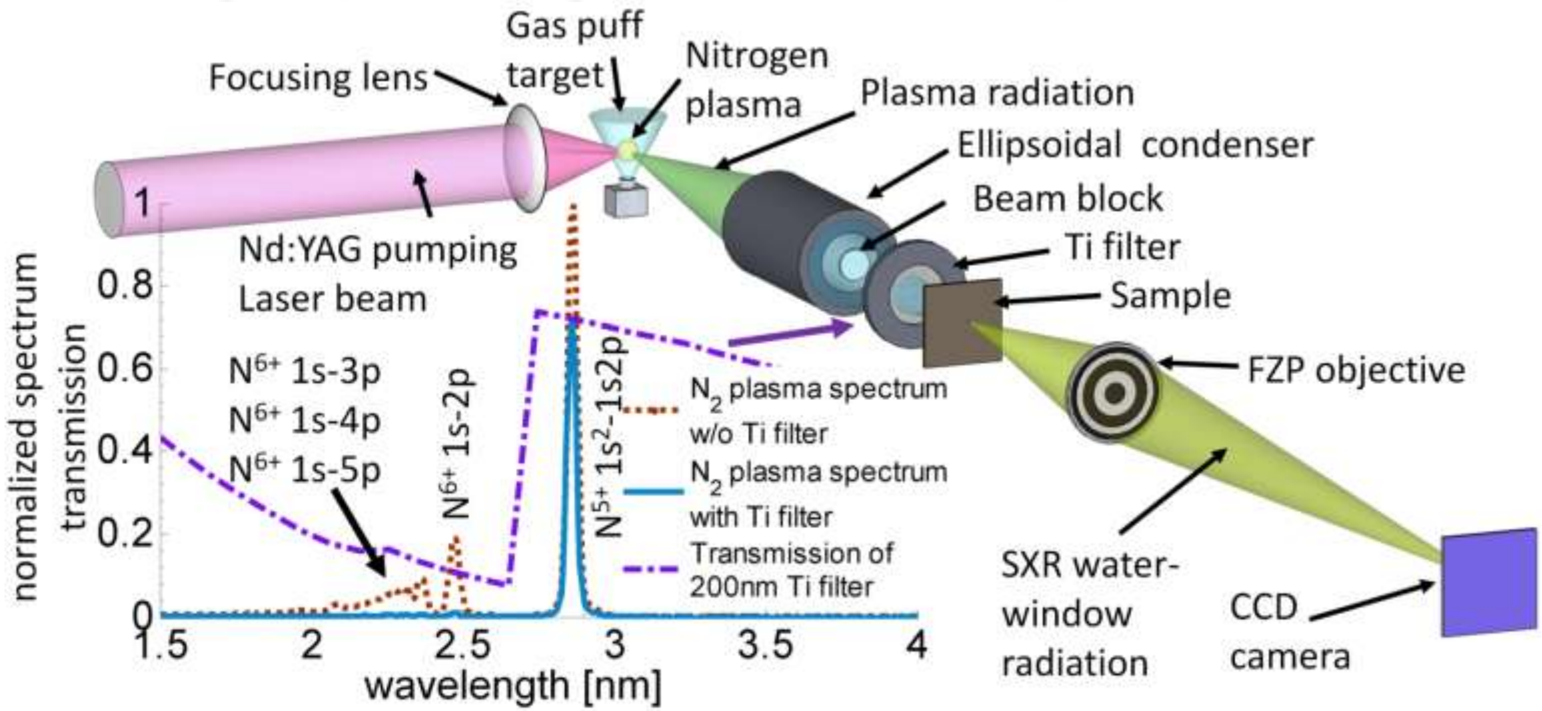

Scheme of the setup and spectrum of the nitrogen plasma source

Double stream N_2/He gas puff target,
N_2=**8bars**, He=**6bars**
TD1=400µs,
PW1=350µs,
TD2=500µs,
PW2=250µs,

Number of photons: ~(7.9+/-0.2)x10^9 /pulse @ λ=2.88nm
Energy: (561+/-17)nJ/pulse and at 10-Hz repetition rate
Inverse relative bandwidth (FWHM): $\lambda/\Delta\lambda$~70, (spec. limit)
Plasma size: ~310x470μm^2

FZP objective:
- Si_3N_4 zoneplate 400nm thick
- D=250µm, Δr=30nm,
- f=2.6mm, λ=2.88nm, NA=0.048

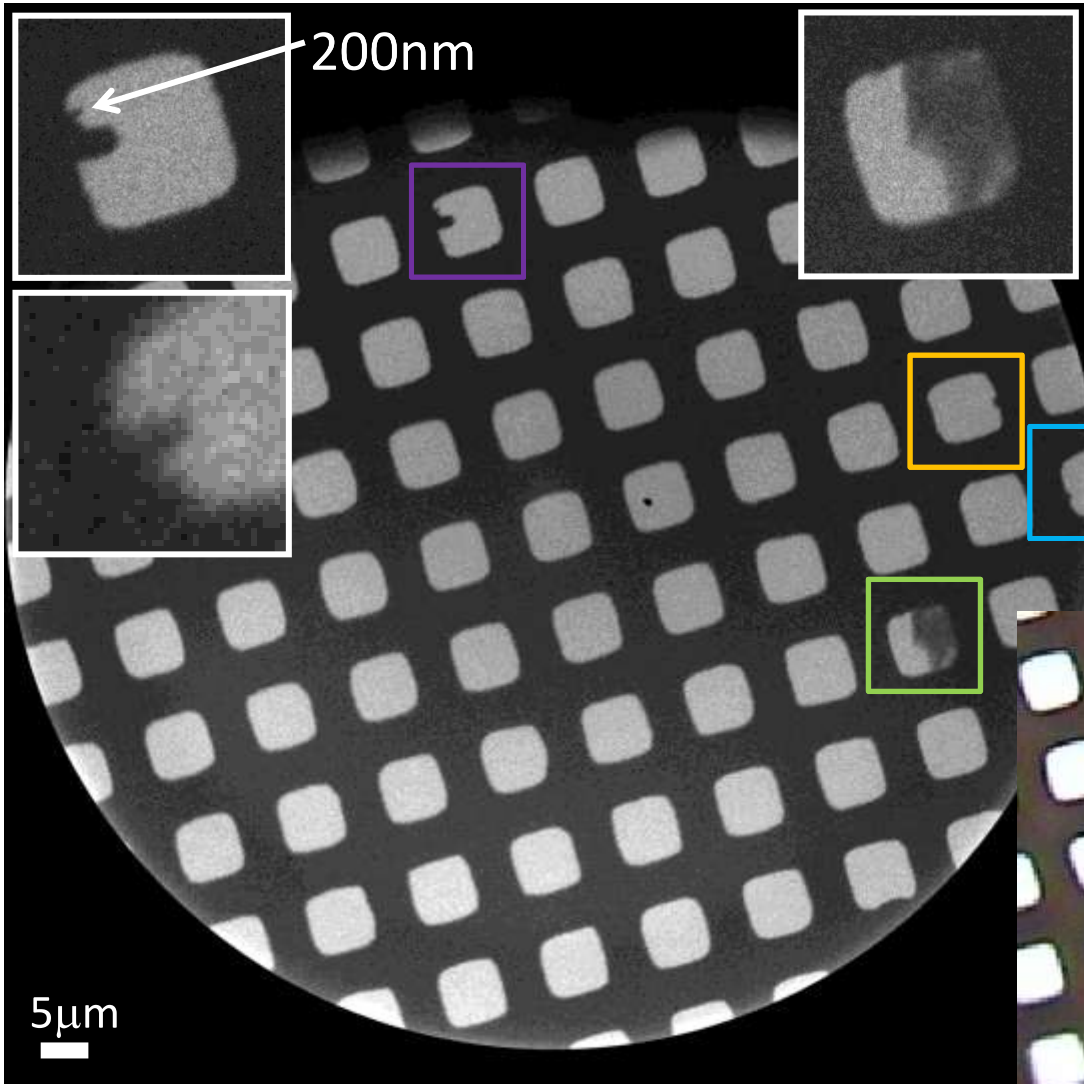

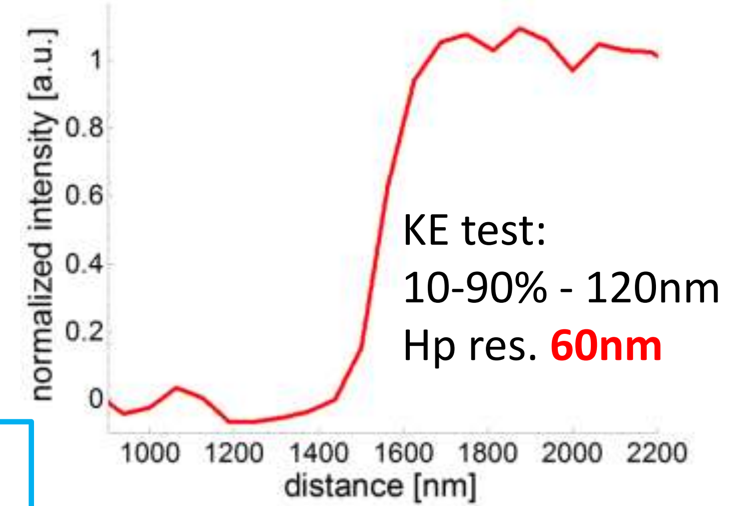

Optical image: 40x objective, NA=0.7

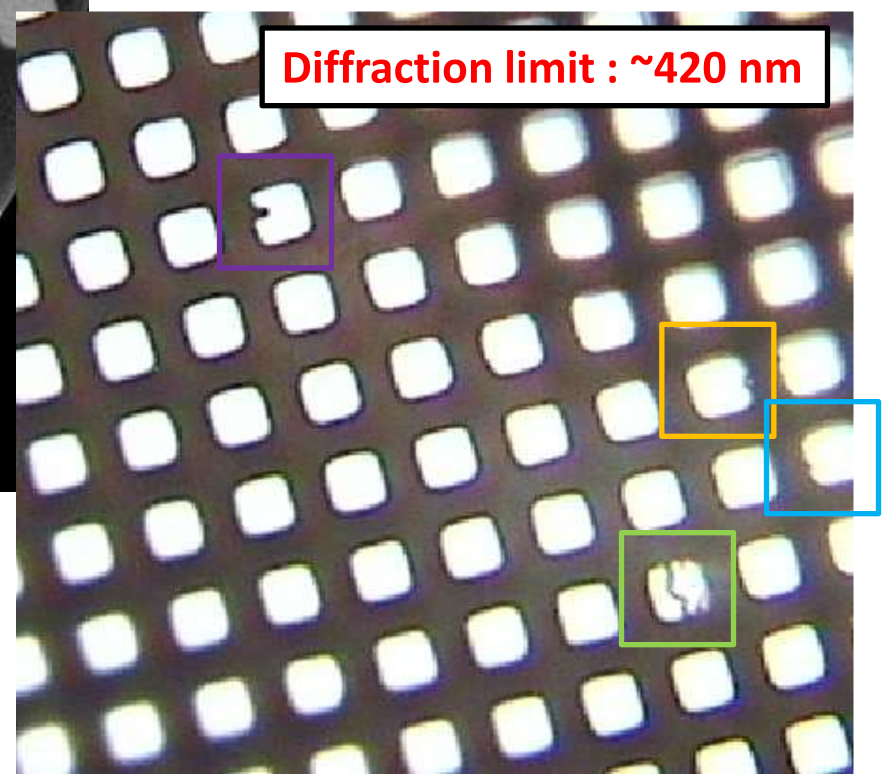

Cu mesh 2000 periods per inch

Exposure: 100 SXR pulses, @10Hz rep. rate, exposure time 12 seconds, T=-20°C, FOV=120µm, res. 60nm, mag. 220x, Great eyes camera 2048x2048 pix, GE2048

Single shot operation and biological samples

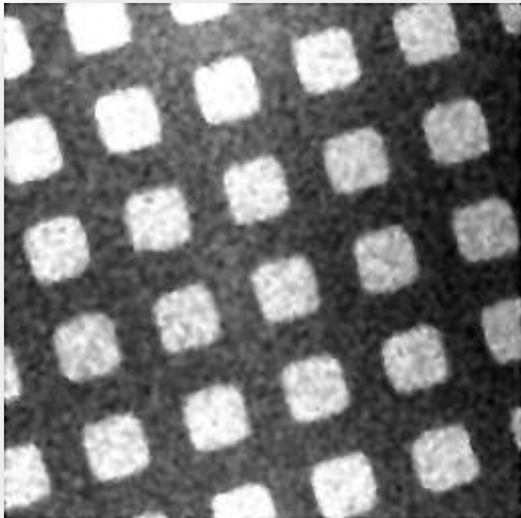

Exposure 1 SXR pulse – 3ns
4x4 CCD binning
spatial resolution ~250-300nm

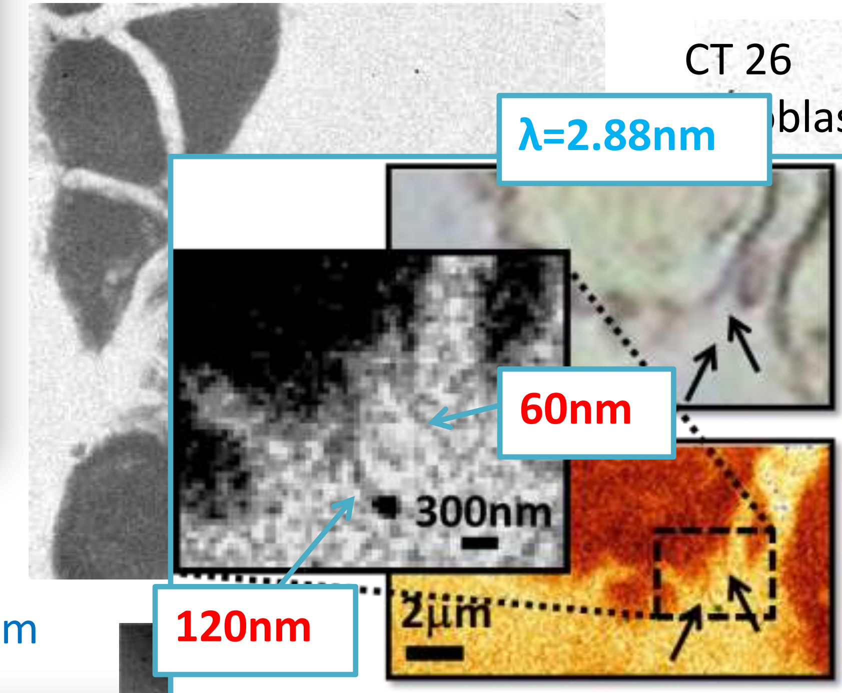

CT 26

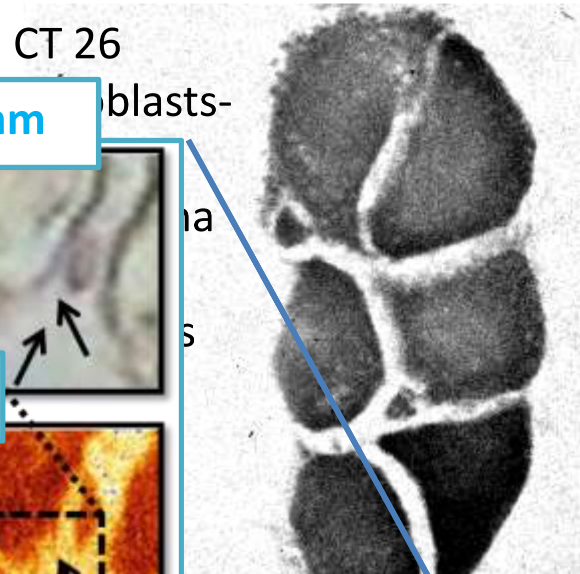

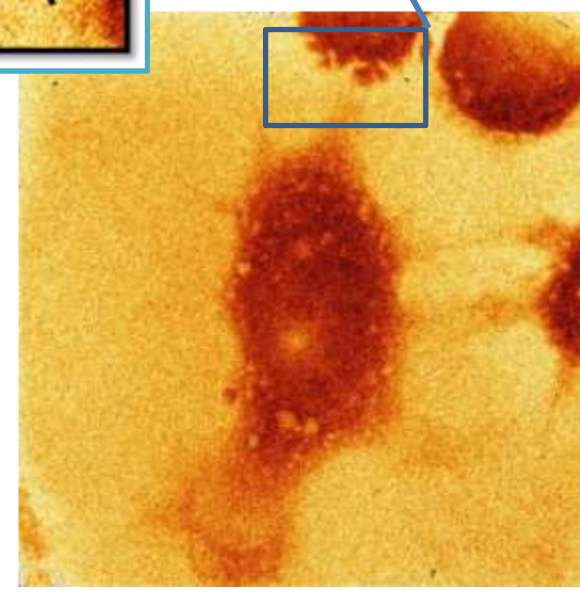

Supercoiled pBR322 DNA (4361bp)- circular double-stranded DNA from Inspiralis, UK, on top of 50nm Si_3N_4 membrane, 100ng/µl

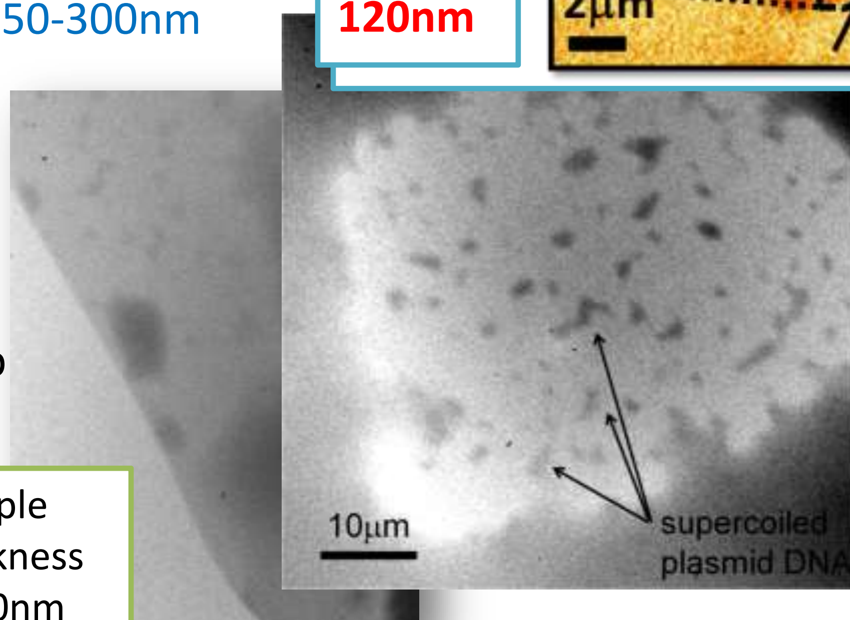

sample thickness ~160nm

P. Wachulak et al., Applied Physics B (2015) , Microscopy and Microanalysis 21, 5, 1214-1223 (2015)

Hippocampal neurons from E17 mouse embryos

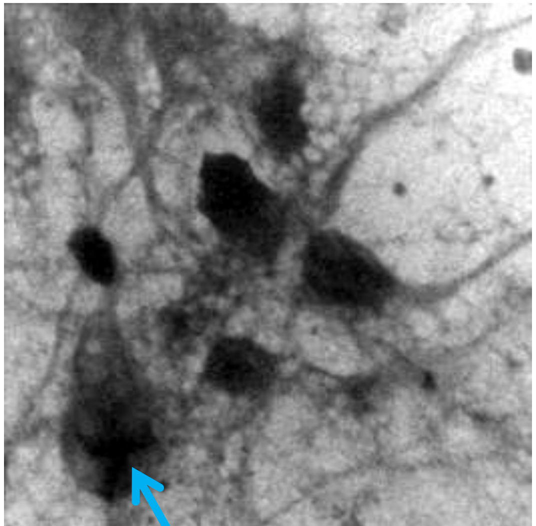

Internal structure visible

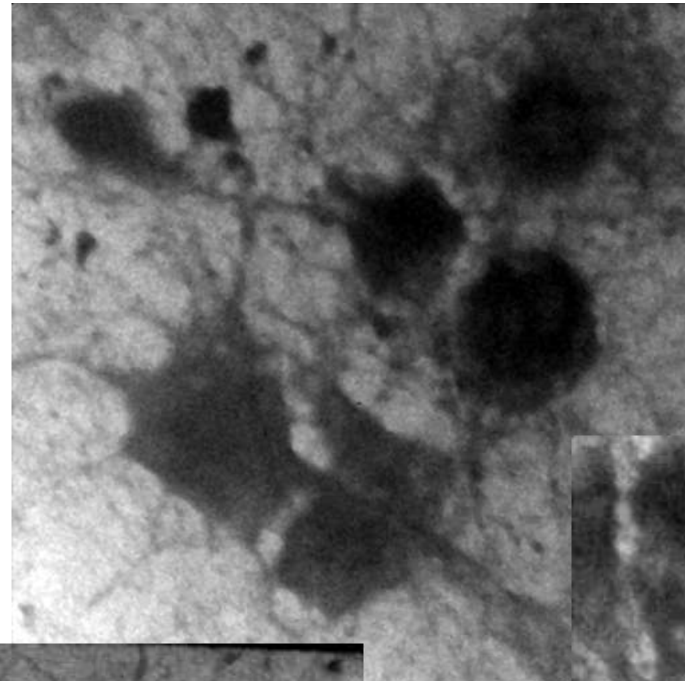

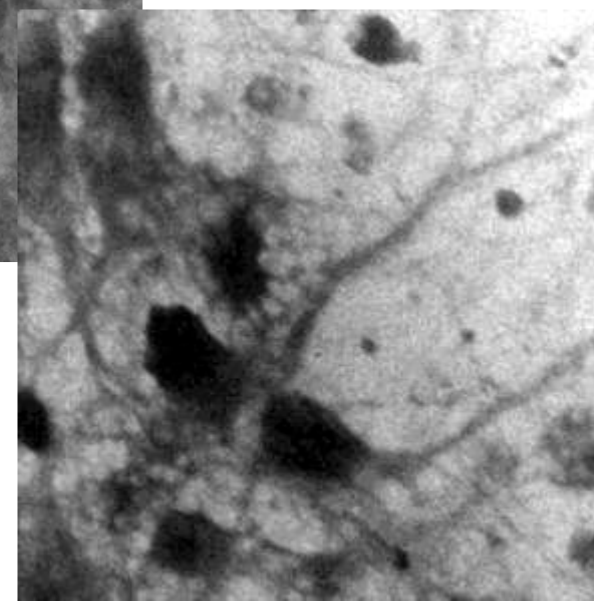

Multiple interconnected neurons

on 50 nm Si_3N_4 membrane,
200 SXR pulses
22 sec, 10 Hz

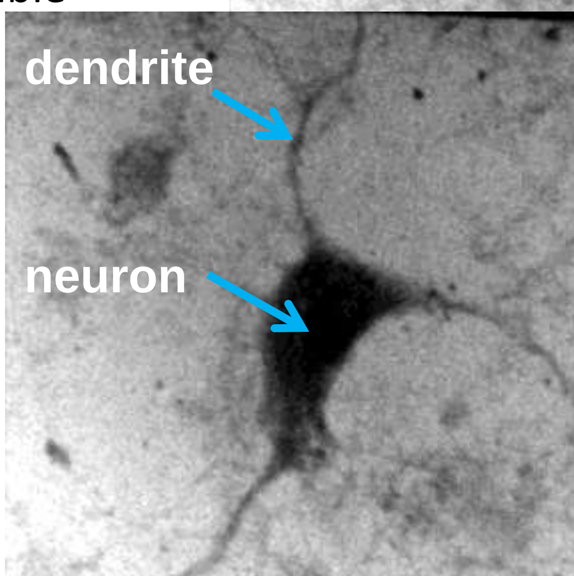

Individual neurons with dendrites

Samples courtesy of M. Odstrčil, Paul Scherrer Institut (Switzerland)

PAUL SCHERRER INSTITUT

P.W. Wachulak,et al., Proc. SPIE 2017

20-nm-resolution SXR microscopy demonstrated by use of multilayer test structures

BERKELEY LAB
LAWRENCE BERKELEY NATIONAL LABORATORY

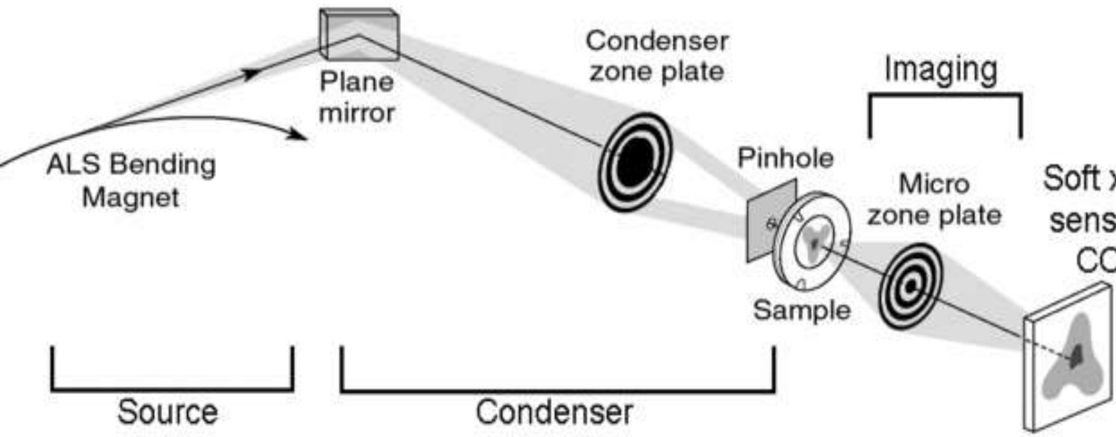

Schematic diagram of the soft x-ray, full-field imaging microscope, XM-1, at the Advanced Light Source (ALS)

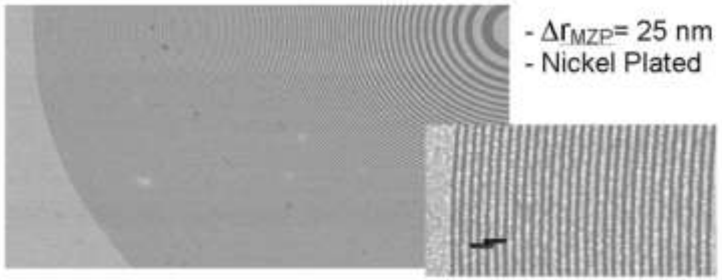

SEM micrograph of a 25-nm outermost-zone-width MZP

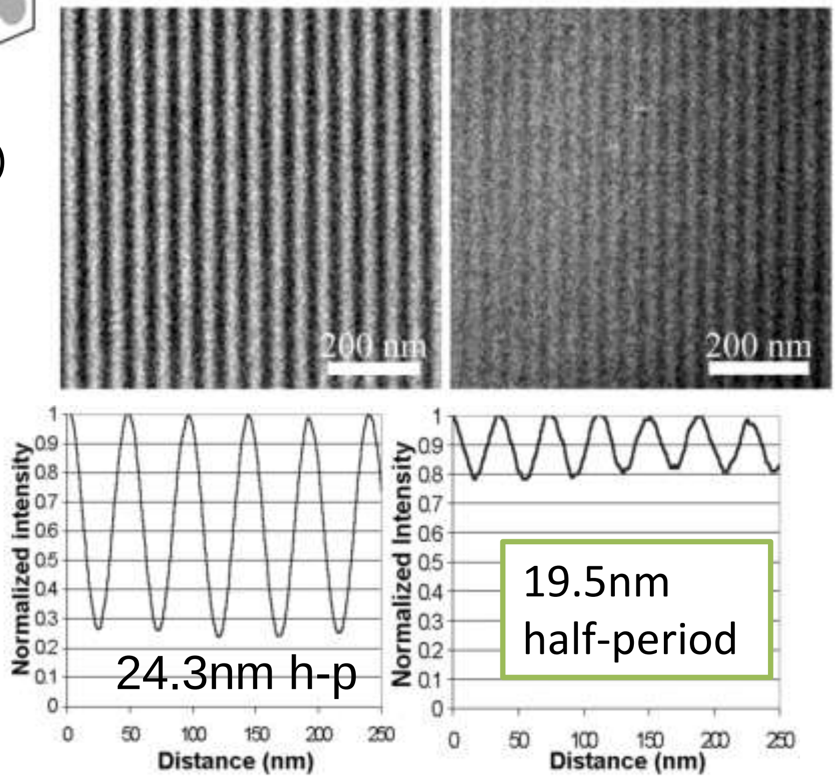

λ=2.07nm (600eV), spatial resolution 20nm (diffraction limit 19nm)

Condensor: D=10mm, 5mm CS, 41700 zones, dr=60nm, NA=0.017, f=289mm

Objective: D=30um, 300 zones dr=25nm, NA=0.04, f=0.362mm

W. Chao, Optics Letters 28, 21 (2003)

Demonstration of 12 nm Resolution Fresnel Zone Plate Lens based Soft X-ray Microscopy

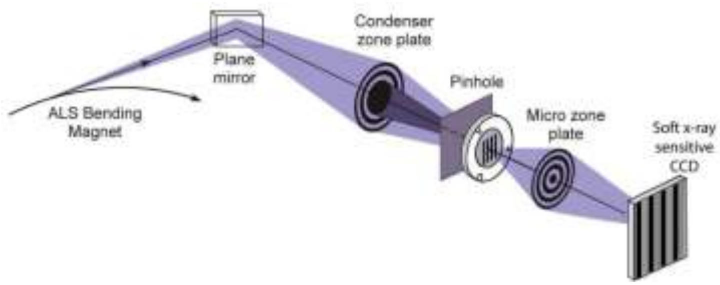

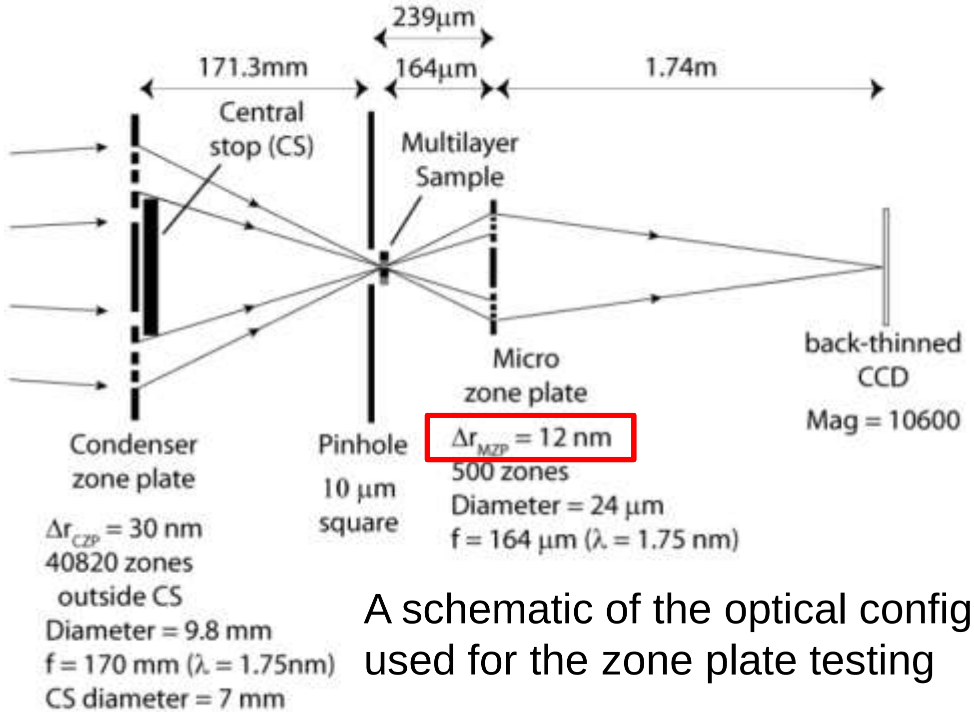

A schematic of the optical configuration used for the zone plate testing

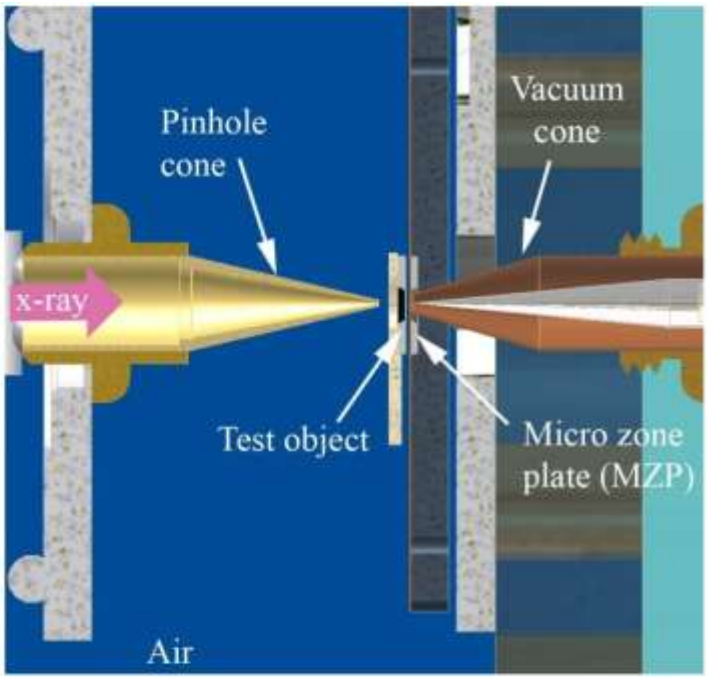

Imaging setup of the test object and the 12 nm zone plate at the XM-1 microscope

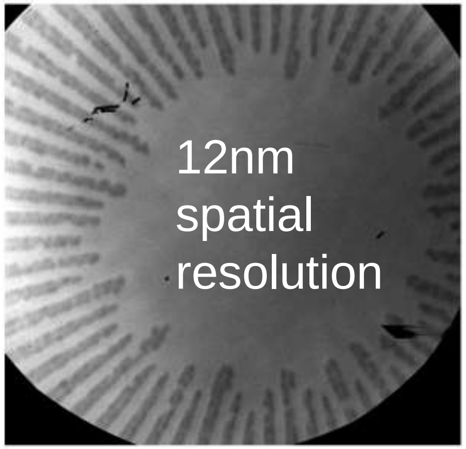

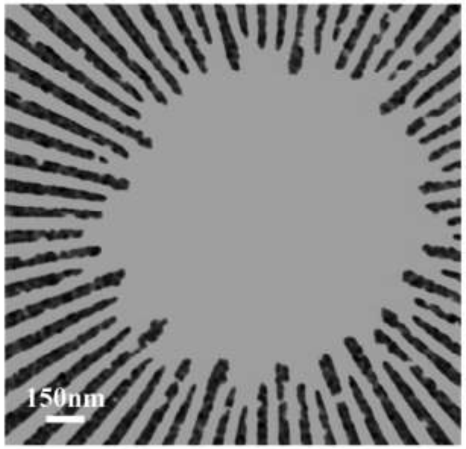

SXR image @ λ=1.75nm TEM image

W. Chao, Optics Express 17, 20 (2009)

Flowchart of the EUV/SXR tomography experiment

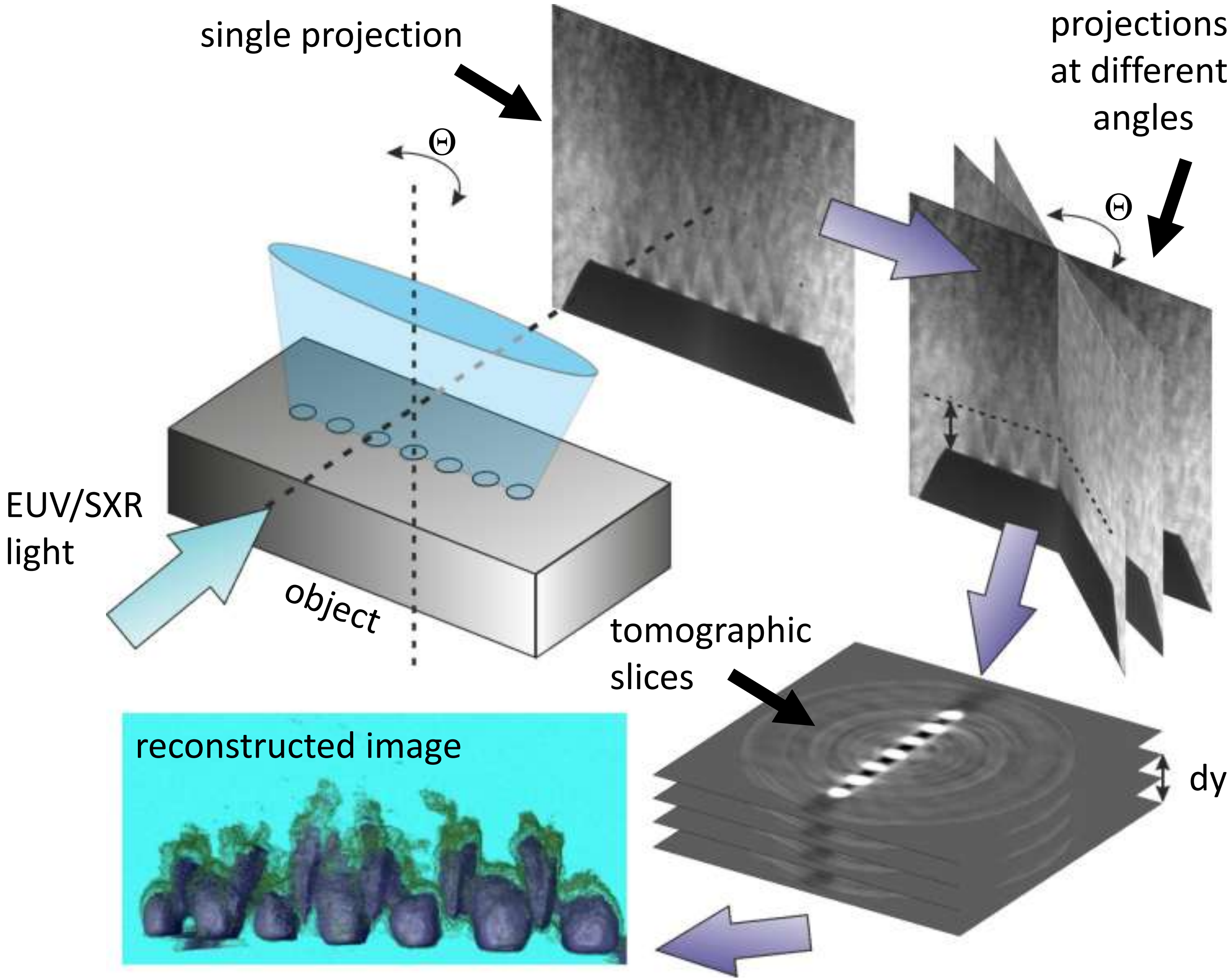

Wachulak et al., Appl. Phys. B, 117, 1, 253-263 (2014),DOI 10.1007/s00340-014-5829-7

Soft X-ray microtomography

National Center for X-ray Tomography

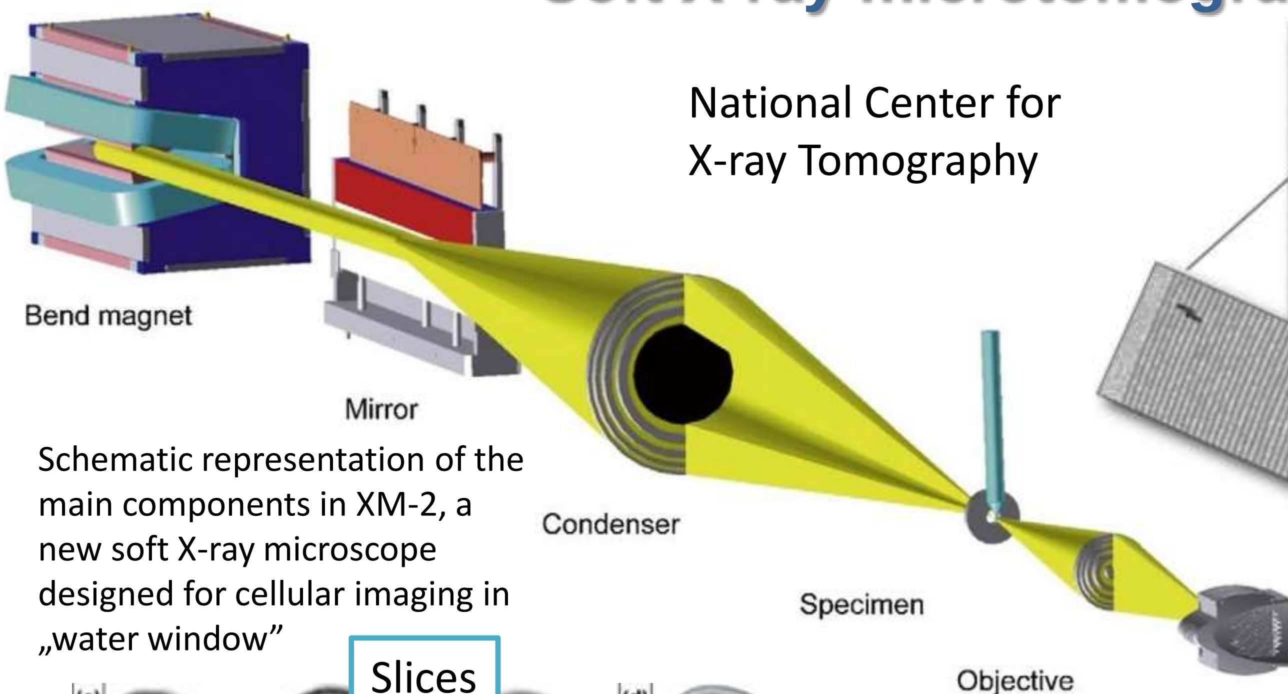

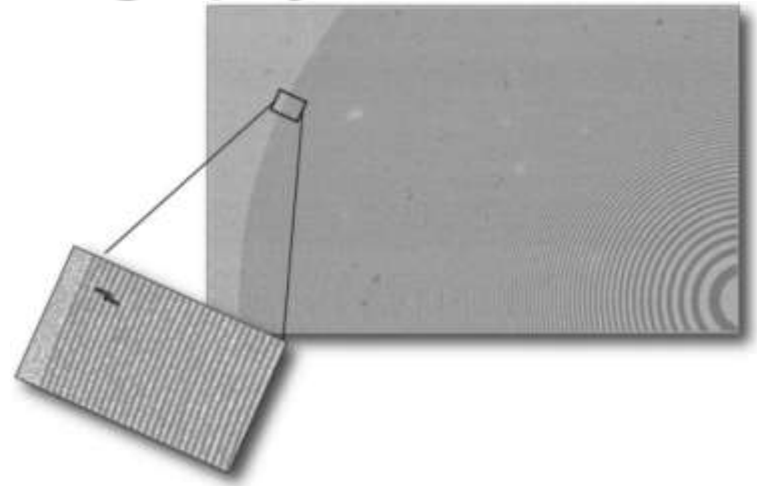

Schematic representation of the main components in XM-2, a new soft X-ray microscope designed for cellular imaging in „water window”

Slices

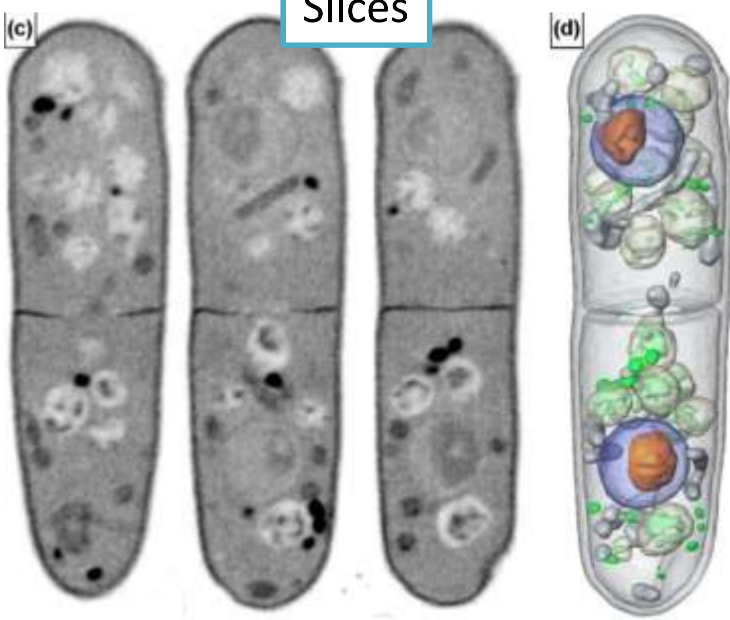

3-D recon-struction

Soft X-ray projection image of cryo-fixed NIH 3T3 cells

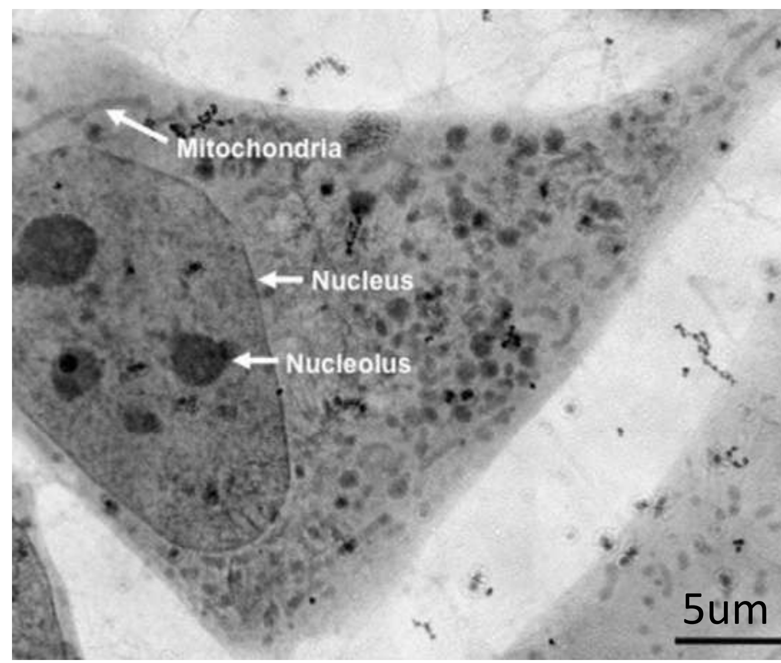

G. McDermott, et al., Trends in Cell Biology 19, 11, 587 (2009)

Soft X-ray microtomography

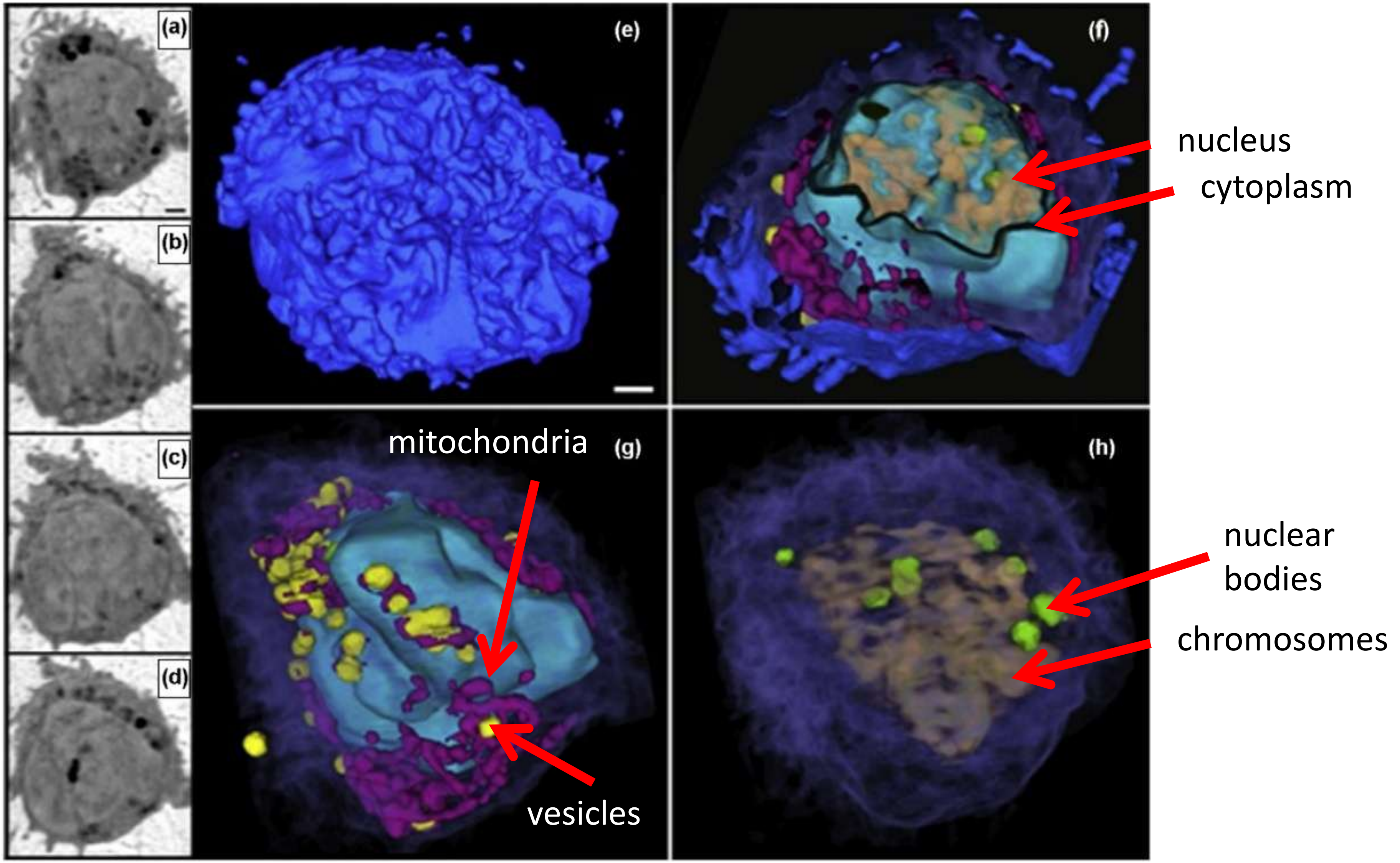

(a-d) slices from the tomographic reconstruction of a cryo-fixed T-cell

(e) cell surface with numerous filopodial extensions
(f–h) section views

G. McDermott, et al., Trends in Cell Biology 19, 11, 587 (2009)

High-resolution computed tomography with a compact soft x-ray microscope

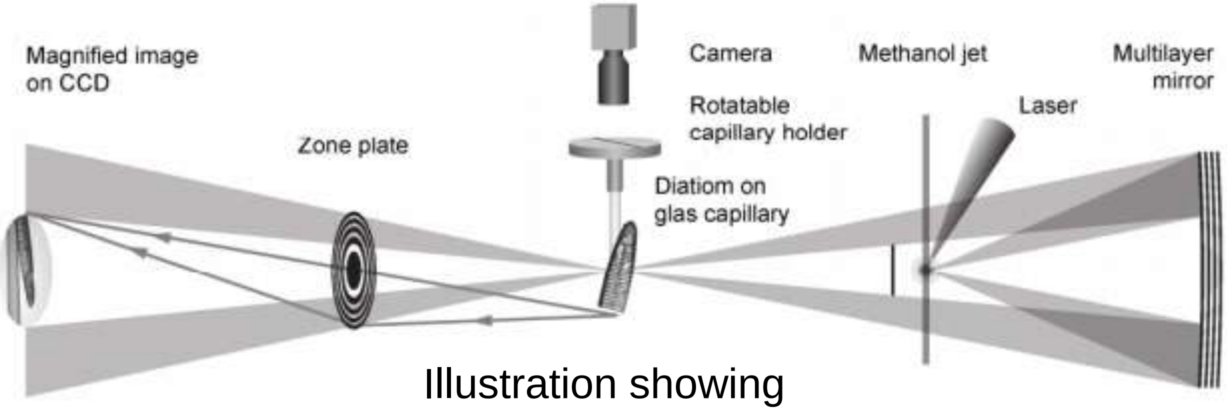

Illustration showing
the arrangement of the microscope

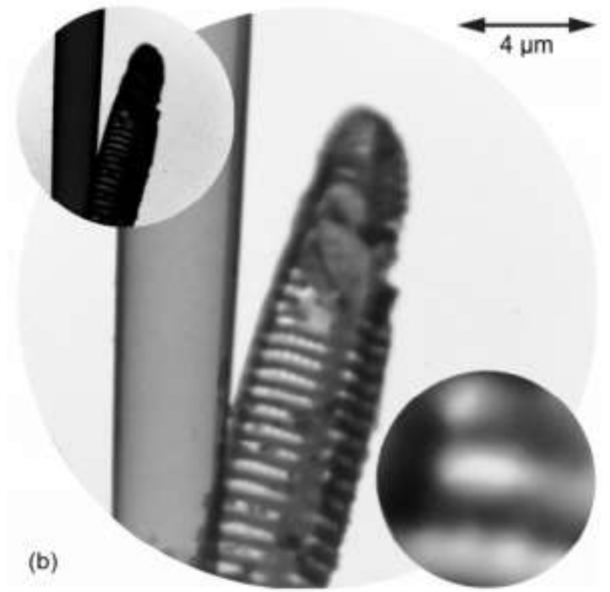

projection image of a diatom

- 100Hz/3ns/100mJ pulses, Nd:YAG 2nd harmonic 532nm
- ethanol droplet target, Cr/Sc condensor mirror, λ=3.37nm,
- 300nm Ti filter, 2E6 photons/um^2/s
- ZP: Ni, D=56um, 468 zones, dr=30nm, f=498um.

Selected slices through the reconstructed tomgram

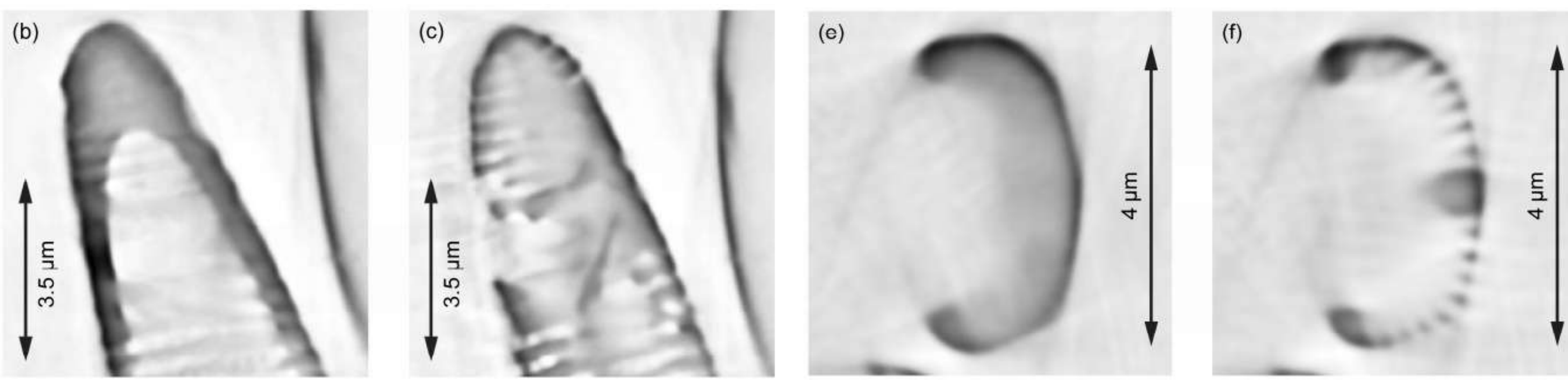

M. Bertilson et al., Optics Express 17, 13, 11057 (2009)

High-resolution computed tomography with a compact soft x-ray microscope

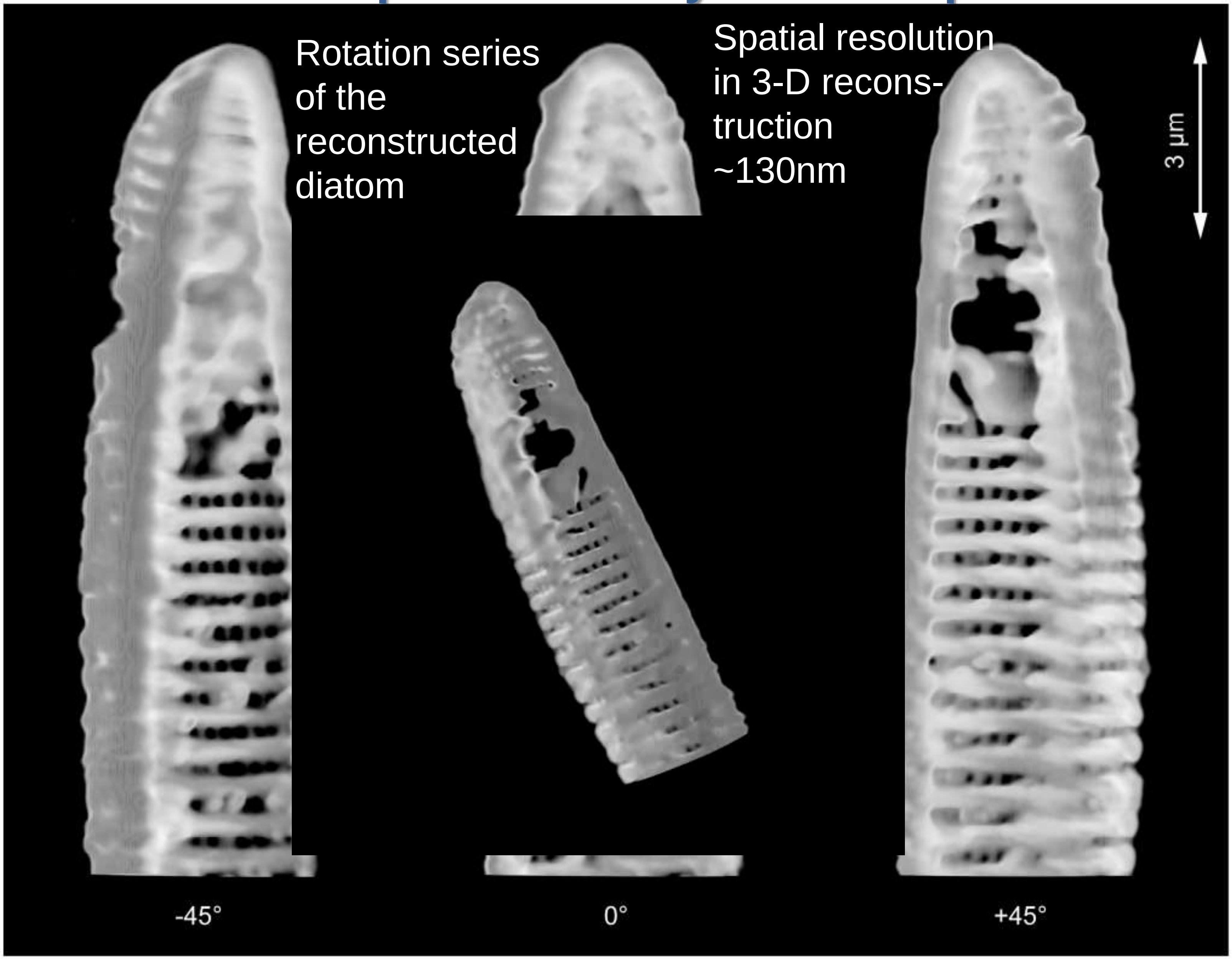

Three-Dimensional GaN-Ga_2O_3 Core Shell Structure Revealed by X-Ray Diffraction Microscopy

Schematic layout of the 3D x-ray diffraction micro-scope, combining *ab initio* phase recovery with tomographic image reconstruction

SPring-8 @ 5 keV

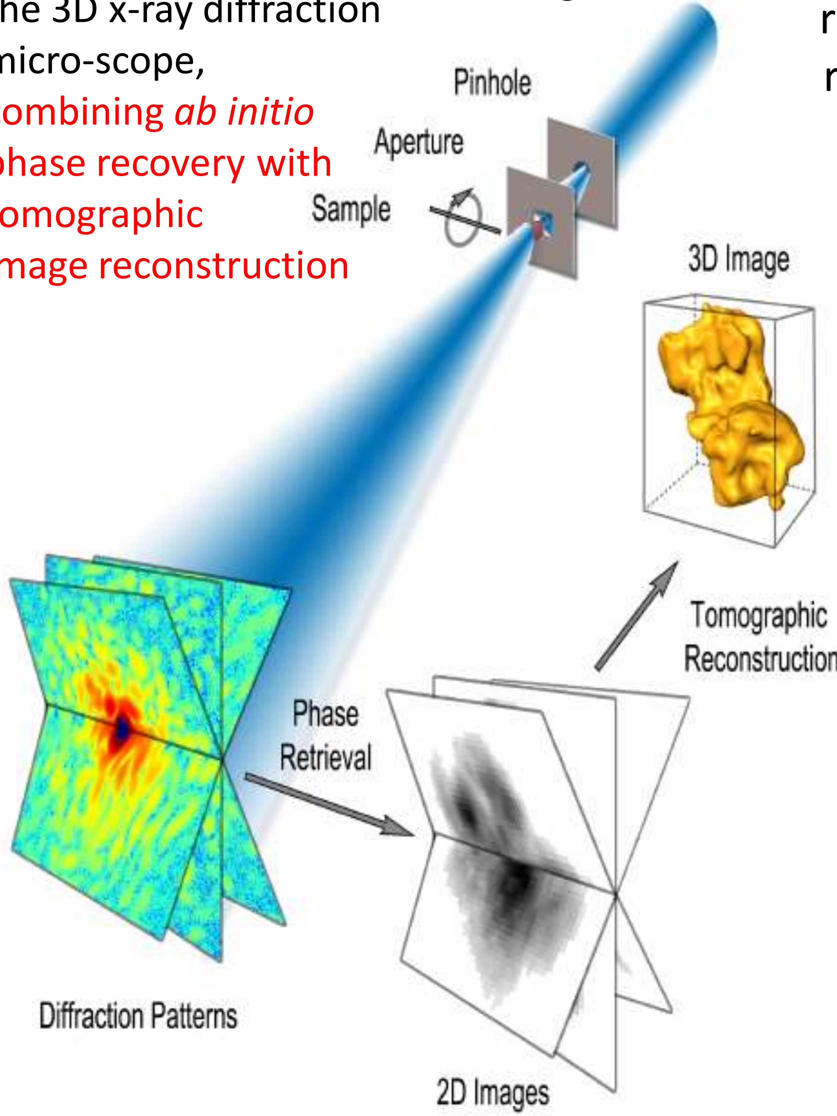

Isosurface rendering of a reconstructed 3D GaN quantum dot particle

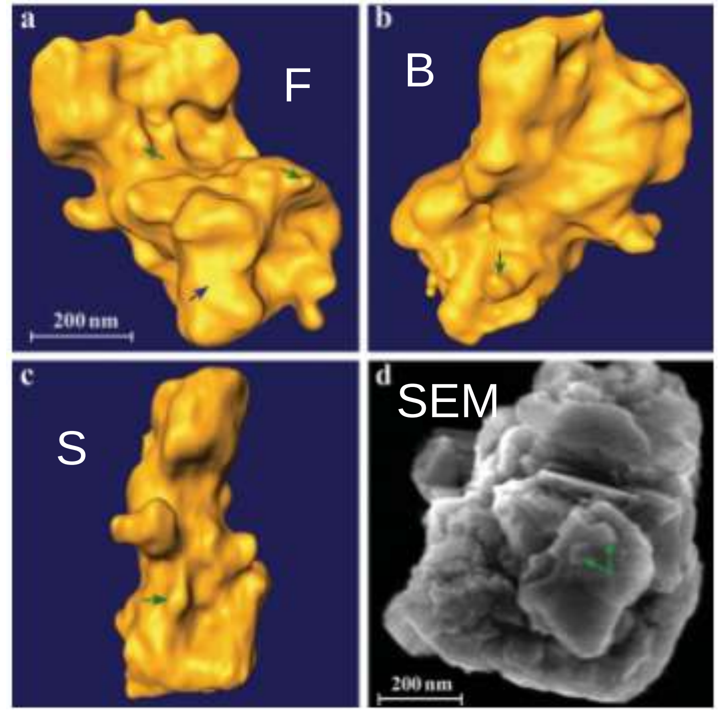

3D internal structure of the GaN quantum dot particle

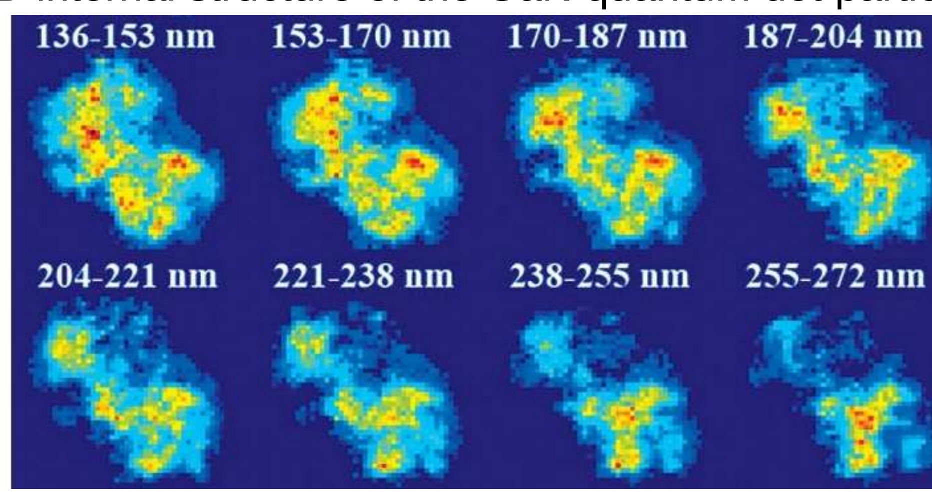

J. Miao et al., PRL 97, 215503 (2006)

Soft X-ray contact microscopy (SXCM)

Environmental specimen chamber

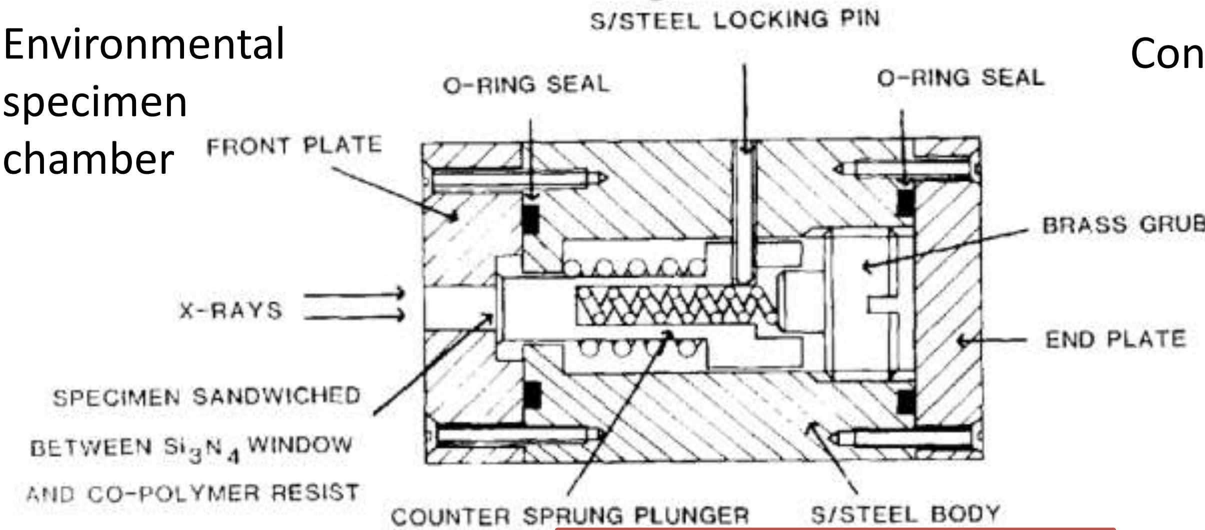

Contact microscopy method

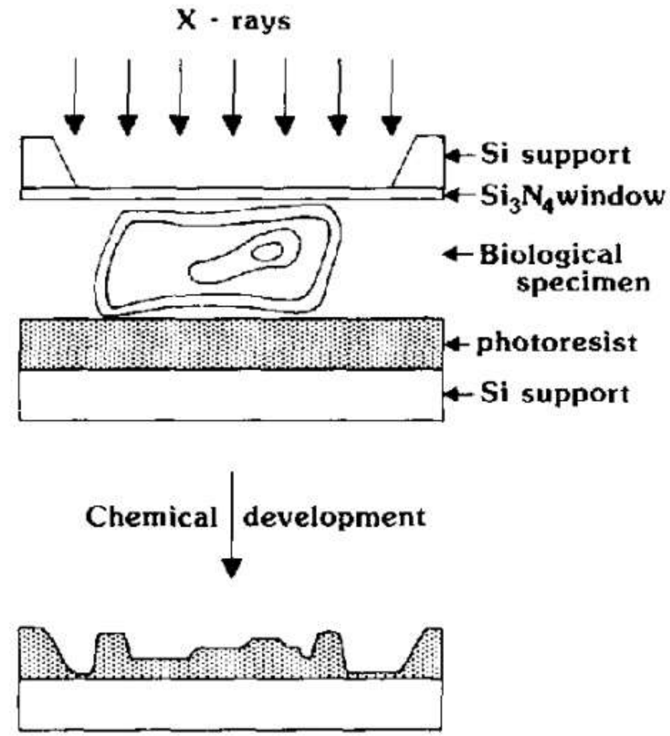

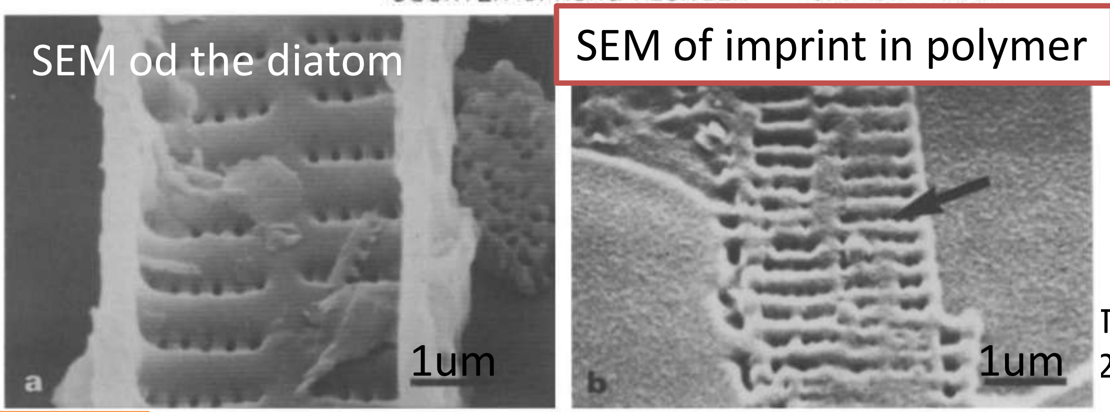

T. W. Ford, et al., Electron Microsc. Rev. 4, 269-292 (1991)

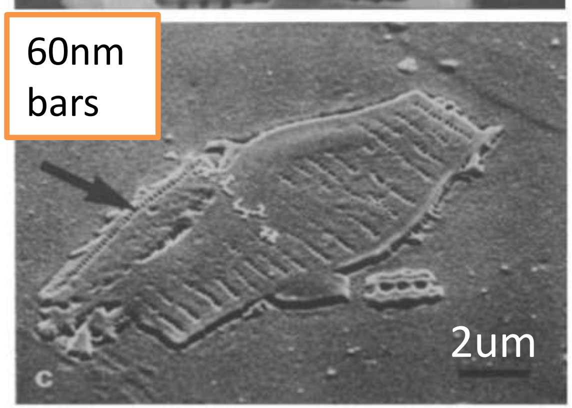

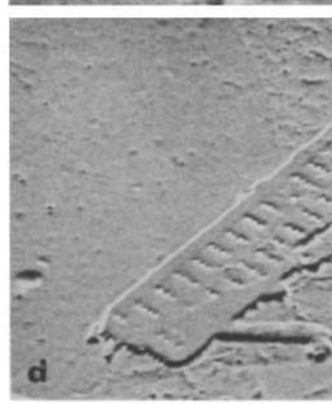

Advantages:

- ✓ the simplest implementation of X-ray microscopy
- ✓ applicable to the large range samples
- ✓ nanoscale resolution and natural contrast
- ✓ no sophisticated optics
- ✓ does not need coherent radiation source
- ✓ possibility of single-shot imaging

Soft X-ray imaging of living cells in water: flash contact soft X-ray microscope

- PMMA photoresist, 40nm spatial resolution
- imaging in water window from LPP source (yttrium target)

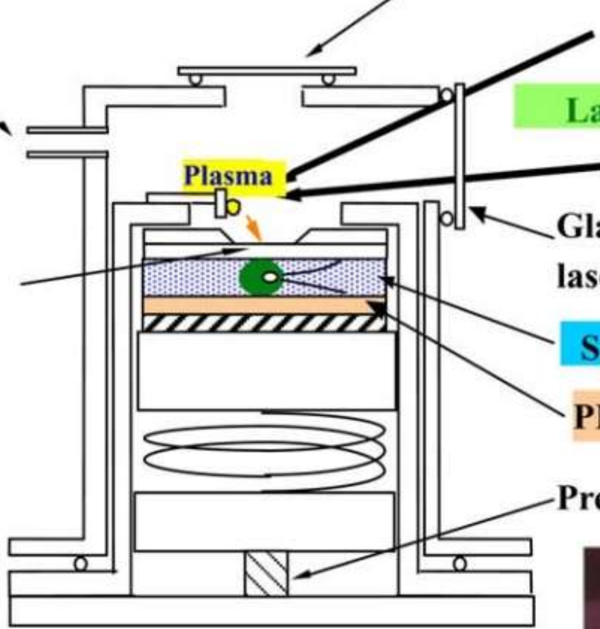

Cross-section of the X-ray exposure chamber

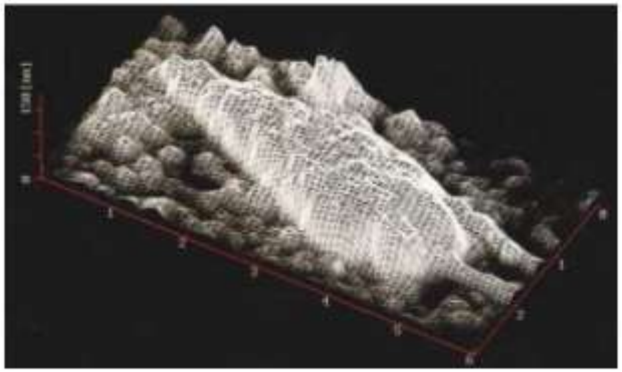

X-ray image of a sea-urchin sperm in seawater

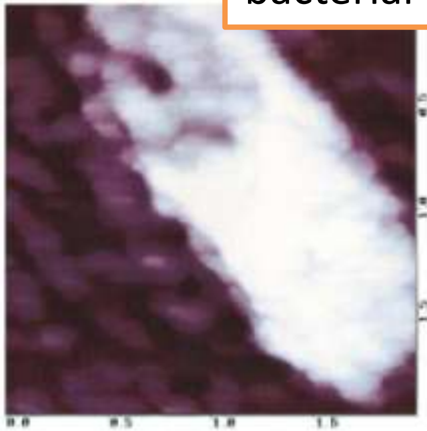

X-ray image of bacterial cell

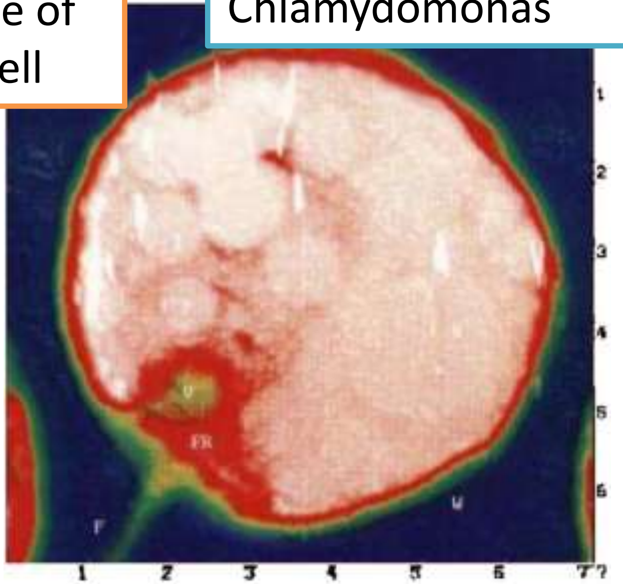

X-ray image of Chlamydomonas

„ The amount of X-ray to make an X-ray image with a spatial resolution of 100 nm is at least more than 10^4 times the dose level that causes biological damage to the specimens"

T. Majima, Trends in Analytical Chemistry 23, 7, 2004

Imaging of chromosomes using contact microscopy

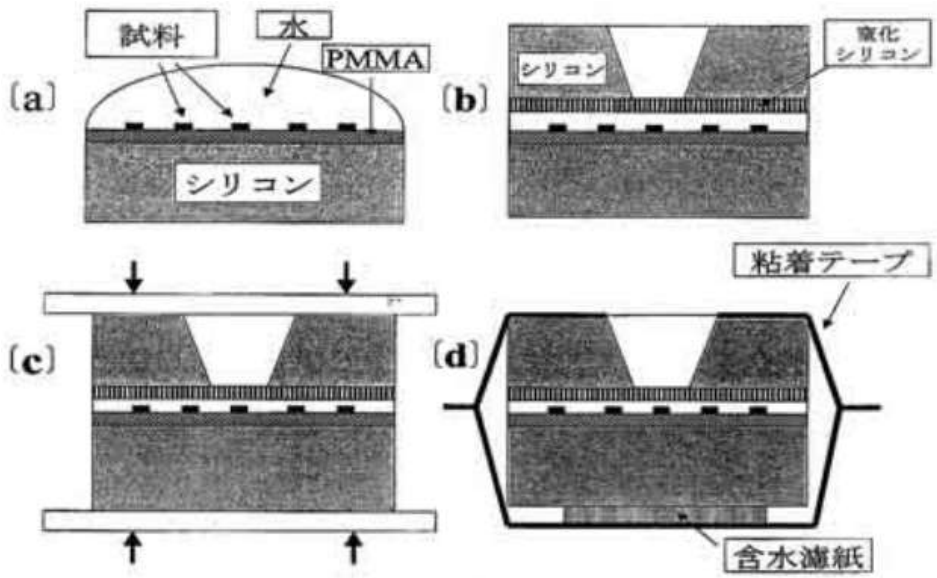

Wet chamber for the sample

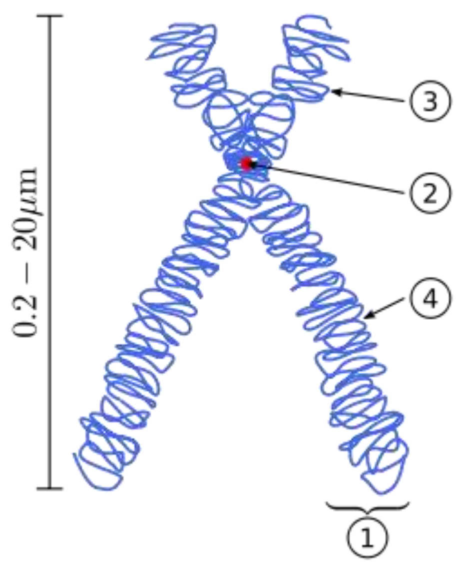

http://en.wikipedia.org/wiki/Chromosome

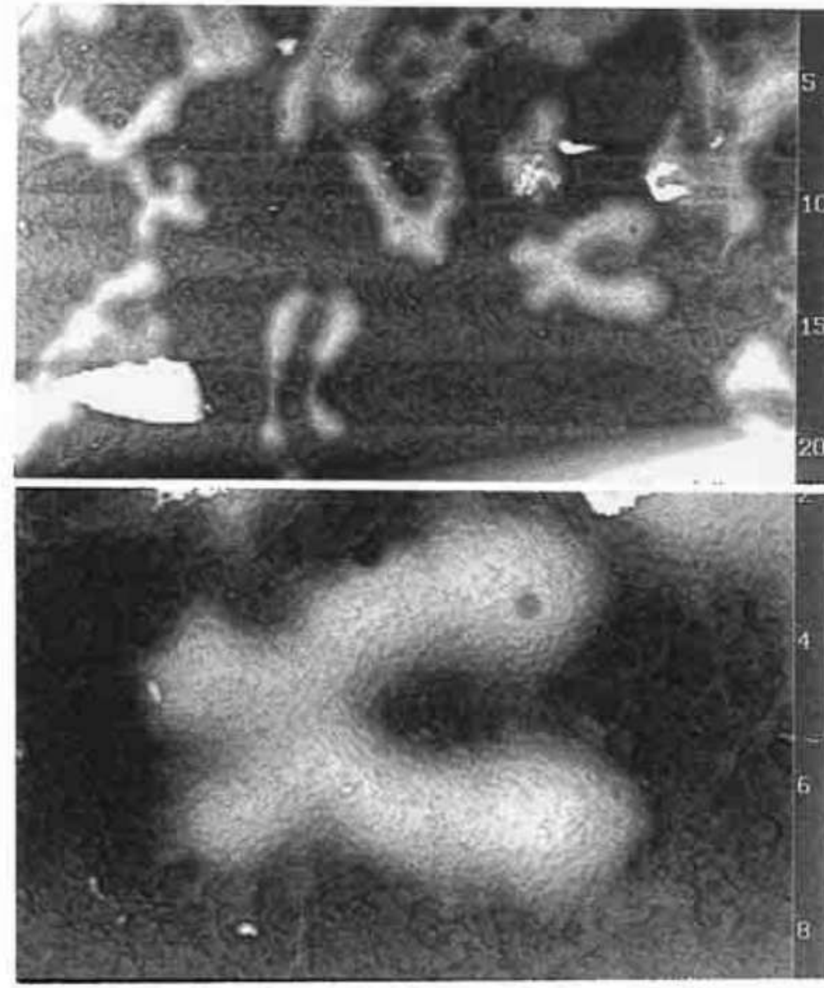

Metaphase chromosomes in the dry state (contact X-ray image)

Y. Kinjo…, H. Fiedorowicz, et al., No. 5 Tokyo Metropolitan Industrial Technology Research Institute research report (2002)

Imaging of fine structures of cellular organelles in hydrated biological cells by a soft x-ray microscope

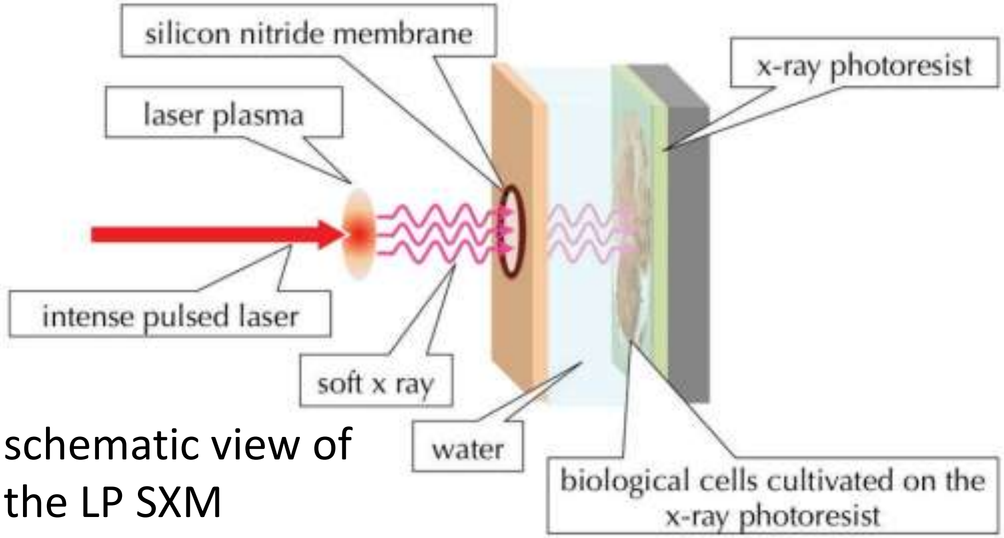

schematic view of the LP SXM

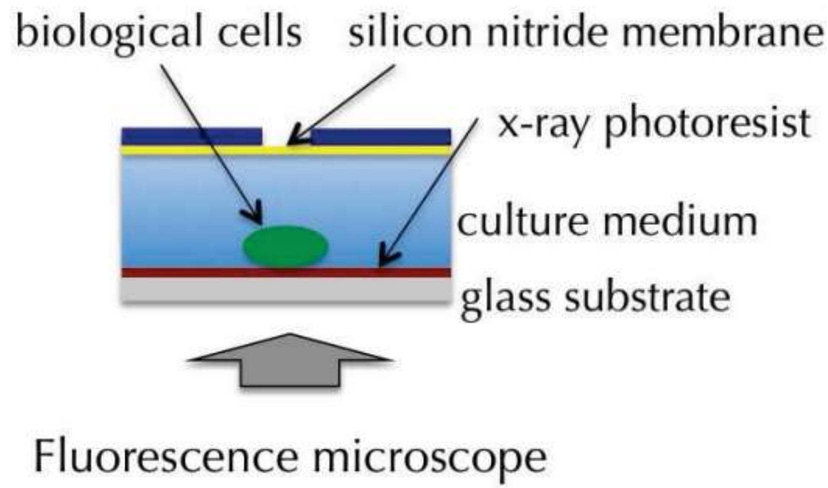

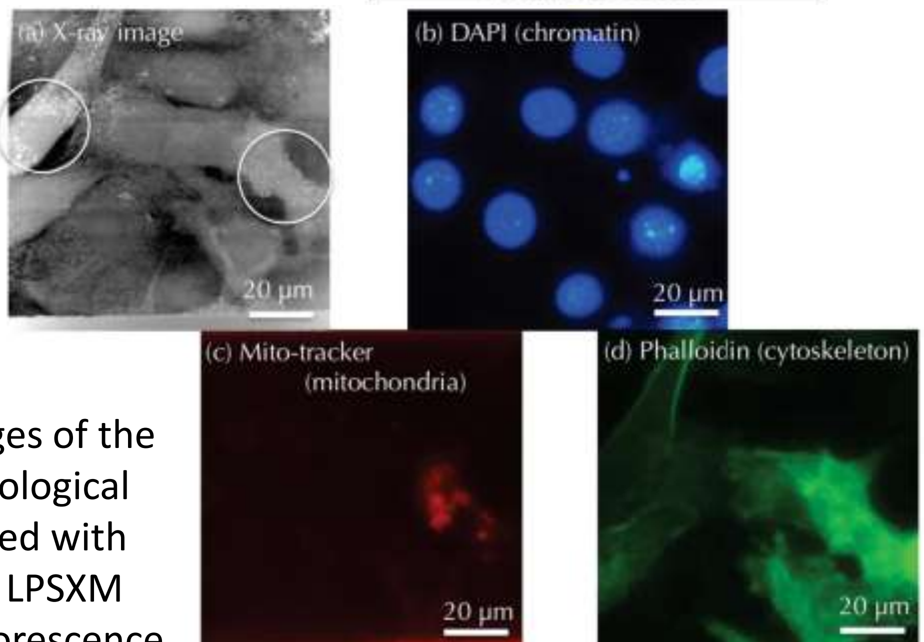

hybrid images of the hydrated biological cells obtained with both of the LPSXM and the fluorescence microscope

SXR with fluorescence microscope

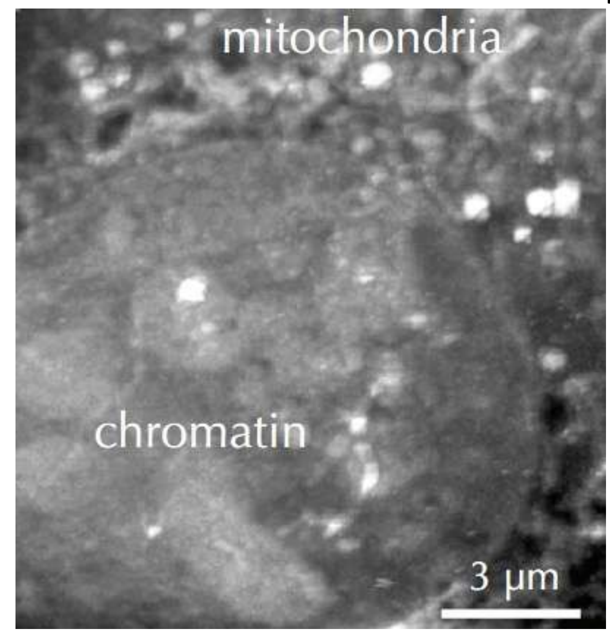

M. Kado et al., Proc. of SPIE 8849, 88490C-1 (2013)

Contact microscopy setup

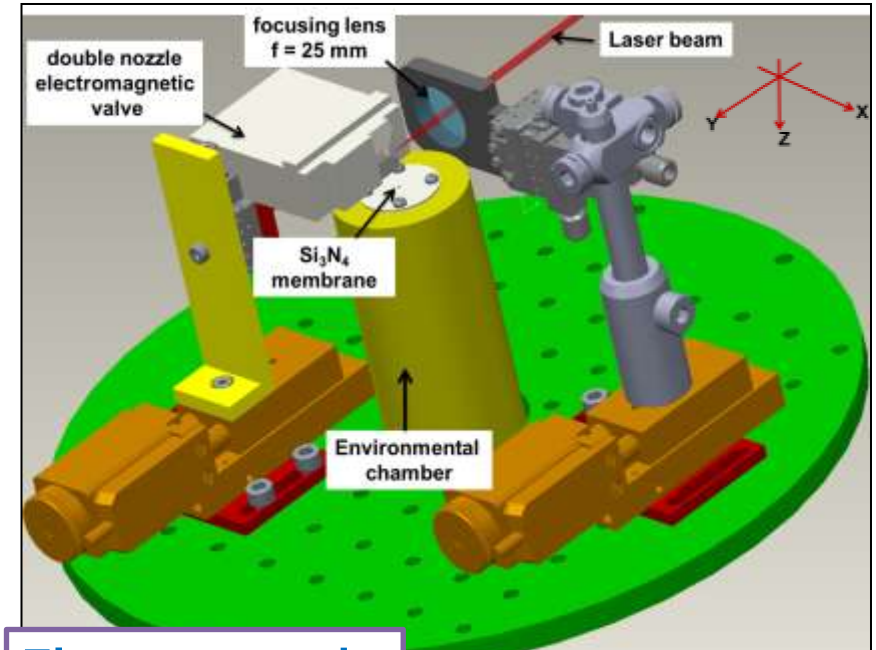

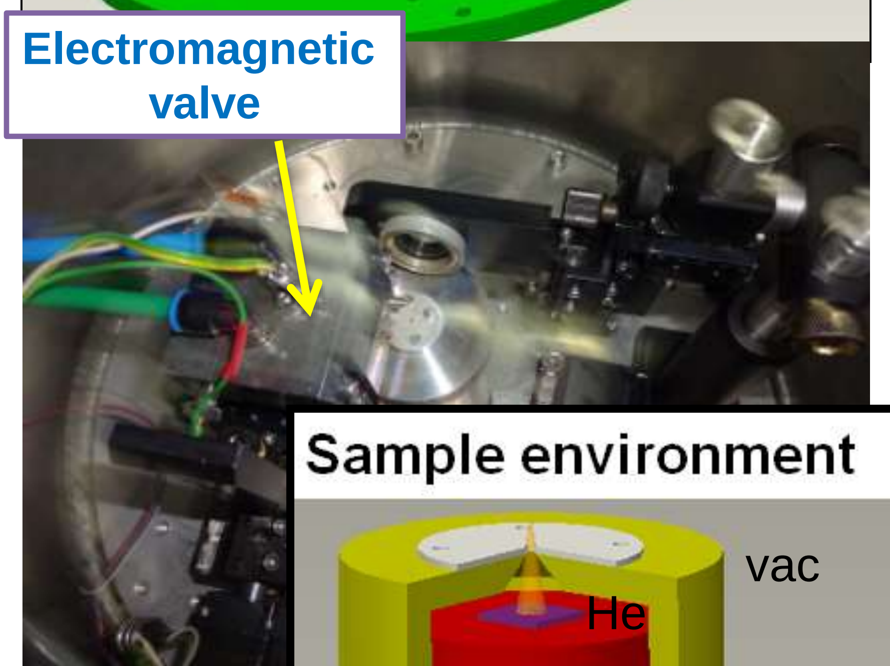

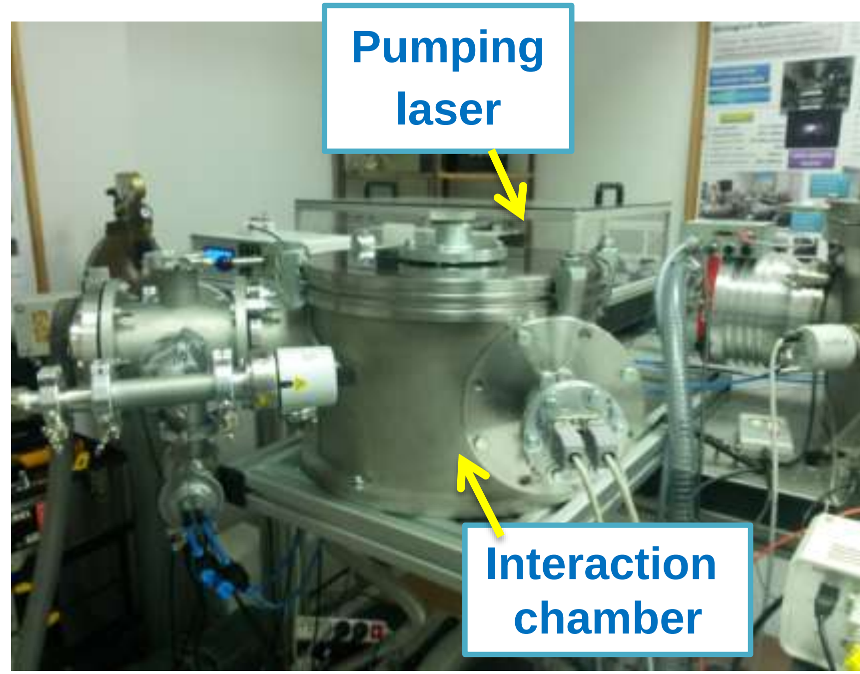

Interaction chamber and components of the source

Pumping laser	Nd:YAG laser (EKSPLA), 740mJ/ 4ns pulse duration,10 Hz repetition rate, λ= 1064 nm
Double nozzle electromagnetic valve	Inner circular: Ø~ 0.4 mm Outer ring: Ø~ 0.7 mm - 1.5 mm
Target gas	Working gas: Ar, Kr, Xe, O_2, N_2 Outer gas : He
Focusing lens	Spherical biconvex lens Focal length: 25 mm

Contact SXR microscopy

Soft X-ray source

Samples on PMMA photoresist

Sample cleaning & photoresist etching
- NaOCl
- MIBK:IPA

Chemical development generates the SXR image of the specimen on the PMMA surface as imprint

Argon plasma source

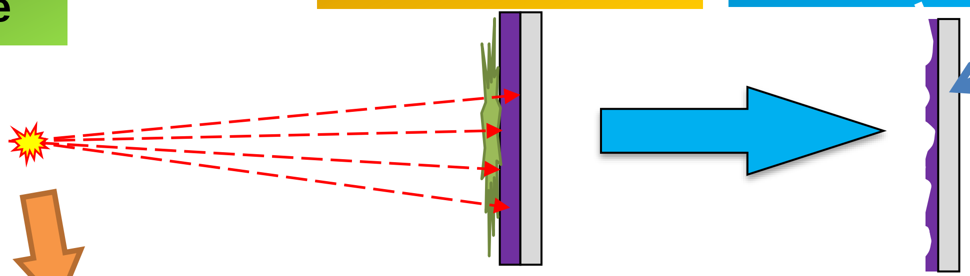

Final inspection with AFM

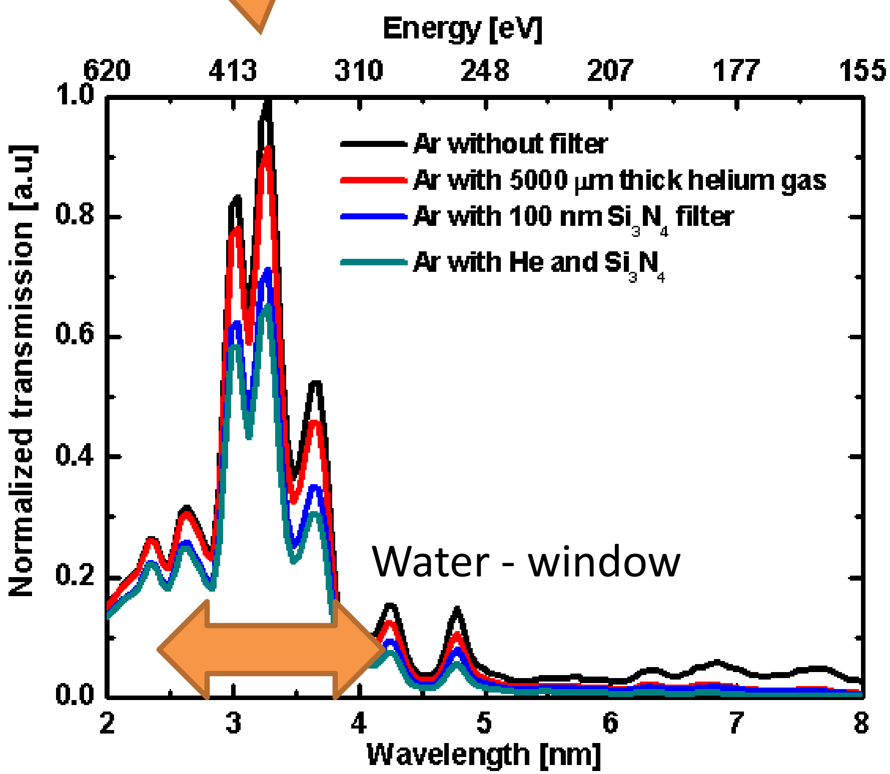

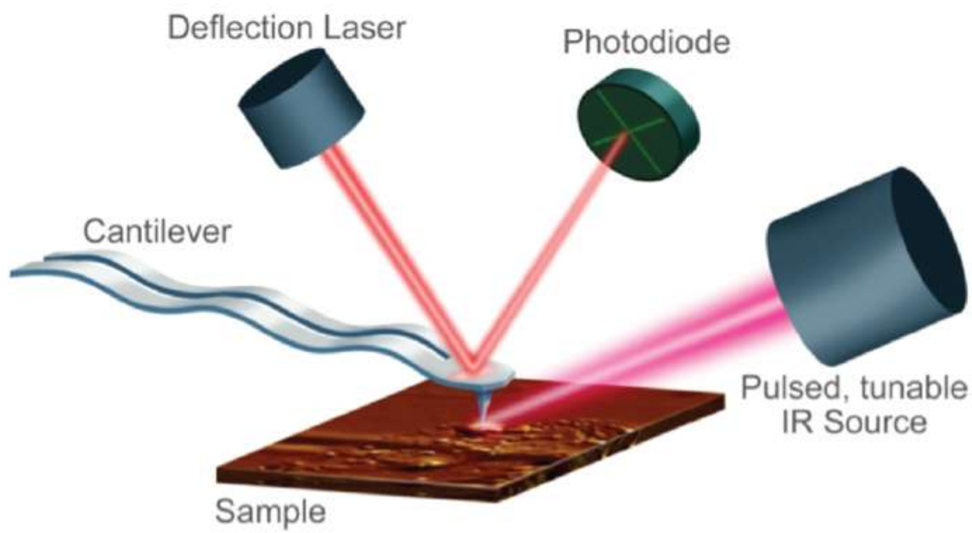

Soft X-ray images by contact microscopy of malignant bladder cancer cells (T24)

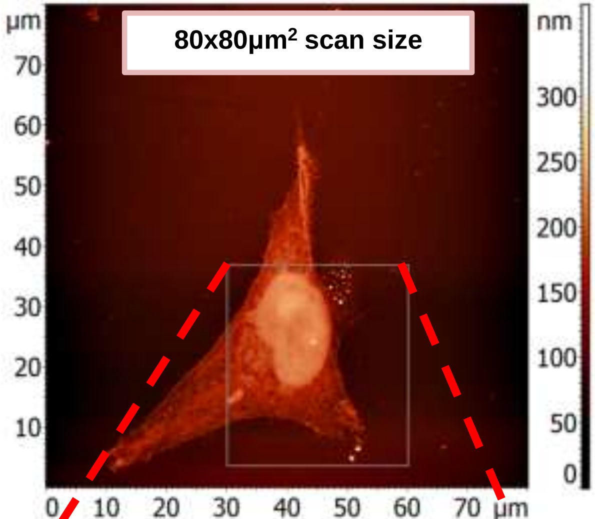

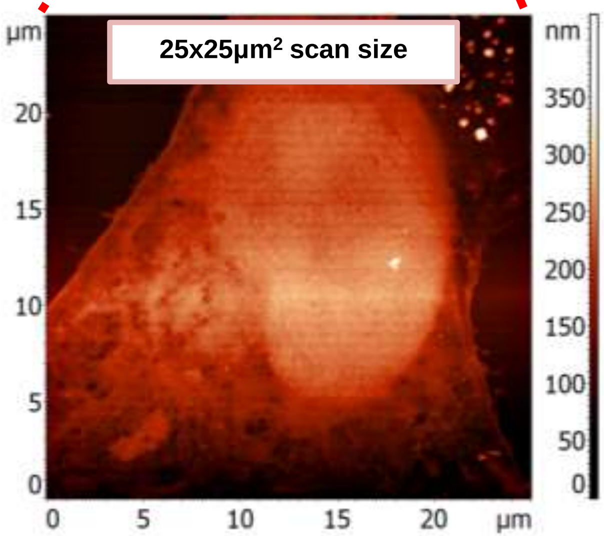

PMMA MW 90k or 350k

SXCM images of bladder cancer cells (T24), 20 laser shots (2 sec exposure time)

AFM images of a developed photoresist

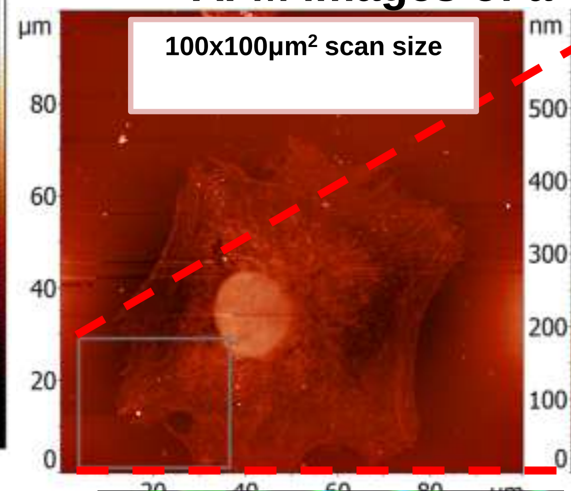

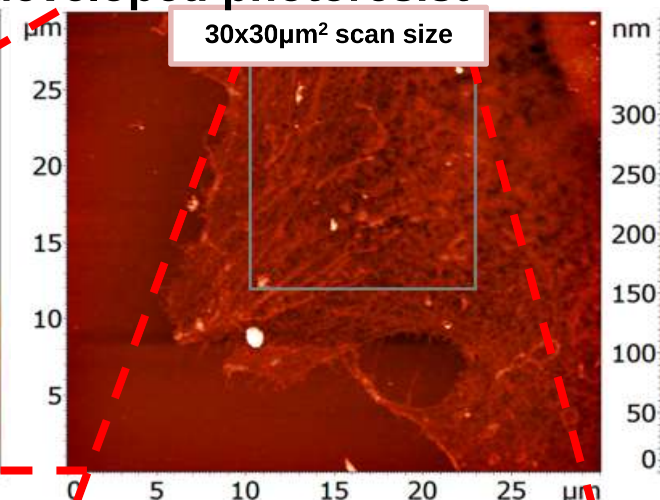

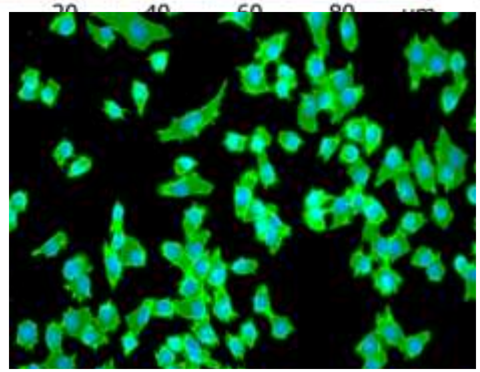

- **Samples stained with Hoechst (Nucleus) and Phalloidin (cytoskeleton)**

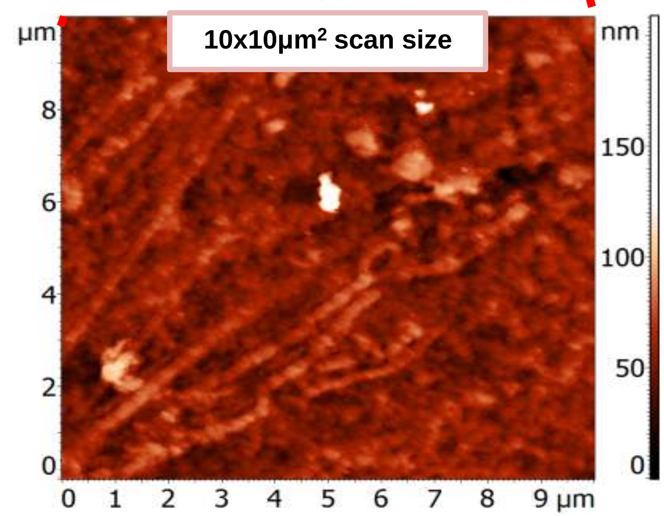

Advantage: during one exposure -> **600x600 μm² imprint.**

If our res. 80nm -> 7.5k x 7.5k (56 Mpix image)

M.G. Ayele, et al., NIMB (2017), DOI: 0.1016/j.nimb.2017.03.082

Soft X-ray images by contact microscopy of fixed epidermal cells (Keratinocytes)

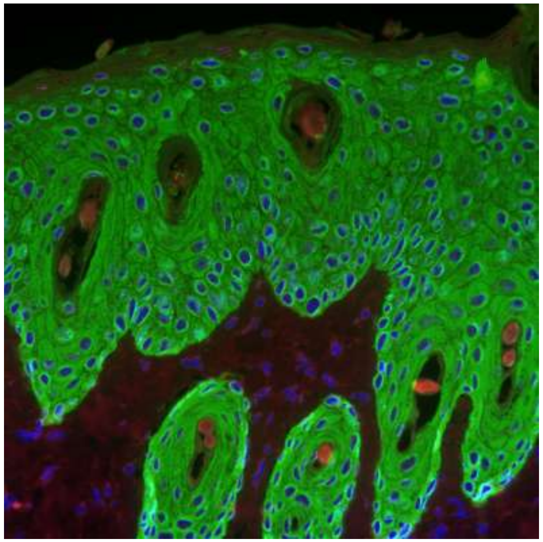

Fluorescence microscope image of Keratinocytes

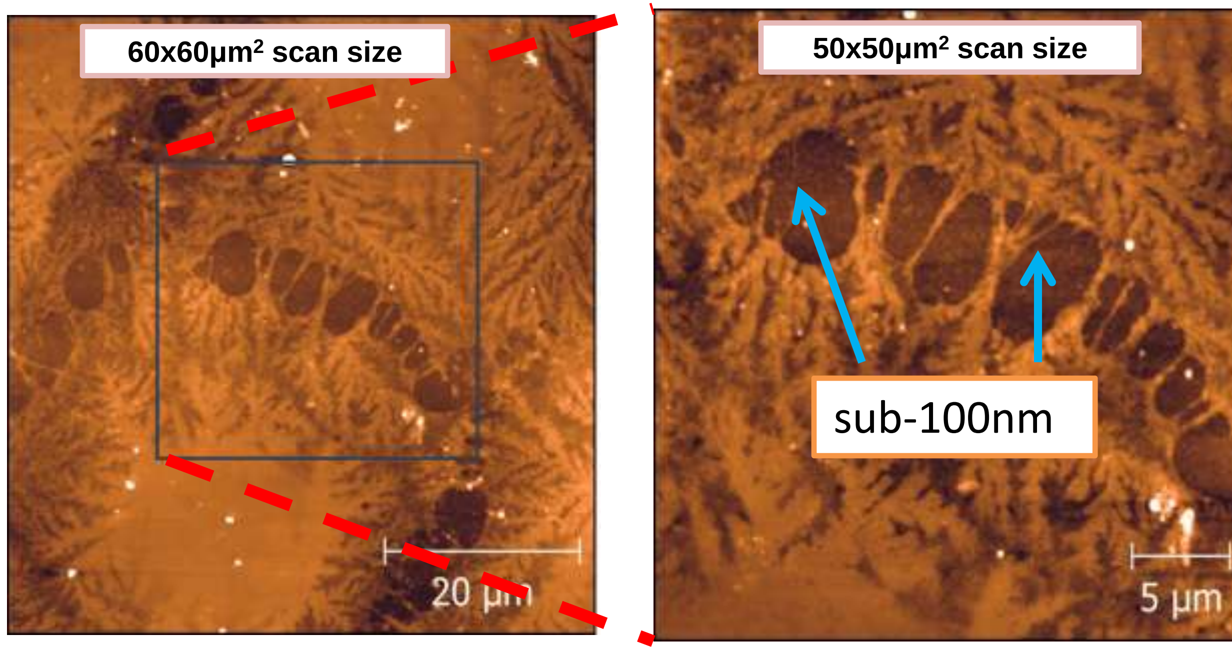

AFM images of a developed photoresist

No. of soft X-ray pulses: 200 SXR pulses
Exposure time: 20 sec
Scan : AFM_NDMT
Tip diameter= 20 nm
Scanning mode: semi-contact
No. points/ scan line: 512 pts
Photo resist development time: 90s
Developer concentration: 1:2 v/v (MIBK:IPA)
Knife-edge resolution 80nm (half-pitch)

Mesfin Ayele, EXTATIC PhD student

EXTATIC Erasmus Mundus

M.G. Ayele et al., Acta Physica Polonica 129, 2, 237-240 (2016),

Contact microscopy SXCM – living samples

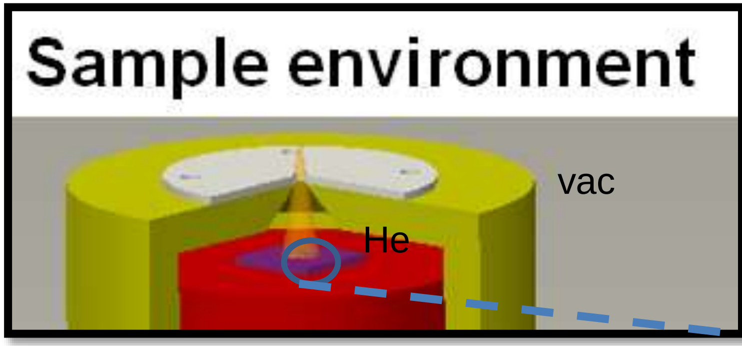

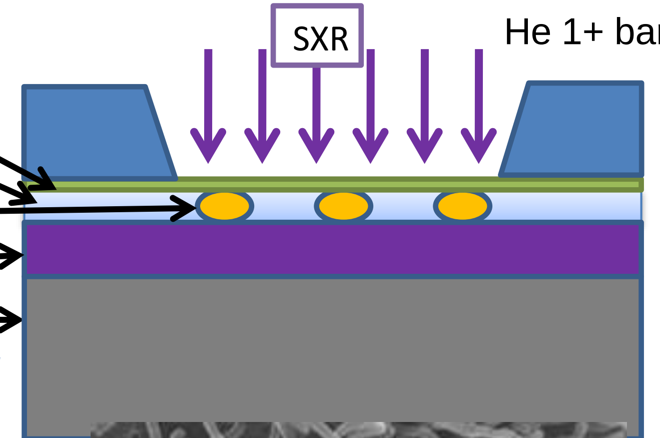

SEM images of the Human prostate cancer cells (DU 145). Scale bar represents 50 µm, 10 µm and 2 µm.

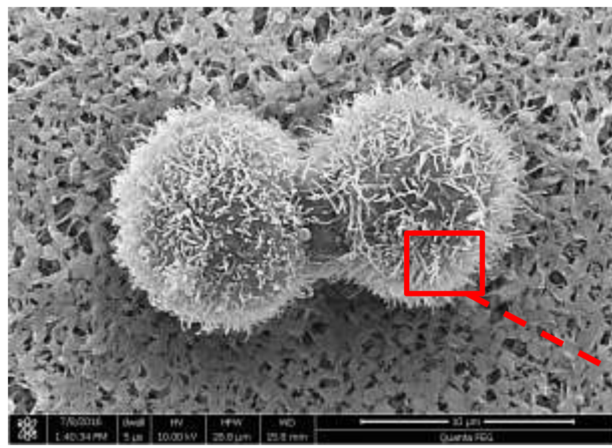

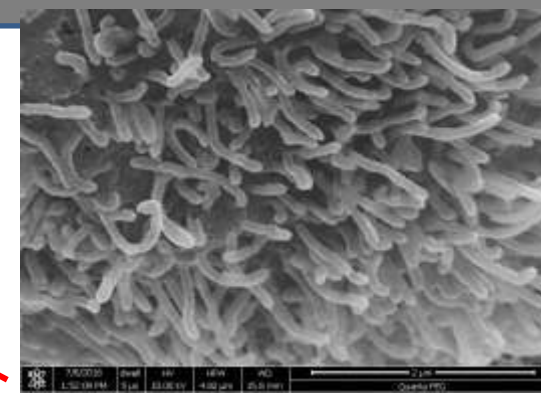

- source emission spectrum: **λ=2.7 - 5 nm,**
- He pressure inside the environmental chamber: **P=1bar (continuous flow)**
- exposure for wet samples **2000-8000 SXR pulses @ 10Hz**
- Recording medium: **500 nm thick PMMA on Si wafer**
- Postprocessing: PMMA developing procedure: **1:1 MIBK:IPA (3 minutes), AFM scan**

AFM image of living prostate cancer cell after the exposure to X-rays in laser plasma based SXCM

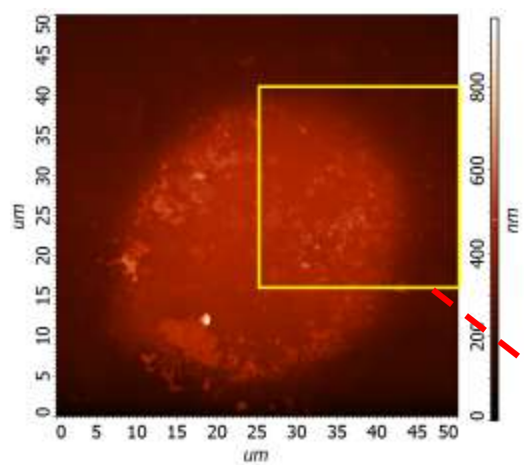

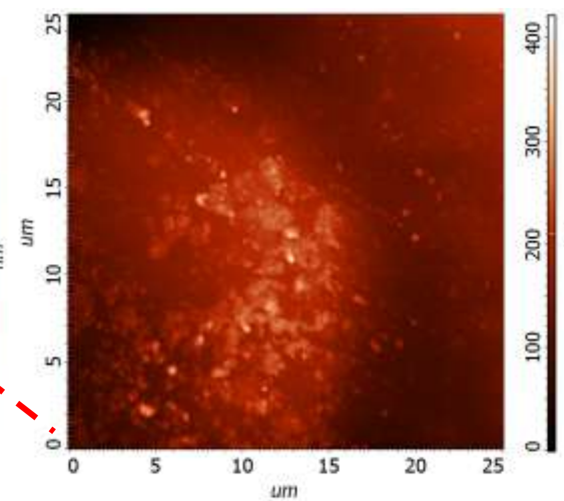

Please see: Paulina Osuchowska, et al. „X-ray microscopy imaging versus other microscopic techniques for analysis of human cancer cells morphology" (poster)

EUV/SXR imaging methods

high energy photons as information carriers

- ✓ EUV holography (Gabor, Fourier)
- ✓ Computer generated holograms
- ✓ Talbot imaging
- ✓ Coherent diffraction (lens-less) imaging
- ✓ Ptychography

coherent

- ✓ Zone plates for various wavelengths
- ✓ EUV microscopy using FZP
- ✓ Scanning EUV microscopy
- ✓ SXR and „water-window" microscopy

better incoherent

- ✓ EUV, SXR HXR tomography
- ✓ Contact microscopy

coh., incoh. are OK

Spatial scales and imaging methods

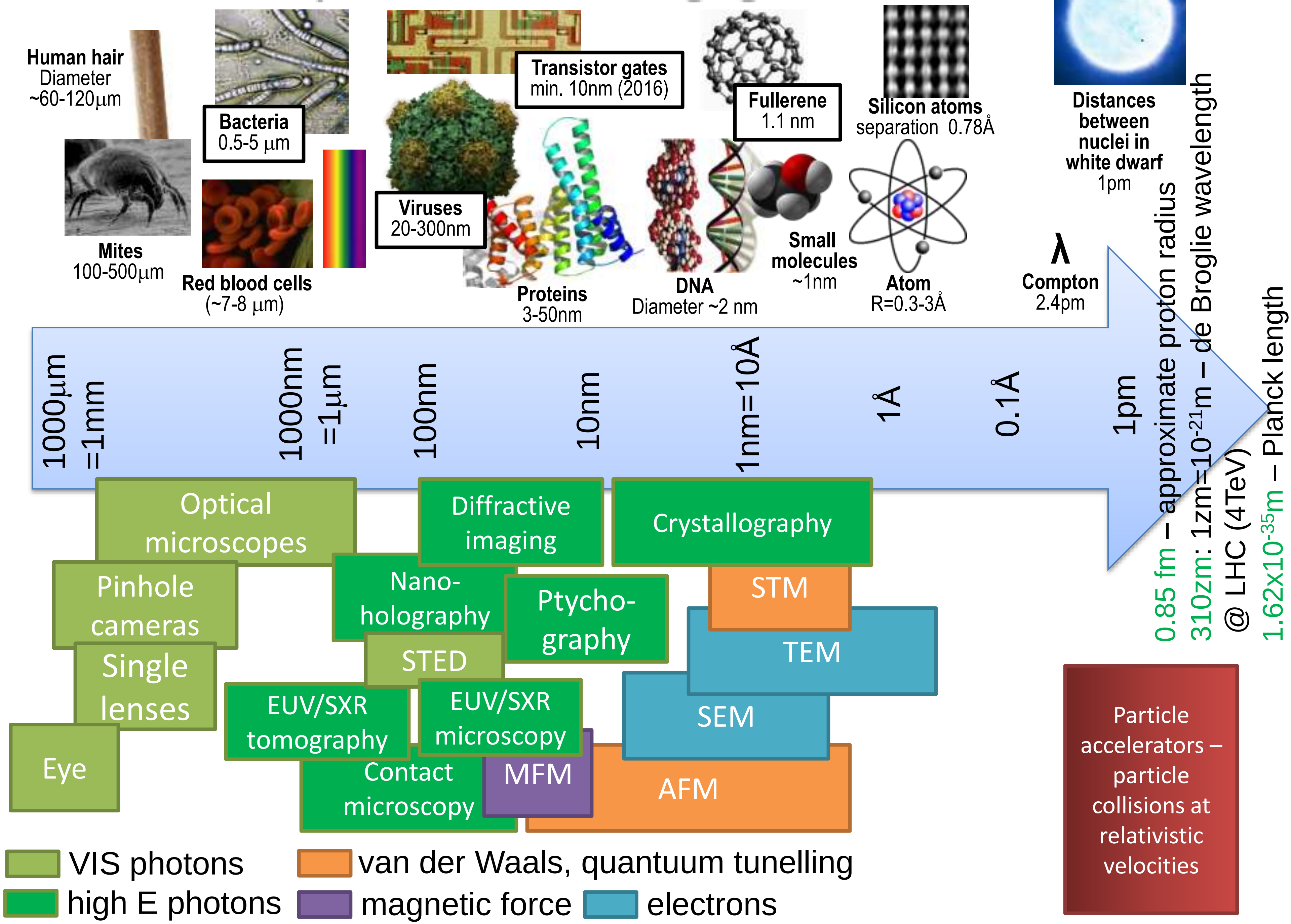

Acknowledgements

LMI

Laser Matter Interaction Laboratory
http://www.ztl.wat.edu.pl/zoplzm/
(in alphabetical order)

D. Adjei, M. Ayele, A. Bartnik, H. Fiedorowicz, T. Fok, R. Jarocki, J. Kostecki, I. Saber, A. Szczurek, M. Szczurek, A. Torrisi, Ł. Węgrzyński
J. Czwartos,

Institute of Physics, PAS (PAN)
A. Baranowska-Korczyc
K. Fronc, D. Elbaum

Czech Technical University
M. F. Nawaz, A. Jancarek, J. Limpouch
S. Salacova, J. Turnova, T. Parkman,

centrum inżynierii biomedycznej
P. Osuchowska, E. Trafny

Rigaku
Rigaku, Inc.
www.rigaku.com
L. Pina

greateyes
M. Regehly
Greateyes, GmbH

Institute of Electrical Engineering, Slovak Academy of Sciences,
Z. Zápražný, D. Korytár

NANO 나노종합팹센터 NATIONAL NANOFAB CENTER
H. T. Kim and S. Ch. Jeon

Astronomical Institute of the ASCR, v.v.i.
i Czech Technical Univ. w Pradze
R. Hudec

PAUL SCHERRER INSTITUT
PSI
M. Odstrcil

Colorado State University
Los Alamos National Laboratory EST. 1943
Colorado University of Colorado at Boulder
EUV
JILA NIST CU
The University of Wisconsin Madison

Engineering Research Center, Colorado State University, University of Wisconsin, Colorado University, JILA, Los Alamon National Laboratory, USA,
M. Marconi, C. Menoni, J. Rocca, R. Bartels, A. Isoyan, R. Sandberg, M. Murnane, H. Kapteyn

Financial support:

- EC's 7. Framework Program LASERLAB-EUROPE III, grant agreement number 284464
- The National Centre for Research and Development, LIDER programme, project no. LIDER/004/410/L-4/12/NCBR/2013
- National Centre for Science, award number DEC-2011/03/D/ST2/00296, UMO-2015/17/B/ST7/03718 , UMO-2015/19/B/ST3/00435
- COST Actions MP0601 and MP1203,
- Audiovisual and Culture Executive Agency (EACEA) Erasmus Mundus Joint Doctorate Programme Project No. 2012-0033
- the European Union's Horizon 2020 research and innovation program, under Laserlab-Europe IV, grant agreement No. 654148.

Laserlab Europe
FNP Fundacja na rzecz Nauki Polskiej
Narodowe Centrum Nauki
LIDER NCBR Narodowe Centrum Badań i Rozwoju
cost MP1203
WAT
ioe
NSF

Thank you